REGULATION OF DYNEIN-DYNACTIN DURING *DROSOPHILA* SPERMATOGENESIS

By

Michael Andrew Anderson

Dissertation

Submitted to the Faculty of the

Graduate School of Vanderbilt University

in partial fulfillment of the requirements

for the degree of

DOCTOR OF PHILOSOPHY

in

Cell and Developmental Biology

December, 2009

Nashville, Tennessee

Approved:

Professor David M. Miller

Professor Laura A. Lee

Professor Ethan Lee

Professor Daniela Drummond-Barbosa

Professor Karen A. Hales

For my family

ACKNOWLEDGEMENTS

First and foremost, I would like to thank my mentor Laura Lee, who has provided me with excellent guidance and support, and given me the confidence to develop into an independent scientist. I would also like to thank Ethan Lee, who always keeps his door open and has never hesitated to offer his advice whenever my project has taken a new direction. I am deeply indebted to fellow members of the Laura and Ethan Lee labs for their camaraderie, generosity, and many insightful discussions. They have truly made my time in graduate school enjoyable and productive. I am particularly appreciative of my benchmate Curtis Thorne, who has shown unbelievable patience in putting up with my many foibles, and has been a true friend.

I would also like to thank the members of my committee: David Miller, Daniela Drummond-Barbosa, and Karen Hales for all of the great advice and support that they have given me over the years. They have truly been excellent role models, and I will continue to aspire to live up to their examples as well as those set forth by Laura and Ethan Lee.

I must also thank my family. They have been a source of encouragement, inspiration, and motivation. I am particularly grateful toward my mother, who instilled in me a love for science, at an early age.

I would not have been able to survive graduate school without the love and support of my fiancée Rebecca Fox, who would never let me give up. I am truly fortunate to have had such a loving, caring, and intelligent woman to spend the last four years of my life with, and I look forward to our future together.

Finally, I am deeply appreciative of the financial support that I have received from the NIH Institutional Predoctoral Program in Developmental Biology training grant (HD-007502) and the NIH Institutional Predoctoral Reproductive Biology training grant (HD-007043).

TABLE OF CONTENTS

LIST OF TABLES

LIST OF FIGURES

CHAPTER I

INTRODUCTION TO DYNEIN AND *DROSOPHILA* SPERMATOGENESIS

Introduction

Cargos are actively transported to specific sites within a cell through the activities of molecular motors that travel along cytoskeletal tracks. Motors belonging to the myosin super family traffic along actin filaments, whereas kinesins and dynein transport cargos along microtubules. The majority of kinesins are involved in plus-end directed transport, whereas dynein is required for powering minus-end directed transport.

Dynein cargos are extremely diverse and can include proteins, mRNAs, chromosomes, and membrane-bound organelles. In addition to transporting cargo, dynein plays key roles during mitotic and developmental processes such as nuclear migration. In dividing cells, dynein facilitates nuclear envelope breakdown, spindle assembly, spindle positioning, and chromosome segregation. During nuclear migration, dynein powers the movement of nuclei down long microtubule tracks to their target sites. Dynein also regulates nuclear positioning within polarized cells and tightly controls their planes of division.

Because of dynein's ability to control such a myriad of functions, its activity must be tightly tailored to meet the needs of the cell. Dynein is composed of multiple subunits, and changes in the composition of these subunits are thought to modulate dynein's activities. Dynein subunits are extensively phosphorylated, and changes in their phosphorylation states can alter dynein's ability to bind cargos and microtubules as well

as its motor activity. Dynein's activities can be further regulated through interactions with its two accessory factors, dynactin and Lissencephaly-1 (Lis1), both of which are essential for dynein's *in vivo* functions. Furthermore, it is now being realized that post-translational modifications of microtubules may provide an additional level of control of dynein's activity.

The focus of my research has been the regulation of dynein during *Drosophila* spermatogenesis. In this chapter, I will provide a brief, general overview of the dynein complex and its interactions with its accessory factors, dynactin and Lis1. I will also discuss how microtubule modifications, specifically acetylation, may be used to regulate dynein's activity. Finally, I will present *Drosophila* spermatogenesis as a model system and will introduce my identification of the conserved gene *asunder* as a novel regulator of dynein.

The Dynein Complex

There are two general forms of dynein: axonemal dynein and cytoplasmic dynein. Axonemal dynein, which provides the force for movement of cilia and flagella, will not be discussed in this chapter. Cytoplasmic dynein is responsible for minus-end directed transport of cargos down microtubule bundles and plays key roles in a variety of biological processes such as nucleus-centrosome interactions, spindle assembly, chromosome segregation, nuclear migration, and cell movement. Cytoplasmic dynein is a large multimeric complex composed of six subunits: two copies of dynein heavy chain, dynein intermediate chain, dynein light intermediate chain, and two of each of the three dynein light chains (Figure 1.1) (reviewed in Susalka and Pfister, 2000).

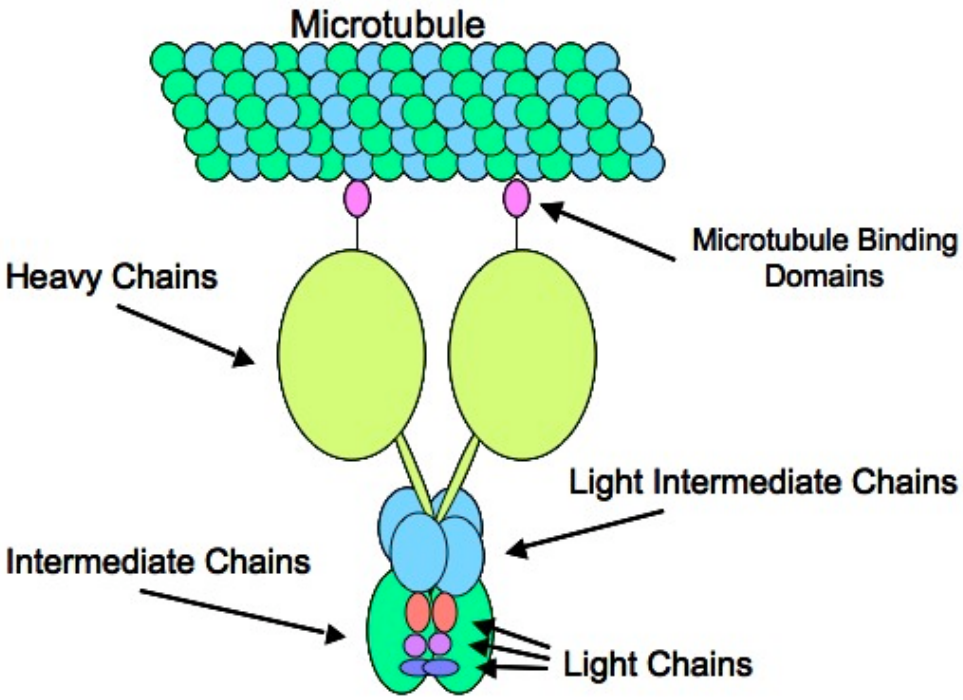

Figure 1.1. The dynein complex. Cartoon depicting the structural and stoichiometric composition of cytoplasmic dynein. Adapted from Susalka and Pfister, 2000.

Dynein heavy chain is approximately 500 kDa in size and consists of two distinct domains, the motor domain and the stem (also known as the tail). The motor domain contains six AAA family ATPase units that power dynein's functions and a "stalk" region through which dynein directly binds microtubules. The stem region, which is positioned at the amino terminus, provides a binding site for the intermediate and light intermediate chains (reviewed in Vallee and Hook, 2006).

Dynein intermediate chains are approximately 70 kDa in size and bind directly to the stem region of dynein heavy chain. Dynein intermediate chains, which are encoded by two genes in vertebrates and one in *Drosophila*, are differentially spliced to produce multiple, tissue-specific isoforms. The dynein intermediate chains directly bind dynein light chains and the dynein adaptor molecule, dynactin, and are required for cargo binding (Karki and Holzbaur, 1995; Susalka and Pfister, 2000; Vaughan and Vallee, 1995).

Dynein light intermediate chains are 50-60 kDa in size and are encoded by two genes in vertebrates and one in *Drosophila* (Mische et al., 2008; Vallee et al., 1989). Dynein light intermediate chains directly bind to the stem region of dynein heavy chain. The dynein light intermediate chains are required for the stability of the dynein complex and for dynein's role in chromosome segregation (Mische et al., 2008; Sivaram et al., 2009).

There are three dynein light chain families: Tctex1, LC8, and Roadblock. The dynein light chains directly bind to sites on the dynein intermediate chain and cooperate with dynein intermediate chain to bind various cargos. Of the three families of dynein light chains, only Tctex1 appears to be nonessential (Li et al., 2004). Vertebrates have at

least two members of each of the dynein light chain families, and the family members are differentially expressed within certain tissues. It has been demonstrated that dynein's cargo binding activities can be modulated through changes in the composition of its light chains, suggesting that light chains within the same family are not functionally equivalent (Chuang et al., 2001; Tai et al., 2001).

Although a great deal is known about the structural composition of the dynein complex, relatively little is known about its regulation. While changes in the composition and phosphorylation states of dynein subunits can modulate dynein's activities, it is believed that dynein's functions are largely controlled through interactions with its accessory factors, dynactin and Lis1 (Farshori and Holzbaur, 1997; Tai et al., 2001).

The Dynactin Complex

Dynactin (for dynein activator) was first identified based on its ability to activate dynein-mediated vesicle mobility in an *in vitro* assay (Gill et al., 1991; Schroer and Sheetz, 1991). Subsequent genetic studies revealed that dynactin is critical for dynein-powered processes *in vivo*, and biochemical studies demonstrated that dynactin directly interacts with dynein (Clark and Meyer, 1994; Holzbaur et al., 1991; Karki and Holzbaur, 1995; McGrail et al., 1995; Plamann et al., 1994; Vaughan and Vallee, 1995). Dynactin is now generally believed to be required for all of dynein's functions (reviewed in Karki and Holzbaur, 1995). Since its discovery, a great deal has been learned concerning dynactin's structure and the physical basis for its interaction with dynein.

Dynactin, like dynein, is a large multimeric complex (~1.2 MDa in size). The dynactin complex is composed of two basic structural units, the rod and the arm. The rod

is the site of cargo binding and is composed of seven proteins: Arp1, Arp11, Actin, CapZ, p25, p27, and p62. The arm mediates binding to both microtubules and dynein and is composed of $p150^{glued}$, p50/dynamitin (DMN), and p24/p22 (Figure 1.2). The stabilities of dynactin subunits are interdependent such that either loss or overexpression of individual components can result in destabilization of the dynactin complex (reviewed in Schroer, 2004).

Dynactin associates with dynein through direct binding between $p150^{glued}$ and the intermediate chain of the dynein complex (Karki and Holzbaur, 1995; King et al., 2003; Vaughan and Vallee, 1995; Vaughan et al., 2002). Interactions between $p150^{glued}$ and dynein intermediate chain appear to be regulated through phosphorylation of a serine residue within dynein intermediate chain (Vaughan et al., 2001). The identity of the kinase responsible for this modification remains elusive (Vaughan et al., 2001). Association of dynactin and dynein is believed to serve two major roles. First, dynactin possesses cargo-binding activity, so it can act as an adaptor protein to link dynein to its cargo (reviewed in Schroer, 2004). Second, dynactin has been shown to enhance the processivity of dynein, allowing dynein to stay associated with microtubules for a longer period of time (Culver-Hanlon et al., 2006; King and Schroer, 2000).

Although dynactin is essential for targeting dynein to cargos, only a fraction of dynactin is associated with dynein within the cell. It is now understood that dynactin has functions that lie outside of the dynein pathway. For example, dynactin has been found to serve as an adaptor protein for two kinesins, kinesin Eg-5 and kinesin-2 (Blangy et al., 1997; Deacon et al., 2003). In addition, dynactin may play a role in anchoring microtubules to the centrosome independently of dynein (Quintyne and Schroer, 2002).

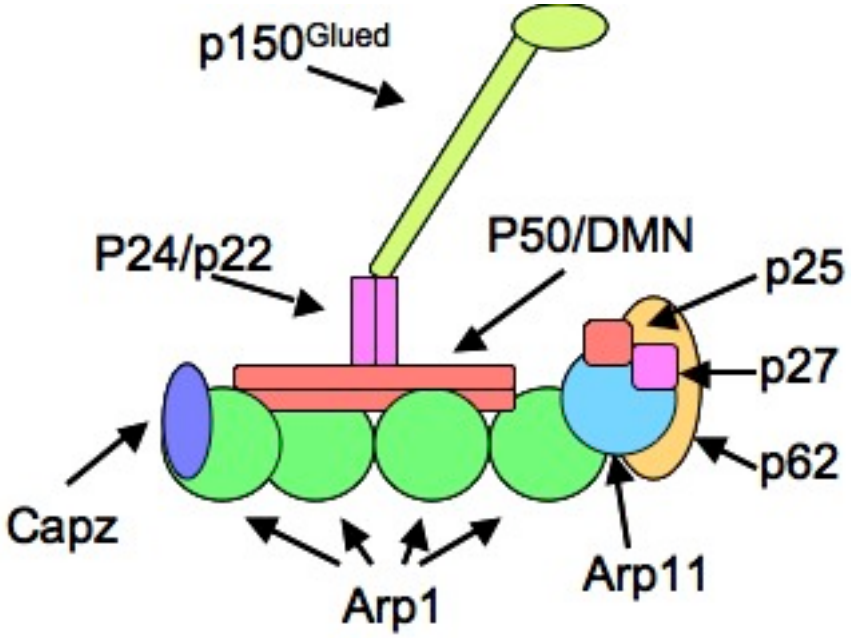

Figure 1.2. The dynactin complex. Cartoon depicting the structural subunits of a dynactin monomer. Adapted from Schroer, 2004.

Lis1

Lissencephaly 1 (Lis1) is highly conserved from yeast to humans. The loss of a single copy of *Lis1* in humans results in a severe developmental disorder known as classical or type I lissencephaly (smooth brain). Patients with type I lissencephaly display severe retardation and epilepsy, and they typically die during early childhood. Lissencephaly is caused by a disruption in neuronal migration during early brain development that results in a drastic reduction in the number of cells within the cerebral cortex (Dobyns and Truwit, 1995). Neuronal migration is initiated when newly formed neurons extend leading processes to a specific site within the nervous system. The nucleus and organelles contained in the cell body then travel along microtubule tracks extending through the leading process to reach their target destination (Hatten, 2002; Rivas and Hatten, 1995). Mouse models have shown that disruption of *Lis1* specifically interrupts the migration of nuclei through the leading processes (Gambello et al., 2003; Hirotsune et al., 1998; Tanaka et al., 2004; Tsai and Gleeson, 2005).

Nuclear positioning and migration are largely dependent on interactions between the nucleus and microtubule organizing centers or cortical microtubule arrays (Reinsch and Gonczy, 1998). Dynein plays an essential role in these processes by promoting associations between the nucleus and microtubules to maintain the position of nuclei within polarized cells and by powering the movement of nuclei down polarized microtubule tracks during nuclear migration (Gonczy et al., 1999; Malone et al., 2003; Morris et al., 1995; Reinsch and Karsenti, 1997; Tsai and Gleeson, 2005). Early genetic studies of nuclear migration involving the mutation of *Lis1* homologs in yeast, *Aspergillus nidulans*, and *Drosophila* revealed that *Lis1* is essential for dynein-mediated

nuclear migration events (Geiser et al., 1997; Lei and Warrior, 2000; Liu et al., 1999; Swan et al., 1999; Willins et al., 1997; Xiang et al., 1995). Subsequent work in mouse models has demonstrated that disruption of nuclear migration in developing neurons of patients with type 1 lissencephaly most likely stems from a loss of dynein activity, further highlighting Lis1's importance as a dynein regulator (Tanaka et al., 2004; Tsai and Gleeson, 2005).

The extent to which Lis1 is required for dynein's activity outside of nuclear migration is unclear; however, a growing body of evidence suggests that Lis1 is required for the majority of dynein's cell-cycle functions. Lis1 colocalizes with dynein at the cell cortex, nuclear periphery, spindle poles, and kinetochores. Furthermore, inhibition of Lis1 disrupts centrosome movements, nuclear envelope breakdown, spindle assembly, and chromosome segregation, all of which are under the control of dynein (Cockell et al., 2004; Coquelle et al., 2002; Faulkner et al., 2000; Hebbar et al., 2008; Li et al., 2005; Tai et al., 2002). Although Lis1 and dynein tightly colocalize at multiple sites, they may be targeted to these sites at least partially independently of one another.

Lis1 possesses two distinct motifs: a Lis homology domain, which promotes self-dimerization, and a WD repeat, located in the C-terminal half of the protein (Ahn and Morris, 2001; Kim et al., 2004; Tai et al., 2002). Lis1 has been shown to directly bind several dynein and dynactin components, including those that regulate its motor and cargo binding activity, through its WD repeat region (Faulkner et al., 2000; Mesngon et al., 2006; Sasaki et al., 2000; Smith et al., 2000; Tai et al., 2002). *In vitro* biochemical studies have suggested that binding of Lis-1 to dynein may stimulate its ATPase activity in a microtubule-dependent manner, thus Lis1 may serve to activate or enhance dynein's

motor activity (Mesngon et al., 2006).

Acetylation of Microtubules

Microtubules are composed of α/β heterodimers that join end-to-end to form long protofilaments. Typically, thirteen protofilaments associate with one another in a staggered arrangement through lateral interactions to form the helical structure of microtubules. Microtubules are selectively modified following polymerization. Common modifications include glutamylation, glycylation, detyrosination, and acetylation (reviewed in Hammond et al., 2008).

Acetylation of microtubules is a reversible modification that occurs at a lysine residue (Lys40) of α-tubulin following microtubule polymerization (reviewed in Westermann and Weber, 2003). Microtubule acetylation is generally observed in stable microtubules, but this modification does not appear to confer stability to microtubules (Palazzo et al., 2003). Early studies in *Chlamydomonas*, *Tetrahymena*, and *Caenorhabditis elegans* involving mutation of α-tubulin's Lys40 residue suggested that microtubule acetylation is not essential for cell survival (Fukushige et al., 1999; Gaertig et al., 1995; Kozminski et al., 1993). Recent work in mammalian systems, however, has revealed that microtubule acetylation contributes to several distinct cellular processes including cell motility and neuronal maturation (Creppe et al., 2009; Hubbert et al., 2002; Saji et al., 2005; Tran et al., 2007).

Acetylation of microtubules is controlled through the activity of acetylases and deacetylases. The enzymatic machinery responsible for microtubule acetylation has been largely elusive; a recent report, however, has implicated the Elongator complex in this

process (Creppe et al., 2009). The Elongator complex, which is composed of six subunits (Elp1-Elp6), catalyzes acetylation of its substrates through a histone acetyltransferase motif in the Elp3 subunit (Svejstrup, 2007; Wittschieben et al., 1999). Creppe and colleagues reported that knockdown of Elongator in developing neurons resulted in defects in neuronal branching due to a loss of microtubule acetylation. Furthermore, they demonstrated that an enriched fraction of Elongator subunit Elp3 was capable of acetylating microtubules *in vitro*, providing strong evidence that Elongator plays a direct role in the acetylation of microtubules (Creppe et al., 2009). Along with its newly discovered role in microtubule acetylation, Elongator is involved in a variety of processes including transcriptional regulation, tRNA processing, kinase signaling, exocytosis, and cell motility (reviewed in Svejstrup, 2007).

As mentioned previously, acetylation is reversible. Two enzymes, HDAC6 and Sirt2, have been shown to catalyze the deacetylation of microtubules both *in vitro* and *in vivo* (Hubbert et al., 2002; Matsuyama et al., 2002; North et al., 2003). HDAC6 and Sirt2 are members of a large family of histone deacetylases, but unlike their fellow family members, they are largely localized to the cytoplasm (Afshar and Murnane, 1999; Barlow et al., 2001; Perrod et al., 2001; Verdel et al., 2000). As with Elongator, both HDAC6 and Sirt2 are thought to act on multiple substrates within several independent pathways.

Acetylation of microtubules has been shown to significantly enhance the binding and activity of both kinesin-1 and dynein (Dompierre et al., 2007; Reed et al., 2006). Selective acetylation of microtubule pools may, therefore, provide superhighways on which microtubule motors travel. Indeed, acetylation of microtubules projecting into select neurites of neuronal CAD cells has been suggested to direct kinesin-1-based

transport to those neurites (Reed et al., 2006). During nuclear migration, the leading process along which dynein transports the nucleus is also heavily acetylated, although the role of acetylation during this process has not been addressed (Umeshima et al., 2007). It is unclear how acetylation of microtubules may stimulate binding of dynein as the acetylated residue of α-tubulin, Lys40, is situated in the lumen of polymerized microtubules and does not contact microtubule motors (Nogales et al., 1998). Study into the regulation of microtubule acetylation is complicated by the fact that the enzymes involved act on multiple substrates in a variety of independent pathways, making mutational analyses of these factors difficult to interpret. The mechanism by which microtubule acetylation regulates dynein and the extent to which it influences cellular processes remains to be determined.

Drosophila Spermatogenesis

Spermatogenesis is a dynamic process in which the cell cycle is coordinated with developmental events to produce haploid sperm capable of fertilizing eggs. The stages of *Drosophila* spermatogenesis have been clearly defined (Figure 1.3) (Fuller, 1993). Germline stem cells at the apical tip of the testis give rise to spermatogonial cells that proceed through four synchronous rounds of mitosis with incomplete cytokinesis to form 16-cell cysts of primary spermatocytes. Following pre-meiotic DNA replication, primary spermatocytes enter a prolonged G2 growth phase. Progression through meiosis I leads to formation of 32-cell cysts of secondary spermatocytes, and further division in meiosis II generates 64-cell cysts of spermatids. Immature, round spermatids differentiate into elongated and individualized sperm that move into the seminal vesicles.

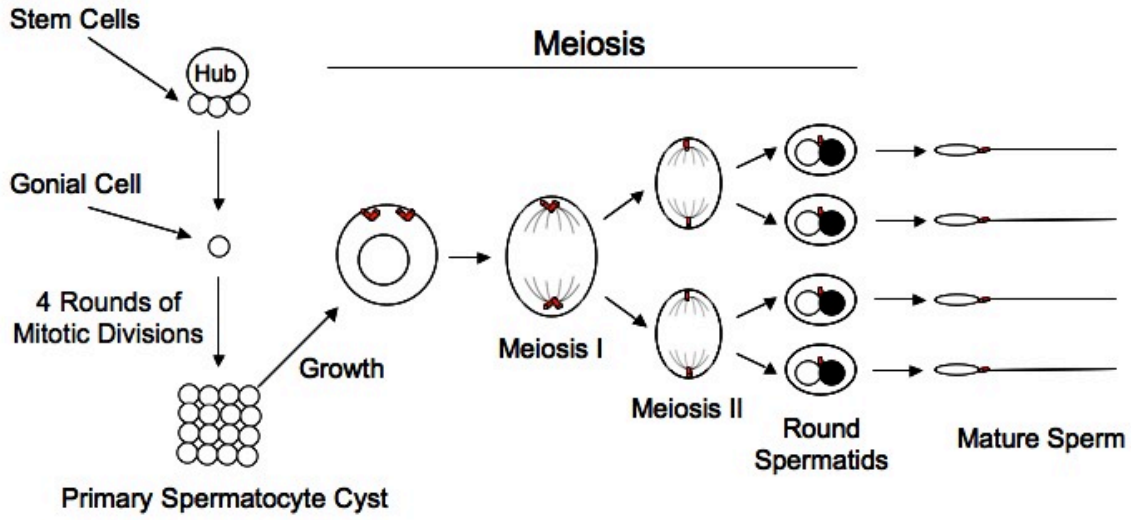

Figure 1.3. Spermatogenesis in the *Drosophila* testis. Diagram depicting the stages of spermatogenesis. Stem cells give rise to mitotic gonial cells. Each gonial cell undergoes four rounds of mitotic divisions to produce 16-cell primary spermatocyte cysts. Primary spermatocytes undergo dramatic growth and progress through the divisions of meiosis I and II to form round spermatids, which differentiate into mature sperm.

During *Drosophila* male meiosis, the centrosomes undergo dramatic changes in position (Figure 1.4) (Fuller, 1993). At completion of premeiotic S phase, the centrosomes of primary spermatocytes undergo migration to the cell cortex. Cortical centrosomes nucleate astral microtubules during late G2 and at entry into prophase will dissociate from the cortex and reform their connections with the nucleus. Once at the nucleus, the centrosomes will separate to opposite poles and direct formation of the meiotic spindle. Cortical centrosome migration is not unique to *Drosophila* spermatogenesis; similar centrosome movements are a key feature of the mitotic cell cycle of polarized epithelial cells (Figure 1.4) (Reinsch and Karsenti, 1994).

A feature that is unique to spermatogenesis in *Drosophila* and other insects is the formation of a mitochondrial aggregate known as the Nebenkern. During meiosis, mitochondria are equally partitioned to daughter cells. At the completion of meiosis, the mitochondria of spermatids will fuse to form a multilayered aggregate known as the Nebenkern. The Nebenkern extends along the length of the sperm axoneme during elongation and provides the energy to power beating of the sperm flagella.

Drosophila melanogaster has proven to be an excellent model system for the study of spermatogenesis. The relatively large size of meiotic spindles of *Drosophila* spermatocytes makes them well suited for cytological examination (Cenci et al., 1994). Due to relaxation of checkpoints, meiotic progression occurs even in the face of errors in spindle assembly (Rebollo and Gonzalez, 2000). Immature spermatids, which are abundant in the testis, are highly regular in appearance; deviations in their uniformity are diagnostic of earlier defects in meiotic divisions. These features, combined with genetic

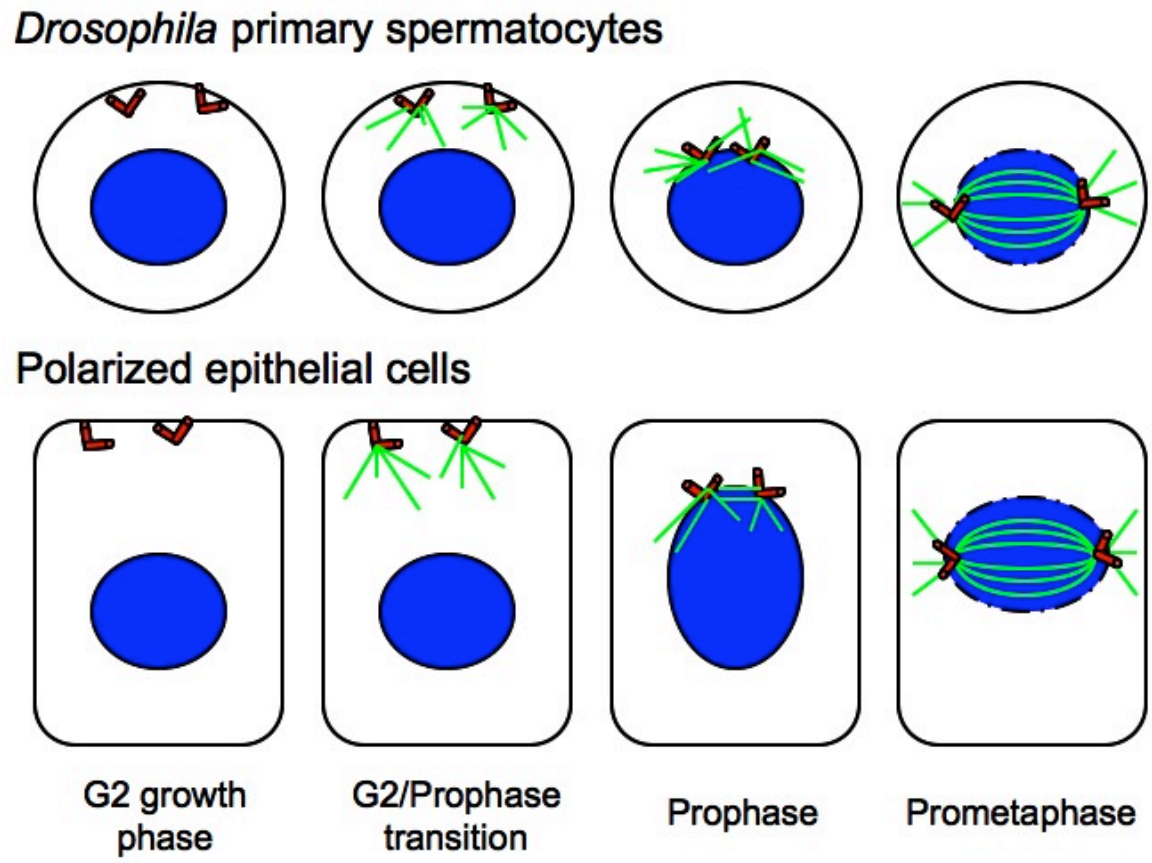

Figure 1.4. Centrosome migration in *Drosophila* primary spermatocytes and polarized epithelial cells. Centrosomes (red) of *Drosophila* primary spermatocytes and polarized epithelial cells associate with the cell cortex at entry into G2. At the completion of G2, the centrosomes nucleate astral microtubules (green) and migrate to the nucleus (blue) at entry into prophase. The centrosomes then travel along the nuclear surface to opposite poles to initiate assembly of the spindle (green) at prometaphase.

tools available in *Drosophila*, have facilitated mutational analysis of male meiosis (Wakimoto et al., 2004).

Dynein-Dynactin in *Drosophila* Spermatogenesis

Dynein is essential for both the meiotic and postmeiotic stages of *Drosophila* spermatogenesis (Anderson et al., 2009; Li et al., 2004). Our lab has demonstrated that dynein displays a dynamic localization pattern during male meiosis (Anderson et al., 2009). During late G2, dynein accumulates at the nuclear surface of primary spermatocytes. At prophase I, dynein accumulates at the centrosomes that have stably reattached to the nucleus. Prometaphase I cells display dynein at both the spindle poles and kinetochores. While the kinetochore localization of dynein is lost at metaphase I, dynein remains at the spindle poles through completion of telophase I. Identical localizations of dynein are seen during meiosis II. At the completion of meiosis, dynein localizes to a hemispherical cap on the nuclear surface and to the periphery of the Nebenkern of round spermatids (Anderson et al., 2009; Li et al., 2004).

Dynein is recruited to the nuclear surface in a multitude of systems, and dynein-mediated interactions between the nucleus and centrosomes have been found to be important for a variety of biological processes, including nuclear envelope breakdown, nuclear positioning, and nuclear migration (Beaudouin et al., 2002; Morris, 2000; Reinsch and Gonczy, 1998; Salina et al., 2002). Recruitment of dynein to the nuclear surface appears to be particularly important during *Drosophila* spermatogenesis. During male meiosis, localization of dynein to the nuclear surface of G2 spermatocytes is required for the stable reattachment of centrosomes to the nucleus at entry into meiotic

prophase and for fidelity of the meiotic divisions (Anderson et al., 2009). In postmeiotic spermatids, perinuclear dynein is required to maintain the attachment between the nucleus and the basal body, which is critical for later stages of spermiogenesis (Anderson et al., 2009; Li et al., 2004).

The mechanism by which dynein is recruited to the nuclear surface is unclear. The *C. elegans* Hook protein ZYG-12, which localizes to the nuclear periphery, tethers dynein to this site in embryos; a similar role for Hook proteins in other species, however, has not been reported (Malone et al., 2003). Nuclear pore complexes have been proposed as likely candidates for sites of dynein attachment as they are unique to the nuclear envelope and span both outer and inner nuclear membranes (Beaudouin et al., 2002; Salina et al., 2002). In support of this model, dynein has been found to physically interact with nuclear pore complex components in bovine zygotes and oocytes (Payne et al., 2003).

My work has shown that dynein's recruitment to the nuclear surface during *Drosophila* spermatogenesis is dependent on the function of the conserved gene, *asunder* (*asun*) (Anderson et al., 2009). *asun* spermatocytes arrest at entry into prophase of meiosis I and contain centrosomes that fail to stably associate with the nucleus. Spermatocytes that overcome this arrest often display severe defects in spindle assembly, chromosome segregation, and cytokinesis. Furthermore, nucleus-basal body coupling is lost in postmeiotic spermatids. Localization of dynein to the nuclear surface of G2 spermatocytes and postmeiotic spermatids is lost in *asun* testes. Intriguingly, dynein's localization to the kinetochores and Nebenkern remains intact in *asun* spermatocytes and spermatids, suggesting that *asun* is specifically required for dynein's localization to the

nuclear periphery (Anderson et al., 2009). In support of this, we have found that both *Drosophila* and human forms of ASUN localize to the nuclear periphery of cultured human (HeLa) cells. Furthermore, *Drosophila* ASUN colocalizes with dynein at the nuclear surface of HeLa cells treated with nocodazole. These observations suggest that ASUN may directly target dynein to the nuclear surface.

While the precise mechanism by which ASUN recruits dynein to the nuclear surface is currently unclear, we have evidence to suggest that ASUN may cooperate with Lis-1 to regulate dynein's activity during *Drosophila* spermatogenesis. My analysis of a male sterile allele of *Lis-1* has revealed that Lis-1 is required for dynein's perinuclear localization and activity during *Drosophila* spermatogenesis. Furthermore, I have found that mutations in *Lis-1* dominantly enhance *asun*.

In the following chapters, I will present my work analyzing the roles of *asun* and *Lis-1* in the regulation of dynein during *Drosophila* spermatogenesis. My identification and characterization of *asun* as a novel regulator of dynein's nuclear localization should provide critical insight into the mechanism underlying dynein's recruitment to the nuclear surface.

CHAPTER II

asunder IS A CRITICAL REGULATOR OF DYNEIN-DYNACTIN LOCALIZATION DURING *DROSOPHILA* SPERMATOGENESIS

Most work described in this chapter has been published (Anderson et al., 2009).

Introduction

Spermatogenesis is one of only a few aspects of *Drosophila* development that requires centrioles. While centrioles appear to be largely dispensable for mitosis, acentriolar spermatocytes form highly abnormal meiotic spindles and do not initiate cytokinesis (Basto et al., 2006; Bettencourt-Dias et al., 2005; Rodrigues-Martins et al., 2008). In addition, centrioles are required in postmeiotic spermatids to form the axoneme (Bettencourt-Dias et al., 2005).

During *Drosophila* male meiosis, centrosomes undergo dramatic changes in position and reductive divisions (Fuller, 1993). In primary spermatocytes, centrosomes separate from the nucleus and move to the cortex following completion of premeiotic S phase. These cortical centrosomes nucleate astral microtubules in late G2 and reassociate with nucleus in early prophase to initiate formation of a bipolar spindle. Centrosome migration during meiosis is thus tightly coupled to the meiotic cell cycle.

Nucleus-centrosome interactions have been shown in many systems to depend on dynein, a minus-end-directed microtubule motor complex (Hook and Vallee, 2006). Dynein also plays key roles in a variety of other biological processes such as spindle assembly, chromosome segregation, nuclear migration, and cell movement. In

Drosophila, dynein regulates many aspects of development, including both male and female gametogenesis (Gepner et al., 1996).

We report here that *asunder* (previously known as *Mat89Bb*) is required in *Drosophila* for male fertility. Primary spermatocytes of *asunder* testes undergo prophase arrest with defects in nucleus-centrosome coupling; cells that overcome arrest exhibit abnormal meiotic spindle assembly, chromosome segregation, and cytokinesis. Additionally, nucleus-basal body associations are disrupted during postmeiotic stages of differentiation. We show that this constellation of defects in germline cells of *asunder* males is likely due to reduced perinuclear localization of dynein-dynactin.

Materials and Methods

Drosophila stocks

y w was used as the "wild-type" stock. *β-tubulin-GFP* flies were a gift from H. Oda and Y. Akiyama-Oda. The *Dmn-GFP* stock has been previously described (Wojcik et al., 2001). *piggyBac* insertion lines *f02815* and *f01662* were from the Exelixis Collection (Harvard Medical School). *asp* alleles were a gift from C. Gonzalez (Rebollo et al., 2004). The following lines were from Bloomington Stock Center: *Df(3R)Exel7329*, *nanos-Gal4-VP16*, *piggyBac* transposase, twe^{1}, $\beta Tub85D^{Drv1}$, fwd^{neo1}, *Df(3L)7C,* $Dhc64C^{4-19}$, $Dhc64C^{6-10}$, *Df(3L)fz-GF3b,* and Gl^{1}.

DNA clones and transgenics

cDNA clone LD33046 encoding ASUN was from the *Drosophila* Gene Collection. A cDNA clone encoding human GCT1 (ID 2989678) was from Open Biosystems. UASp-Myc-ASUN was created by subcloning of PCR-amplified coding sequence from LD33046 into a modified version of UASp that confers an N-terminal Myc tag (Rorth, 1998). For male germline expression of fluorescently tagged ASUN, cDNA encoding ASUN with an N-terminal GFP or Cherry tag was subcloned into testis expression vector tv3 (gift from J. Brill) (Wong et al., 2005). Two independent transgenic lines with male germline expression of GFP-ASUN were used in this study: line 16 (chromosome III) to demonstrate perinuclear localization of GFP-ASUN (Figure 2.15) and line 11 (chromosome II) for all other experiments. Transgenic lines were generated by *P*-element-mediated transformation via embryo injection (Rubin and Spradling, 1982).

Cytological analyses of live and fixed testes

Live testes cells were prepared for examination by phase contrast or fluorescent microscopy as described (Kemphues et al., 1980). Methanol fixation (for immunofluorescence and visualization of cells expressing β-tubulin-GFP) was performed as follows: slides of squashed testes were snap-frozen, immersed in methanol for 10 minutes at -20˚C after coverslip removal, and washed twice in phosphate-buffered saline. Formaldehyde fixation (for actin staining and visualization of cells co-expressing Cherry-ASUN and DMN-GFP) was performed as described (Gunsalus et al., 1995).

Primary antibodies were used as follows: rat anti-α-tubulin (Mca77G, 1:500, Accurate Chemical & Scientific Corp.), mouse anti-γ-tubulin (GTU-88, 1:250, Sigma),

mouse anti-Cyclin A (A12, 1:50, Developmental Studies Hybridoma Bank), mouse anti-Cyclin B (F2F4, 1:50, Developmental Studies Hybridoma Bank), and mouse anti-dynein heavy chain (P1H4, 1:150) (McGrail and Hays, 1997). The following antibodies were used to assess centrosome integrity: rabbit anti-CNN (1:1000), rabbit anti-SPD-2 (1:200), rabbit anti-D-PLP (1:250), rabbit anti-SAS-4 (1:100), and rabbit anti-TACC (1:500) (gifts from J. Raff except for anti-CNN, a gift from W. Theurkauf). Cy2- and Cy3-conjugated secondary antibodies were used at 1:800. Actin individualization cones were stained with Alexa Fluor 594 phalloidin (1:100, Invitrogen). Fixed samples were mounted in phosphate-buffered saline with DAPI (0.2 μg/ml) to visualize DNA.

Fluorescent images were obtained using one of two microscopes: Nikon Eclipse 80i with Plan-Apo 100x and Plan-Fluor 40x objectives or Zeiss Axioplan with Neo-Fluor Ph2 40x objective. Bright field images of whole testes were obtained using a Zeiss Stemi 2000-CS stereoscope. Phase contrast images were captured using one of three microscopes: Nikon Eclipse 80i with Plan 20x Ph1 objective, Zeiss Axiophot with Neo-Fluor Ph2 40x objective, or Zeiss Axioplan with Neo-Fluor Ph2 40x objective. The ratio of the intensity of perinuclear to cytoplasmic DMN-GFP signal and of cytoplasmic to nuclear Cherry-ASUN signal in individual G2 spermatocytes was determined using Adobe Photoshop.

Mammalian cell transfection, staining, and microscopy

HeLa cells were maintained in Dulbecco's modified Eagle Medium (DMEM) containing 10% fetal bovine serum. Plasmids for expression of N-terminally tagged versions of *Drosophila* ASUN and/or human GCT1 (GFP or Myc, respectively)

generated by subcloning into pCS2 were transfected into cells using Lipofectamine 2000 (Invitrogen) according to manufacturer's directions.

Cells were plated on fibronectin-coated coverslips 21 hours post-transfection and fixed three hours later. For direct GFP fluorescence alone or in combination with phospho-histone H3 or Myc immunostaining, cells were fixed 20 minutes with 4% formaldehyde in CBS (10 mM MES pH 6.1, 138 mM KCl, 3 mM $MgCl_2$, 2 mM EGTA, 0.32 M sucrose). For direct GFP fluorescence in combination with dynein intermediate chain staining, cells were fixed 5 minutes at -20˚C in methanol. Cells were permeabilized 10 minutes with 0.5% Triton X-100 in Tris-buffered saline. For nocodazole treatment, cells were exposed to 5 μg/ml nocodazole for 3 hours prior to fixation. Primary antibodies were used as follows: mouse anti-c-Myc (9E10, 1:1000), rabbit anti-phospho-histone H3 (Mitosis Marker, 1:200, Upstate Antibody), and mouse anti-dynein intermediate chain (74.1, 1:100, Santa Cruz). Fluorescently conjugated secondary antibodies were used at 1:5000. Slides were mounted in Vectashield with DAPI (Vector Labs). Images were acquired using a Nikon Eclipse 80i microscope equipped with a CoolSNAP ES camera (Photometrics) and Plan-Apo 60X objective. For experiments involving quantification, at least 400 cells per condition were scored.

RT-PCR

RNA was extracted from testes of newly eclosed males using RNA STAT-60 (Tel-Test, Inc.). RT-PCR was performed using Ready-To-Go RT-PCR Beads (GE Healthcare). 5' and 3' regions of *asun* (Products 1 and 2, respectively) were amplified using the following primer sets: 5'-gccgcgcattcccaacaagg-3' (1F), 5'-

gcggcatttccagcaagact-3' (1R), 5'-actaaatgccaccacaatgc-3' (2F), and 5'-gcgtcccgagaaatccaatc-3' (2R). A region of *Mst89B*, which is expressed specifically in the testes, was amplified as a positive control using the following primer set: 5'-tgcaacctcaagttcagtcg-3' (Mst89B-F) and 5'-gcgtcccgagaaatccaatc-3' (Mst89B-R) (Stebbings et al., 1998).

Immunoblots

Protein extracts were prepared by homogenizing dissected testes from newly eclosed males in SDS sample buffer. The equivalent of two testes pairs was loaded per lane. Proteins were transferred to nitrocellulose for immunoblotting using standard techniques. Primary antibodies were used as follows: mouse anti-Cyclin A (A12, 1:50, Developmental Studies Hybridoma Bank), rabbit anti-Cyclin B (Rb271, 1:2000, gift from D. Glover), mouse anti-actin (pan Ab-5, 1:1000, NeoMarkers), mouse anti-dynein heavy chain (P1H4, 1:2000) (McGrail and Hays, 1997), mouse anti-dynein intermediate chain (74.1, 1:1000, Santa Cruz), mouse anti-Dynamitin (1:250, BD Biosciences), and mouse anti-tubulin (DM1α, 1:7000). HRP-conjugated secondary antibodies and chemiluminescence were used to detect primary antibodies.

Results

***asunder* is required for male fertility**

Mat89Bb (*Maternal transcript 89Bb*) was originally identified by virtue of its rich expression in *Drosophila* ovaries (Stebbings et al., 1998). In a *Drosophila* genome-scale

biochemical screen, we identified Mat89Bb as a substrate of the kinase encoded by *pan gu* (*png*) that is required in the early embryo (Lee et al., 2005). To assess *Mat89Bb*'s developmental role, we obtained a candidate mutant (Figure 2.1A). *f02815* is a *piggyBac* insertion in the second intron of *Mat89Bb* predicted to remove the C-terminal 64 residues from the full length (689-amino acid) protein (Thibault et al., 2004). Homozygous $Mat89Bb^{f02815}$ adults are viable and appear normal. Unexpectedly, we found that $Mat89Bb^{f02815}$ males are almost completely sterile (Table 2.1), whereas mutant females have only slightly decreased fertility (data not shown). We have changed the *Mat89Bb* gene name to "*asunder*" ("*asun*") to better reflect its loss-of-function phenotype as described below.

To elucidate the basis for the male-sterile phenotype of $asun^{f02815}$ flies (referred to herein simply as "*asun*"), we first assessed whether they were capable of producing mature sperm. We dissected whole testes with attached seminal vesicles from males withheld from females to allow accumulation of sperm. Although the overall size and shape of *asun* testes (Figure 2.1C) were similar to that of wild type (Figure 2.1B), suggesting normal proliferation of sperm progenitor cells, their seminal vesicles were largely empty. Mature sperm formed in small amounts in *asun* testes were immotile or weakly motile (data not shown). Germline expression of Myc-tagged ASUN using the UAS-Gal4 system fully restored motile sperm production and fertility to *asun* males (Figure 2.1D; Table 2.1) (Brand and Perrimon, 1993) (Rorth, 1998). Thus, *asun* is required for spermatogenesis in *Drosophila*.

Table 2.1. Quantification of defects in onion-stage spermatids and sterility of *asun* males

Genotype[a]	n[c]	Nebenkern to nuclei ratio (%Cells)						Macro/ micronuclei (%Cells)	Male fertility (%WT)[e]
			Abnormal						
		1:1	1:2	1:3	1:4	1:≥5	Total		
Wild type	2948	100	0	0	0	0	0	0	100
f02815[b]	616	33	16	10	23	18	67	47	8
f02815/Df(3R)Exel7329	100	9	28	15	33	15	91	56	6
f02815 revertant	2220	100	0	0	0	0	0	0	90
UASp-Myc-asun/Y; f02815	2463	67	n.d.[d]	n.d.	n.d.	n.d.	33	n.d.	22
nanos-Gal4-VP16, f02815	1462	44	n.d.	n.d.	n.d.	n.d.	56	n.d.	0
UASp-Myc-asun/Y;f02815/ nanos-Gal4-VP16, f02815	2297	100	0	0	0	0	0	0	111

[a]All genotypes are w^-.
[b]*asun* allele.
[c]n = Number of onion-stage spermatids scored. Testes from 15 males were scored per genotype.
[d]n.d. = Not determined.
[e]Single adult males (two days old) were placed in vials with five wild-type virgin females (two days old) and allowed to mate for five days. The mean number of adult progeny eclosed per vial is shown as a percentage of wild type (50 males tested per genotype).

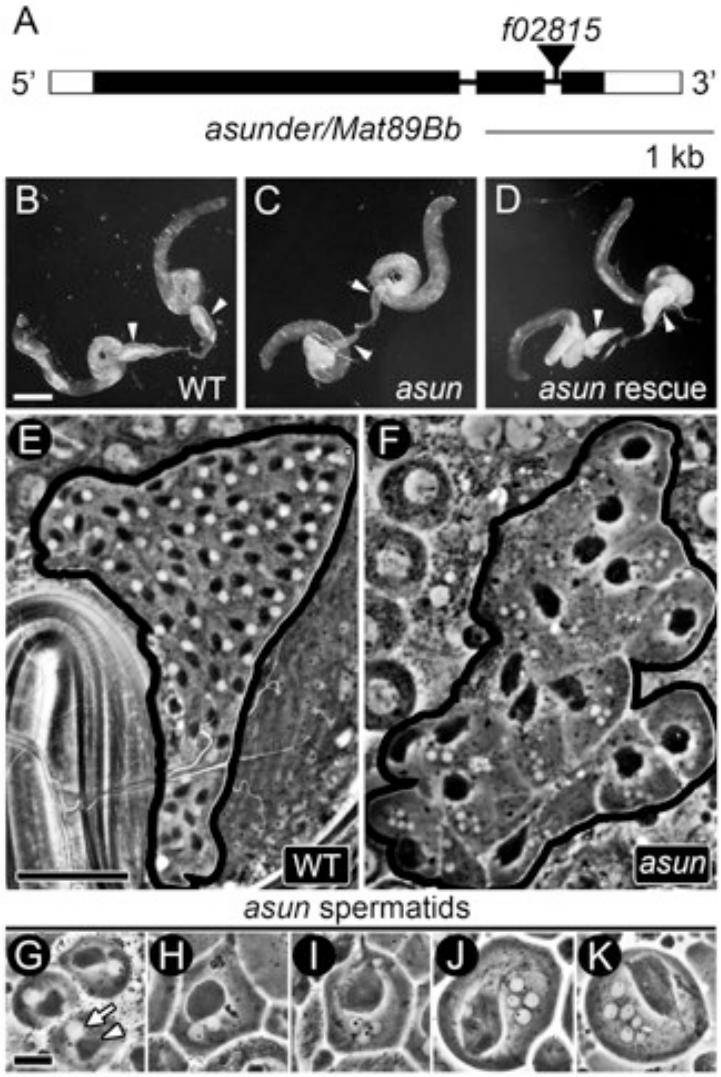

Figure 2.1. *asun* males are sterile. (A) *asun* gene structure. Coding regions and UTRs are represented as filled and unfilled boxes, respectively, introns as thin lines, and *piggyBac* transposon *f02815* as a triangle. (B-D) Testes of males separated from females for six days. Arrowheads, seminal vesicles. (B) Wild-type seminal vesicles engorged with mature sperm. (C) Flaccid *asun* seminal vesicles indicate failed spermatogenesis. (D) Transgenic Myc-ASUN restores sperm to *asun* seminal vesicles. Bar, 250 μm. (E-K) Phase-contrast micrographs of testes. (E,F) Cysts of onion-stage spermatids; black lines mark cyst boundaries. (E) Wild-type cyst with normal complement of 64 cells, each containing a phase-light nucleus and phase-dark Nebenkern of similar size. (F) *asun* cyst of 16 cells, most with one large Nebenkern and several nuclei of variable size. Bar, 50 μm. (G-K) Range of *asun* onion-stage spermatid phenotypes. (G) Cell with normal (1:1) ratio of Nebenkern to nuclei. (H-K) Cells with abnormal ratios of Nebenkern to nuclei (1:2 (H), 1:3 (I), 1:4 (J), and 1:6 (K)) and nuclei of variable size. Bar, 10 μm.

asun spermatids display irregularities in nuclear size and number

To determine which steps of spermatogenesis were impeded in *asun* males, we used phase contrast microscopy to examine germline cells within live squashed preparations of dissected testes. Intact cysts of *asun* primary spermatocytes contained exactly 16 cells (50/50 cysts), indicating that the four mitotic spermatogonial divisions occurred; furthermore, *asun* spermatogonial cells appeared normal (data not shown). When we examined cysts of postmeiotic spermatids in *asun* testes, however, abnormalities in both cell number and morphology were apparent.

Wild-type spermatids in the "onion" stage (named for their tightly wrapped mitochondrial membranes that resemble onion layers in cross section) have one phase-light nucleus associated with one phase-dark mitochondrial aggregate, the Nebenkern (Figure 2.1E) (Fuller, 1993). Because nuclear diameter correlates with chromosome content at this stage, errors in chromosome segregation during meiosis yield variably sized nuclei (Gonzalez et al., 1989). Although fusion of interconnected cells within the same cyst commonly occurs during squashing of wild-type testes, resulting in the spurious appearance of multi-nucleated spermatids, a 1:1 ratio of Nebenkern to nuclei is maintained. Inhibition of meiotic cytokinesis following nuclear division leads to alterations in this ratio because the Nebenkern fuse into a single large mass within multi-nucleated cells (Liebrich, 1982).

We found that most *asun* cysts have reduced numbers of onion-stage spermatids, sometimes as few as 16, with a variable number of irregularly sized nuclei and one large Nebenkern (Figure 2.1, F-K). Such defects are indicative of severe disruptions in chromosome segregation and cytokinesis during the preceding meiotic divisions (Fuller,

1993). These phenotypes were fully rescued by germline expression of Myc-ASUN or reverted to wild type by precise excision of *f02815* (Table 2.1). Thus, *asun* is required for normal male meiosis.

The frequency of spermatid defects increased when *f02815* was placed in *trans* to a small chromosomal deficiency that removes *asun*. Whereas 67% of $asun^{f02815}$ spermatids were multi-nucleated, and 47% had variably sized nuclei, the frequency of these phenotypes increased to 91% and 56%, respectively, in hemizygotes, suggesting that $asun^{f02815}$ may have residual function (Table 2.1). Consistent with these data, we detected a truncated *asun* transcript in $asun^{f02815}$ testes by RT-PCR (Figure 2.2).

Centrosomes fail to stably attach to the nucleus in *asun* primary spermatocytes

Because the phenotypes that we observed in *asun* spermatids were diagnostic of earlier disruptions in the meiotic divisions, we shifted our focus to spermatocytes. To aid in this analysis, we crossed into the *asun* background a transgene that ubiquitously expresses fluorescently labeled β-tubulin (Inoue et al., 2004).

Entry into M phase in primary spermatocytes is marked by centrosome migration, chromosome condensation, and the appearance of specific microtubule structures (Cenci et al., 1994; Rebollo et al., 2004). Paired asters (centrosomes with associated astral microtubules) formed at the cell cortex in late G2 migrate inward from the cortex and stably attach to the nuclear envelope in prophase I (Figure 2.3, A and E). Asters then separate from each other and move along the nuclear surface to opposite poles to establish the meiotic spindle. In *asun* spermatocytes, we observed normal cortical positioning in G2 and release of centrosomes upon M-phase entry; subsequent nucleus-

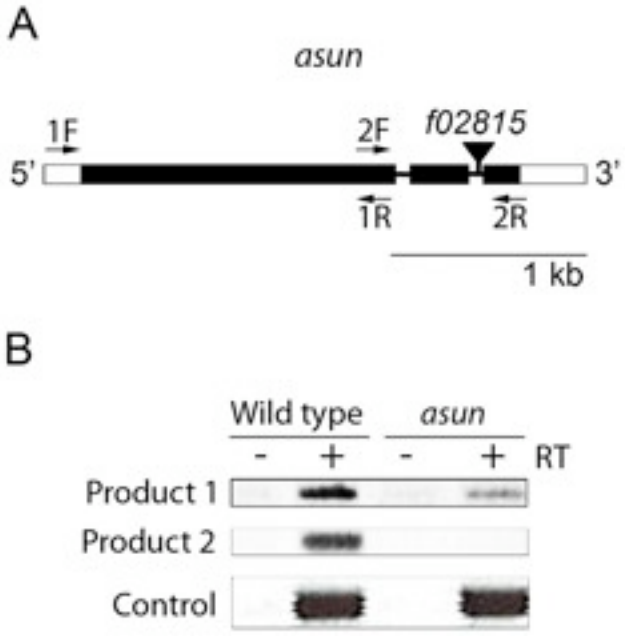

Figure 2.2. *asun*^{f02815} males express a truncated *asun* transcript in the testes. (A) *asun* gene structure (see Figure 2.1A for description). Arrows indicate positions of primers used for RT-PCR. (B) In *asun*^{f02815} testes, the 5'-end of the *asun* transcript (Product 1) was present at decreased levels relative to wild type, whereas the 3'-end of the *asun* transcript (Product 2) was not detected. Transcript encoded by the male germline-specific gene *Mst89B* (Stebbings et al., 1998) was PCR-amplified as a control.

centrosome coupling, however, was defective (Figure 2.3, B, D, and F-H; data not shown).

We observed a striking loss of association between asters and the nucleus during prophase in *asun* primary spermatocytes by direct visualization of β-tubulin-GFP (Figure 2.3, B-D). We confirmed the identity of these free asters by staining for γ-tubulin, a centrosomal marker (Figure 2.3, F-H). We chose the gene name "*asunder*" (set apart in position or space) on the basis of this phenotype. The number of asters per *asun* prophase spermatocyte ranged from two to four (Figure 2.3, B-D and F-H), likely due to premature reduction of centrosomes that normally occurs during meiosis. Quantification of these defects revealed that the majority of prophase I spermatocytes from *asun* homozygous and hemizygous males contain unattached, divided asters (Figure 2.3I). Furthermore, a disproportionately high number of primary spermatocytes from *asun* homozygous and hemizygous males were found to be in prophase (Figure 2.3J), indicative of arrest upon M-phase entry. *asun* spermatocytes appear to normally accumulate Cyclin A and Cyclin B during prophase I, and *asun* testes display elevated levels of Cyclin A and Cyclin B consistent with an increased fraction of cells at prophase I (Figure 2.4).

Meiotic spindle assembly and chromosome segregation are aberrant in *asun* spermatocytes

Although *asun* spermatocytes arrest in prophase I, they can evade arrest and proceed through both meiotic divisions. In wild-type spermatocytes, chromosomes segregate evenly to daughter cells along a bipolar spindle during meiosis I and II (Figure 2.5, A and B). In contrast, the vast majority of *asun* spermatocytes that progress through

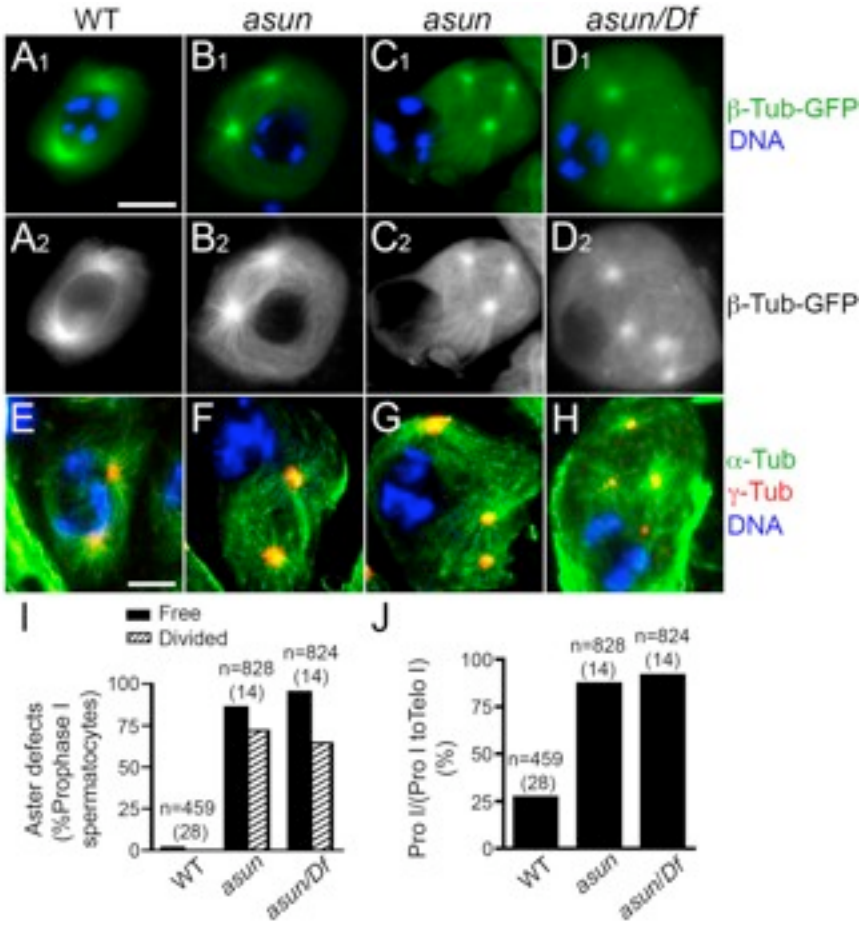

Figure 2.3. Loss of nucleus-centrosome attachments in *asun* spermatocytes. (A-H) Prophase I spermatocytes expressing β-tubulin-GFP (green in A1-D1; grayscale in A2-D2) or stained for microtubules (α-tubulin; green) and centrosomes (γ-tubulin; red) (E-H). DNA is in blue. In wild-type spermatocytes (A,E), centrosomes migrate from cortex and attach to nucleus. Most *asun* spermatocytes have two (B,F), three (C,G), or four (D,H) unattached centrosomes; spermatocytes in D and H are from hemizygotes. Bar, 10 μm. (I,J) Quantification of aster defects (I) and prophase arrest (J) of *asun* spermatocytes. Relative to wild type, *asun* testes contain an increased fraction of Prophase I (Pro I) through Telophase I (Telo I) spermatocytes that are in Prophase I. n, number of prophase I spermatocytes (I) or prophase I through telophase I spermatocytes (J) scored per genotype. Number of males analyzed per genotype is in parentheses. Free, cells with unattached asters. Divided, cells with three or four asters. *Df*, *Df(3R)Exel7329*.

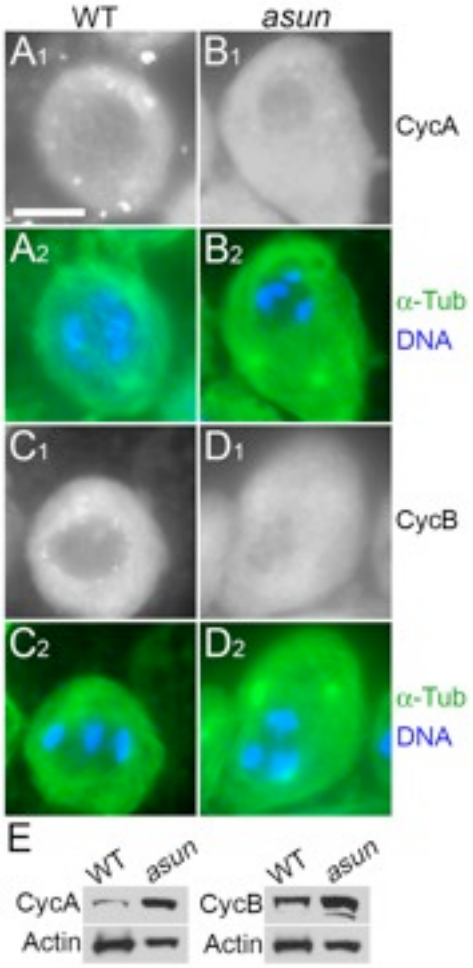

Figure 2.4. Normal levels of Cyclin A and Cyclin B in *asun* prophase I spermatocytes and testes extracts. (A-D) Prophase I spermatocytes stained for Cyclin A (red in A1,B1; grayscale in A2,B2) or Cyclin B (red in C1,D1; grayscale in C2,D2). Microtubules (α-tubulin) are stained in green and DNA in blue. Cyclin A and Cyclin B levels in prophase I spermatocytes of *asun* testes (B and D, respectively) are comparable to that of wild type (A and C, respectively). Bar, 10 μm. (E) Immunoblots showing normal levels of Cyclin A and Cyclin B in *asun* testes extracts. Loading control: anti-α-tubulin.

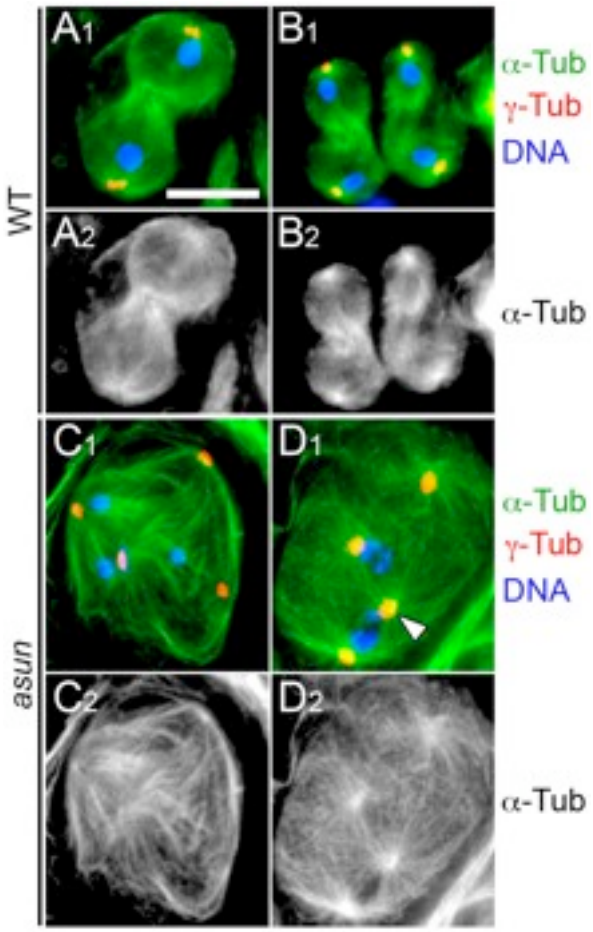

Figure 2.5. Aberrant spindle assembly and chromosome segregation in *asun* spermatocytes. Meiotic cells stained for α-tubulin (green in A1-D1; grayscale in A2-D2), centrosomes (γ-tubulin; red), and DNA (blue). Wild-type primary (A) and secondary (B) spermatocytes in telophase segregate DNA equally to daughter cells. (C,D) Representative *asun* primary spermatocytes. (C) Unequal segregation of DNA masses to three poles of a tetrapolar spindle. (D) Two spindles sharing a pole (arrowhead). Bar, 10 μm.

the meiotic divisions exhibit gross defects in spindle assembly (e.g. tetrapolar spindles) and chromosome segregation (Figure 2.5, B and C). We infer that these defects in spindle assembly and chromosome segregation occur upon resumption of M-phase by *asun* spermatocytes that underwent premature division of centrioles during a prolonged prophase I. Although *Drosophila* spermatocytes are capable of forming acentrosomal spindles when nucleus-centrosome coupling is disrupted, we have not observed acentrosomal spindles in *asun* spermatocytes (Rebollo et al., 2004).

Late events of spermatogenesis are disrupted in *asun* males

In *Drosophila*, key events of spermatid differentiation (e.g. elongation and individualization) can proceed even in the face of severe meiotic defects (Alphey et al., 1992; Castrillon et al., 1993). Indeed, postmeiotic stages of spermatogenesis are present in *asun* testes despite the disruptions in meiosis that we have reported herein. We examined postmeiotic spermatids in *asun* testes to determine if *asun* regulates late spermatogenesis.

Axoneme assembly is directed by a centriole-derived basal body that embeds in the nuclear envelope immediately after meiosis (Figure 2.6, A and C). We found that nucleus-basal body coupling is impaired in *asun* spermatids that have failed to undergo meiotic cytokinesis (Figure 2.6B). Despite the absence of nucleus-basal body interactions, axonemes nonetheless nucleate from the free basal bodies of *asun* spermatids (Figure 2.6D).

Formation of the sperm axoneme initiates onion-stage spermatid elongation. During elongation of wild-type spermatids, nuclei with their associated basal bodies are

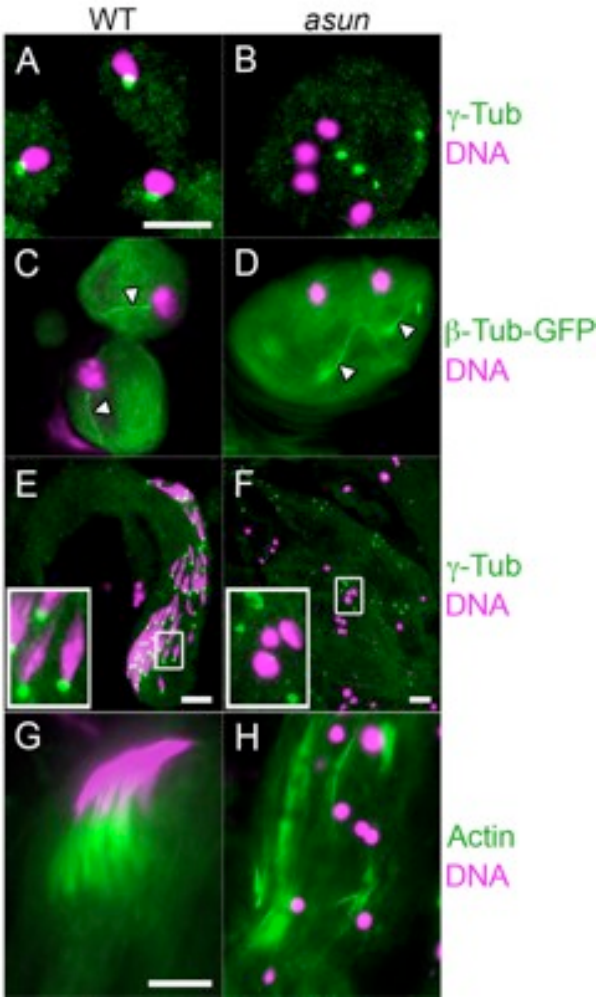

Figure 2.6. Loss of nucleus-basal body attachment and individualization defects of *asun* spermatids. (A,B) Onion-stage spermatids stained for basal bodies (γ-tubulin; green) and DNA (magenta). Basal bodies embed in the nuclear envelope after meiosis in wild-type spermatids (A) but fail to attach to nuclei of *asun* spermatids (B). (C,D) Onion-stage spermatids expressing β-tubulin-GFP (green) stained for DNA (magenta). Sperm axonemes (arrowheads) nucleate from attached basal bodies in wild-type spermatids (C) and from free basal bodies in *asun* spermatids (D). (E,F) Elongating spermatids stained for basal bodies (γ-tubulin; green) and DNA (magenta). Insets show enlarged views of boxed regions. (E) As wild-type spermatids elongate, basal bodies remain attached to nuclei that acquire a spiculated shape. (F) Disorganized bundles of elongating *asun* spermatids with dispersed basal bodies and round nuclei. (G,H) Bundles of individualizing spermatids stained for actin (green) and DNA (magenta). (G) In wild-type spermatids, actin cones formed at each nucleus move as a unit along the bundle length. (H) In *asun* spermatids, disorganized actin cones are found along the bundle length. Bars, 10 μm.

positioned at the proximal tips of growing bundles, and the nuclei undergo a change in morphology from round to needle-like (Figure 2.6E). The nuclei and basal bodies of *asun* spermatids in elongating bundles, however, are often randomly distributed throughout the length of the bundle, and nuclei remain round (Figure 2.6F).

Spermatid individualization occurs as actin cones assembled at the nucleus move down the axoneme, pushing out excess cytoplasm and remodeling cell membranes as they travel the bundle length. Wild-type actin cones form synchronously and migrate as a unit (Figure 2.6G). *asun* actin cones, however, appear to move down the axoneme independent of one another and are typically dispersed along the entire bundle length (Figure 2.6H). Thus, *asun* is required for some, but not all, events of late spermatogenesis.

Dynamic localization of dynein-dynactin throughout *Drosophila* spermatogenesis

Our analysis of the *asun* male-sterile phenotype strongly suggested that *asun* plays a critical role in the formation and/or maintenance of nucleus-centrosome/basal body interactions. Using a panel of antibodies directed against centrosomal proteins, we found that the free asters of *asun* spermatocytes stained positively for all markers tested (Figure 2.7) (Basto et al., 2006; Gergely et al., 2000; Martinez-Campos et al., 2004) (Dix and Raff, 2007). Thus, loss of nucleus-aster attachments in *asun* spermatocytes does not appear to be due to a global defect in centrosome composition.

Migration of centrosomes from the cortex to the nucleus in *Drosophila* primary spermatocytes, a prerequisite step to form nucleus-centrosome attachments, depends upon microtubules, actin, and *abnormal spindle* (*asp*) function {Kemphues, 1982

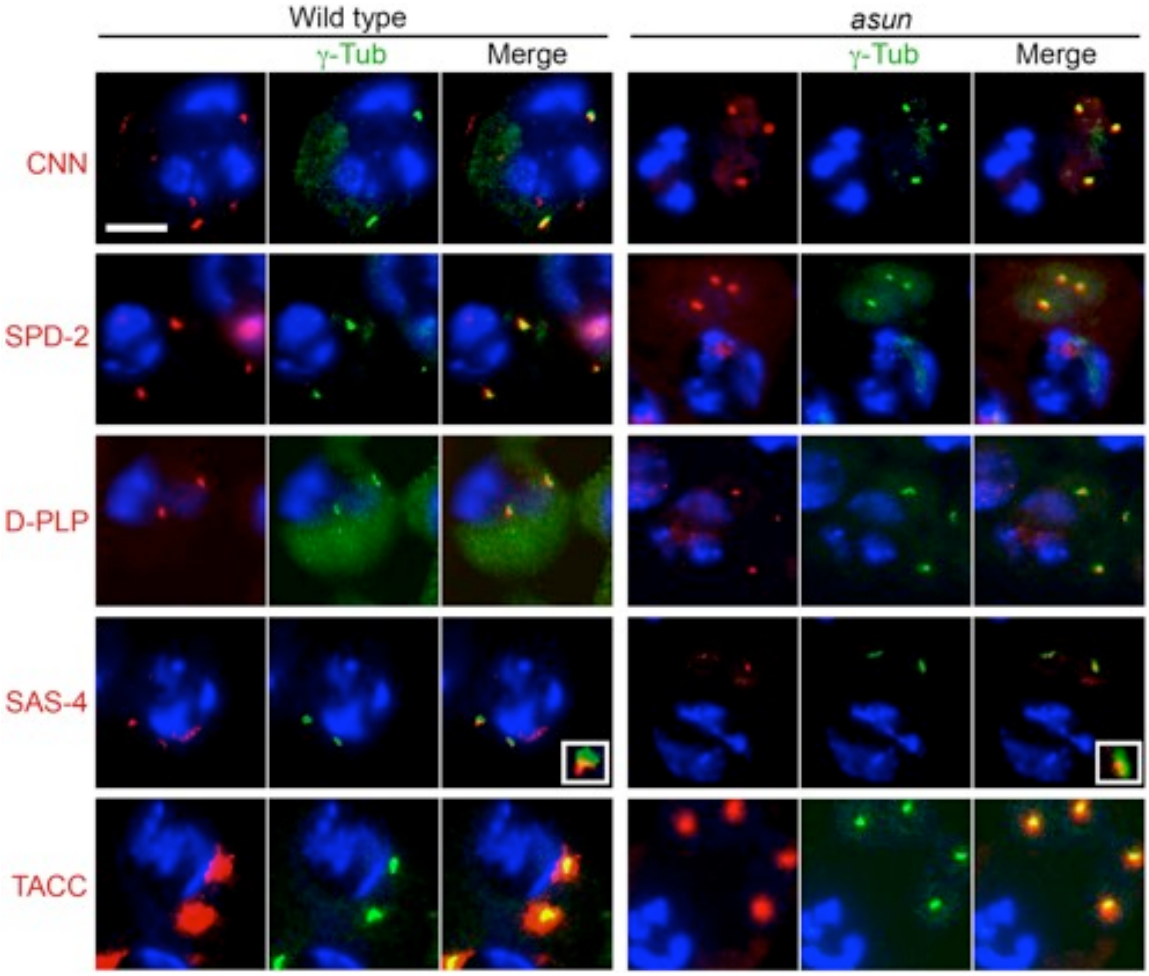

Figure 2.7. Normal centrosomes in *asun* spermatocytes. Wild-type and *asun* testes were stained for γ-tubulin (green) to mark the position of the centrosomes, DNA (blue), and the indicated centriole/centrosome components (red). *asun* late primary spermatocytes exhibited staining comparable to that of wild type for all components tested. CNN, Centrosomin; SPD-2, Spindle defective 2; D-PLP, Pericentrin-like protein; TACC, Transforming acidic coiled-coil protein. Insets show enlarged views of SAS-4 localization on centrosomes.

#116}(Giansanti et al., 1998; Gunsalus et al., 1995; Rebollo et al., 2004; Wakefield et al., 2001). In *asun* spermatocytes, actin arrays appear grossly normal, and astral microtubule arrays are similar in size to those of wild type (compare Figure 2.3, B to A and F to E; data not shown). In contrast to *asp*, centrosomes of *asun* spermatocytes appear to disassociate from the cell cortex normally upon M-phase entry, suggesting that *asun* mediates a subsequent event required for nucleus-centrosome coupling (Figure 2.3, A and B).

Dynein-dynactin has been shown to play an essential role in anchoring both centrosomes and basal bodies to the nucleus. Dynein-dynactin is recruited to the nuclear periphery in a variety of systems, and this localization has been shown to be critical for centrosome attachment in *C. elegans* embryos (Gonczy et al., 1999; Salina et al., 2002) (Malone et al., 2003). Loss of dynein in *Drosophila* embryos results in failure of centrosomes to stably attach to nuclei, and nucleus-basal body interactions are lost in *Drosophila* spermatids null for *tctex-1*, which encodes a dynein light chain (Li et al., 2004; Robinson et al., 1999). We therefore chose to examine dynein-dynactin localization during spermatogenesis in *asun* males.

Dynamic localization of dynein at meiotic spindle poles and kinetochores has been observed in grasshopper and crane-fly spermatocytes (Fabian and Forer, 2005; King et al., 2000). Localization of dynein-dynactin during *Drosophila* male meiosis, however, has not been reported to our knowledge. We first established the normal localization pattern of dynein and dynactin in wild-type spermatocytes by examining fixed cells stained for dynein heavy chain and living cells expressing a GFP-tagged version of

Dynamitin (DMN), the p50 subunit of dynactin (McGrail and Hays, 1997; Wojcik et al., 2001).

Whereas dynein is evenly dispersed in the cytoplasm of early G2 spermatocytes, it accumulates on the nuclear periphery by late G2 (Figures 2.8A; data not shown). Dynein concentrates near asters attached to the nucleus in prophase I and at spindle poles and kinetochores in prometaphase I (Figure 2.8, B and C). Kinetochore localization is lost in metaphase I as dynein further concentrates at spindle poles, where it persists during anaphase I and telophase I (Figure 2.8, D-F). We observed an identical pattern of dynein localization during meiosis II (data not shown). As previously reported, we detected a hemispherical cap of dynein on nuclei of onion-stage spermatids; interestingly, the site of nucleus-basal body attachment lies directly in the middle of this cap (Figure 2.8, G and H) (Li et al., 2004; Wei et al., 2008). We observed an essentially identical localization pattern throughout spermatogenesis for the DMN subunit of dynactin (Figure 2.9, A and B; data not shown). We also detected a weak enrichment of dynein-dynactin at the Nebenkern surface that has not been previously reported to our knowledge (Figure 2.10A; data not shown).

asun is required for dynein-dynactin localization throughout spermatogenesis

We found dynein-dynactin localization to be severely disrupted in *asun* spermatocytes and spermatids. Dynein rarely localized to the nuclear periphery in late G2 *asun* spermatocytes (Figure 2.8I; 35/320 cells scored) or in arrested *asun* spermatocytes with free asters (Figure 2.8J; 0/167 cells scored). Even in *asun* primary spermatocytes that overcame the G2 arrest and formed spindles, dynein localization to spindle poles was

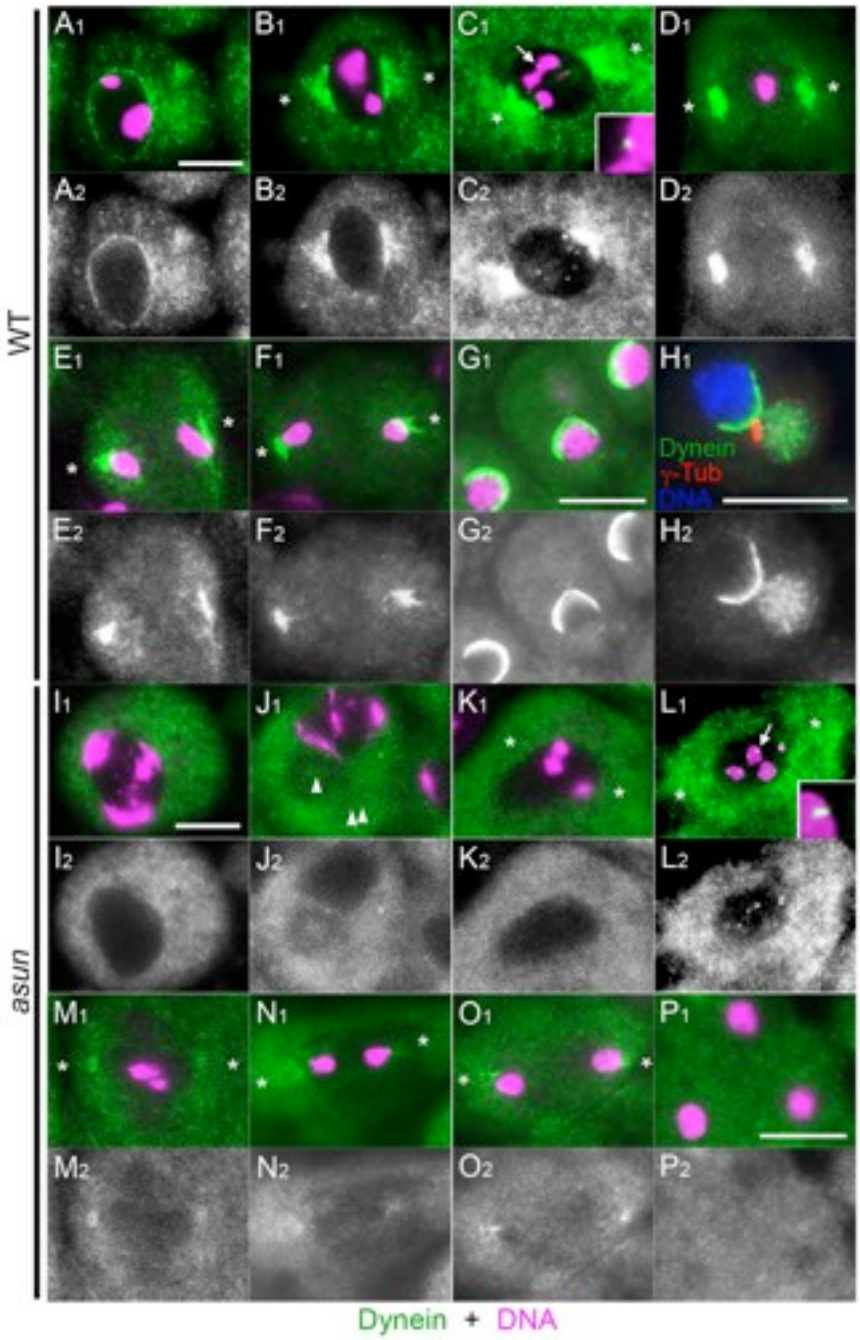

Figure 2.8. Disrupted dynein localization in *asun* spermatocytes and spermatids. Wild-type (A-G) and *asun* (I-P) primary spermatocytes and onion-stage spermatids stained for dynein heavy chain (green in A1-G1, I1-P1; grayscale in A2-G2, I2-P2). DNA is in magenta. α-Tubulin staining (not shown) was used to determine cell-cycle stage and spindle pole positions (asterisks). (A-F) Wild-type spermatocytes. Dynein localizes uniformly to surface of late G2 nuclei (A), near centrosomes attached to the nucleus in

Figure 2.8 continued: prophase (B), and at spindle poles and kinetochores (arrow, enlarged in inset) in prometaphase (C). Kinetochore localization is lost at metaphase (D). Dynein remains at spindle poles in anaphase (E) and telophase (F). (G,H) In wild-type spermatids, dynein localizes to a hemispherical cap on the nucleus. (H) Triple staining for dynein (green in H1; grayscale in H2), basal bodies (γ-tubulin; red), and DNA (blue) reveals proximity of basal body to dynein cap. (I-O) *asun* spermatocytes. Dynein fails to localize to the nuclear periphery in late G2 (I) and is dispersed in the cytoplasm. *asun* spermatocytes arrest in prophase I (J) with free asters (arrowheads) and no spindle, although some form bipolar spindles in prophase (K) and proceed through prometaphase (L), metaphase (M), anaphase (N), and telophase (O). In both cases, dynein localization to the nuclear periphery and spindle poles is absent or greatly reduced relative to wild type, whereas localization to prometaphase kinetochores (arrow in L, enlarged in inset) appears normal. (P) Dynein does not localize to a hemispherical nuclear cap in *asun* spermatids. Bars, 10 μm.

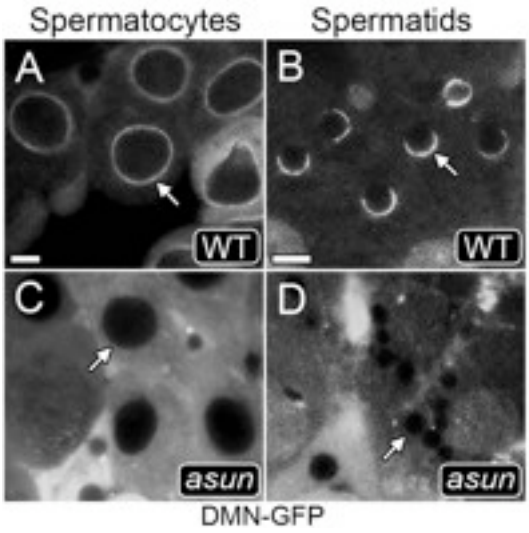

F**igure 2.9. Disrupted dynactin localization in *asun* spermatocytes and spermatids.** Wild-type (A-B) and *asun* (C-D) primary spermatocytes and onion-stage spermatids expressing DMN-GFP. Dynactin is at the nuclear periphery (arrows) in wild-type G2 spermatocytes (A) and onion-stage spermatids (B), but not in *asun* spermatocytes (C) and spermatids (D). Bars, 10 μm.

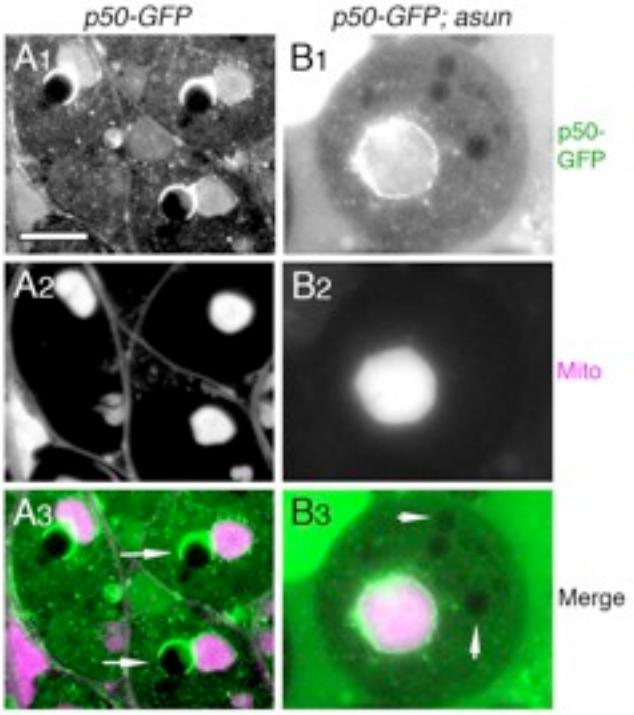

Figure 2.10. Dynactin localizes to the Nebenkern of wild-type and *asun* spermatids. Wild-type (A) and *asun* (B) spermatids expressing DMN-GFP (grayscale in A1,B1; green in A3,B3). Mitochondria exhibit autofluorescence under UV light revealing the Nebenkern (grayscale in A2,B2; magenta in A3,B3). Arrows mark nuclei. In wild-type spermatids (A), DMN-GFP localizes to the surface of Nebenkern and nuclei. In *asun* spermatids (B), DMN-GFP is present at the Nebenkern surface but absent at the nuclear surface. Bar, 10 μm.

greatly reduced relative to wild type from prophase through telophase (Figure 2.8, K-O). *asun* secondary spermatocytes also exhibited decreased dynein at spindle poles (data not shown). Dynein appeared to accumulate normally, however, on kinetochores of *asun* prometaphase spermatocytes with bipolar spindles (Figure 2.8L; 64/64 cells). Dynein did not form a hemispherical nuclear cap in multi-nucleated *asun* onion-stage spermatids, although very weak perinuclear localization was occasionally seen in *asun* spermatids with wild-type morphology (Figure 2.8P; data not shown). A severe reduction in the localization of the DMN subunit of dynactin to the nuclear periphery and to spindle poles throughout spermatogenesis was similarly observed in *asun* testes (Figure 2.9, C and D; data not shown). In contrast, localization of dynein-dynactin to the Nebenkern surface appeared to be normal in *asun* spermatids (Figure 2.10B; data not shown).

Despite the loss of dynein-dynactin localization during meiotic and postmeiotic stages of spermatogenesis in *asun* males, we found that protein levels of DHC64C and Cdic, core dynein components (heavy and intermediate chains, respectively), are not reduced in *asun* testes (Figure 2.11A). Likewise, we found that protein levels of DMN, a core dynactin component, are not reduced in *asun* testes (Figure 2.11B). These results strongly suggest that *asun* is required for localization, but not stability, of dynein-dynactin during spermatogenesis.

Loss of perinuclear dynein localization is not a general feature of male-meiotic mutants

Loss of dynein-dynactin localization in *asun* spermatocytes and spermatids could be a general consequence of meiotic failure. To test this possibility, we examined dynein localization to the nuclear surface in four other male-meiotic mutants: *twine* (*twe*),

βTubulin85D (*βTub85D*), *abnormal spindle* (*asp*), and *four wheel drive* (*fwd*). Spermatocytes of *twe* or *βTub85D* males arrest at the G2/M-phase transition due to loss of Cdk1-Cyclin B activity or microtubules, respectively (Alphey et al., 1992; Kemphues et al., 1982). In spermatocytes lacking *asp*, which encodes a microtubule-associated protein, the two pairs of centrioles fail to migrate from the plasma membrane back to the nucleus during prophase and instead remain located at the plasma membrane throughout meiosis (Rebollo et al., 2004; Wakefield et al., 2001). *fwd* spermatocytes undergo nuclear divisions, but meiotic cytokinesis fails, resulting in the formation of multi-nucleated spermatids (Brill et al., 2000). We found that dynein accumulates to normal levels on the nuclear periphery of spermatocytes and spermatids of all four mutants tested (Figure 2.12), indicating that perinuclear localization of dynein in the male germline occurs via a microtubule-independent mechanism and that loss of dynein localization in *asun* testes is not likely to be a secondary or indirect consequence of disruption of meiosis.

Genetic enhancement of *asun* by dynein-dynactin components

We hypothesized that loss of perinuclear dynein-dynactin is the underlying basis for the defects observed in *asun* spermatocytes. As a test of this model, we assessed whether reduction of the gene dosage of either of two dynein-dynactin components would enhance the *asun* phenotype: DHC64C (dynein heavy chain) or Glued (Gl), the p150 subunit of dynactin (Holzbaur et al., 1991). Introduction into the *asun* background of a single copy of $Dhc64C^{4-19}$ (null allele), $Dhc64C^{6-10}$ (hypomorphic allele), or *Df(3L)fz-*

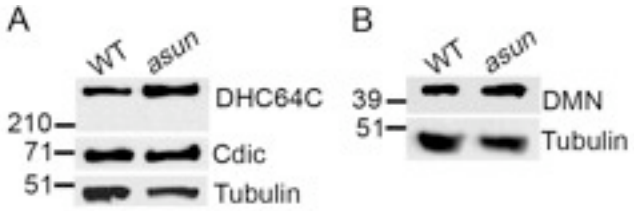

Figure 2.11. Normal levels of dynein-dynactin components in *asun* testes extracts. Dynein and dynactin immunoblots. (A) Normal levels of dynein heavy and intermediate chains (DHC64C and Cdic, respectively) in *asun* testes extracts. (B) Normal level of DMN in *asun* testes extracts. Loading control: anti-α-tubulin.

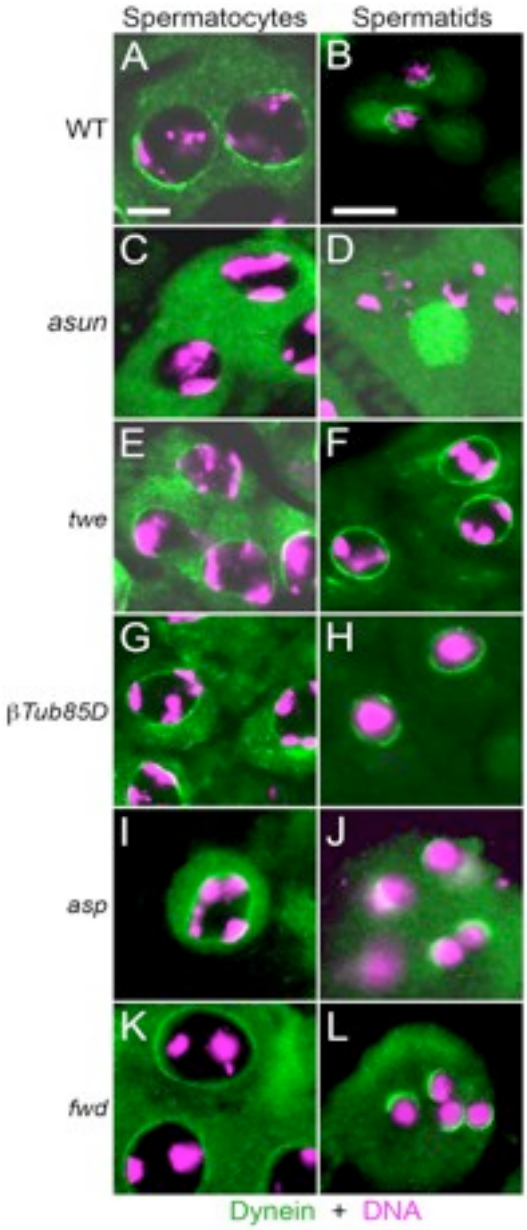

Figure 2.12. Dynein localization in other male-meiotic mutants. Fixed testes from wild-type (A,B), *asun* (C,D), *twe*^{1} (E,F), *βTub85D*^{Drv1} (G,H), *asp*^{E3}/*asp*^{L1} (I), and *fwd*^{neo1}/*Df(3L)7C* (J) males were stained for dynein heavy chain (green) and DNA (magenta). In contrast to *asun*, dynein localizes to the nuclear periphery in spermatocytes and spermatids of other male-meiotic mutants. Perinuclear localization of dynein is expanded in *twe* and *β2tub* spermatids relative to wild type.

GF3b (genomic deficiency that deletes *Gl*) significantly increased the incidence of multi-nucleated spermatids (from 64% to 93%, 84%, and 88%, respectively); dominant enhancement of *asun* by Gl^1 (dominant-negative allele) did not reach statistical significance (Figure 2.13). As controls, one copy of any of these alleles in an otherwise wild-type background had no apparent effect on spermatogenesis (data not shown). These genetic data support our model that loss of dynein-dynactin function is responsible for the meiotic defects of *asun* spermatocytes.

ASUN and dynactin undergo coincident changes in localization in primary spermatocytes

To gain insight into the mechanism by which ASUN promotes dynein-dynactin localization during spermatogenesis, we examined its localization pattern. We established transgenic lines that express fluorescently tagged versions of ASUN in postmitotic germ cells of the testis under the control of the male-specific *βTub85D* promoter (Wong et al., 2005). These transgenes could fully rescue the sterility of *asun* males and did not perturb spermatogenesis in wild-type flies (data not shown). Using a combination of fluorescent and phase-contrast microscopy, we assessed ASUN localization throughout male meiosis.

Using this approach, we found that ASUN exhibits stage-specific localization in G2 spermatocytes (Figure 2.14, A-C). The G2 phase of primary spermatocytes can be divided into six stages (S1-S6) based on the appearance of cytoplasmic and nuclear structures (Cenci et al., 1994). In stage S3-S4 cells, ASUN is largely restricted to the nucleus (253/253 cells). In stage S5 cells, ASUN localization ranges from mostly nuclear to being partitioned between the nucleus and cytoplasm (Figure 2.14, A and B). By stage

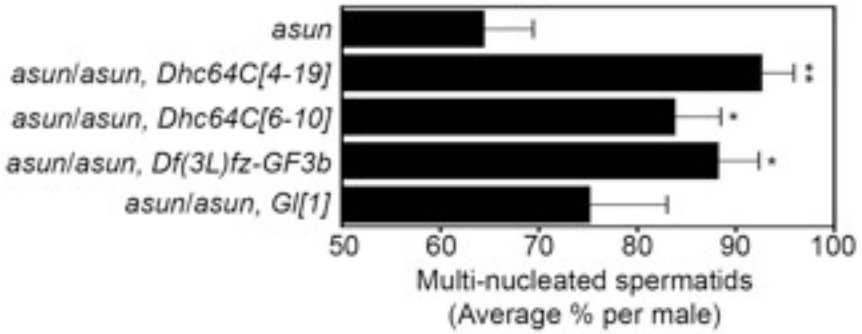

Figure 2.13. Dominant enhancement of *asun* by dynein-dynactin. *asun* is dominantly enhanced by mutation of genes that encode core dynein-dynactin components. Bars represent the average percentage of multi-nucleated onion-stage spermatids per male of the indicated genotypes (15 males analyzed per genotype). Error bars represent SEM. Significant differences compared to *asun* were determined by a two-tailed unpaired Student's *t*-test. Single and double asterisks represent *P*-values <0.01 and <0.0001, respectively.

S6, which precedes centrosome migration and entry into M phase, ASUN is distributed between the cytoplasm and nucleus (Figure 2.14C; 236/236 cells). ASUN remains dispersed throughout the cell until the completion of meiosis when it becomes restricted from nuclei of onion-stage spermatids (Figure 2.14D; data not shown). Based on these observations, we infer that a pool of ASUN is released from the nucleus to the cytoplasm during the S5 stage of G2 spermatocytes.

Although the localization patterns of ASUN and dynein-dynactin differ during spermatogenesis, we found that the timing of the nuclear-to-cytoplasmic movement of a pool of ASUN in G2 spermatocytes coincides tightly with that of dynein-dynactin recruitment to the nuclear surface. As described above for ASUN, we used a combination of fluorescent and phase-contrast microscopy to more precisely define the timing of the perinuclear recruitment of GFP-tagged DMN in living G2 spermatocytes. In stage S3-S4 cells, perinuclear DMN was undetectable (248/248 cells). DMN first accumulates on the nuclear surface during stage S5 (Figure 2.14, E and F) and uniformly localizes there by stage S6 (Figure 2.14G; 144/145 cells). When we examined primary spermatocytes expressing both Cherry-ASUN and DMN-GFP, we found a strong temporal correlation between the nuclear-to-cytoplasmic movement of a pool of ASUN and perinuclear accumulation of DMN (Figure 2.14, I-L). These results are consistent with a model in which release of a pool of ASUN from the nucleus to the cytoplasm in G2 primary spermatocytes stimulates recruitment of dynein-dynactin to the nuclear periphery.

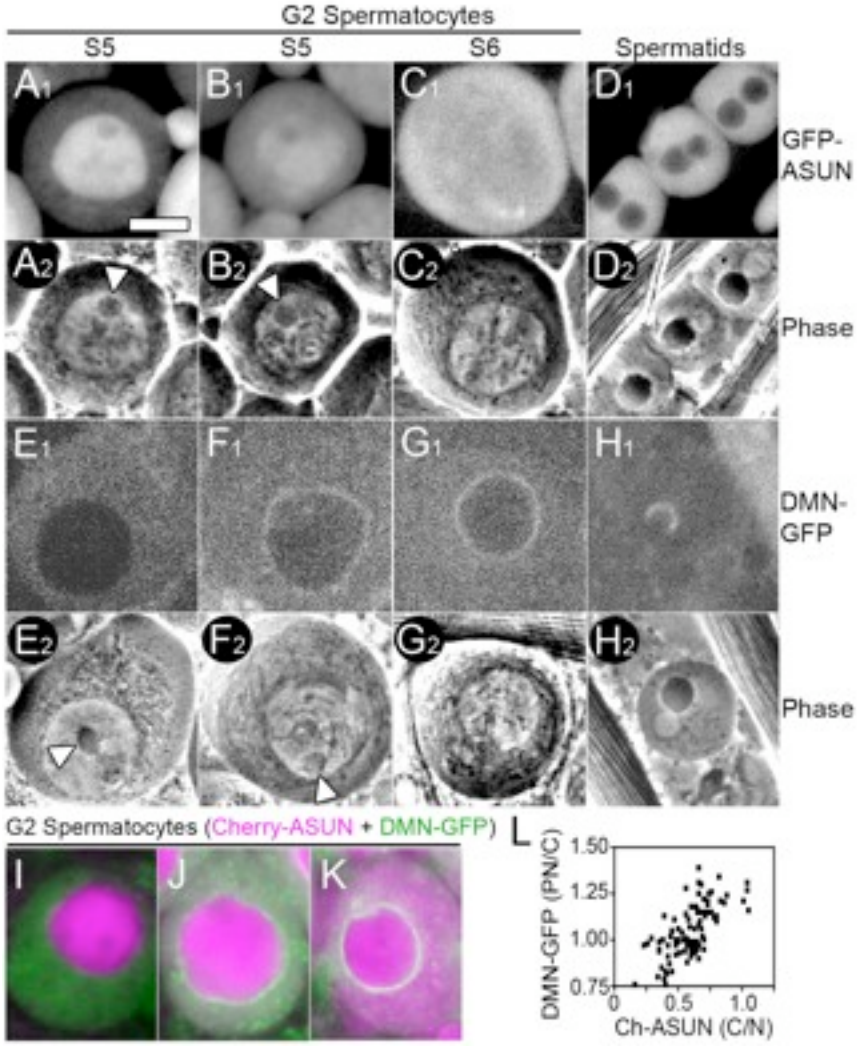

Figure 2.14. Coincident localization changes of ASUN and dynactin in primary spermatocytes. (A-D) Matched fluorescent (A1-D1) and phase-contrast (A2-D2) images of representative G2 spermatocytes (A-C) and onion-stage spermatids (D) expressing GFP-ASUN. (A,B) In S5 spermatocytes, GFP-ASUN is largely nuclear (A) or in both nucleus and cytoplasm (B). Arrowheads mark intact nucleoli characteristic of this stage. (C) S6 spermatocyte with uniformly distributed GFP-ASUN. (D) GFP-ASUN is excluded from spermatid nuclei. (E-H) Matched fluorescent (E1-H1) and phase-contrast (E2-H2) images of G2 spermatocytes (E-G) and onion-stage spermatids (H) expressing DMN-GFP. (E,F) S5 spermatocytes with DMN-GFP uniformly distributed in cytoplasm (E) or at nuclear surface (F). Arrowheads mark intact nucleoli characteristic of this stage. (G) S6 spermatocyte in which DMN-GFP has accumulated at the nuclear periphery. (H) DMN-GFP is localized to a hemispherical cap on the nucleus of spermatids. (I-K) Fluorescent images of representative G2 spermatocytes co-expressing Cherry-ASUN (magenta) and DMN-GFP (green). (I) Evenly distributed cytoplasmic DMN-GFP with minimal cytoplasmic Cherry-ASUN. (J) Low levels of perinuclear DMN-GFP with increased cytoplasmic Cherry-ASUN. (K) High levels of perinuclear DMN-GFP with

Figure 2.14 continued: Cherry-ASUN uniformly distributed between nucleus and cytoplasm. Bar, 10 μm. (L) Scatter plot displaying the relationship between release of Cherry-ASUN from the nucleus and accumulation of DMN-GFP at the nuclear periphery in late G2 primary spermatocytes. Each data point represents a single spermatocyte for which the ratio of the intensity of peripheral nuclear to cytoplasmic DMN-GFP signal is plotted against the ratio of the intensity of cytoplasmic to nuclear Cherry-ASUN signal.

Perinuclear localization of ASUN

To assess whether the localization of ASUN is conserved, we expressed fluorescently tagged *Drosophila* ASUN in cultured mammalian (HeLa) cells and examined its subcellular distribution. Similar to our observations in the *Drosophila* male germline, we found that GFP-ASUN localization in HeLa cells ranged from predominantly nuclear, partitioned between the nucleus and cytoplasm, to predominantly cytoplasmic (Figure 2.15, A-C). Strikingly, we found that GFP-tagged *Drosophila* ASUN localized to the perinuclear region in ~40% of transfected cells (Figure 2.15D). Essentially identical results were obtained using a Myc-tagged version of GCT1, the candidate human homolog of ASUN, underscoring the possibility that ASUN's functions are conserved in higher organisms (Figure 2.15, D-F; data not shown).

Dynein-dynactin has been reported to localize to the nuclear surface during the G2/prophase transition in cultured mammalian cells (Hebbar et al., 2008; Salina et al., 2002). Based on the perinuclear enrichment of both GFP-ASUN and Myc-GCT1 in transfected HeLa cells, we investigated the possibility that ASUN and dynein-dynactin may interact at the nuclear surface. In our hands, we detected only a weak perinuclear localization of dynein in HeLa cells at G2/prophase by immunofluorescence (data not shown). Treatment of cells with nocodazole, which destabilizes microtubules, has been shown to transiently enhance the perinuclear localization of dynein-dynactin in prophase cells (Hebbar et al., 2008). We therefore examined nocodazole-treated HeLa cells expressing GFP-ASUN to assess whether dynein and GFP-ASUN co-localize on the nuclear surface at the G2/prophase transition. We found that GFP-ASUN localized to the nuclear surface in >80% of prophase cells (Figure 2.15G). Furthermore, we found that

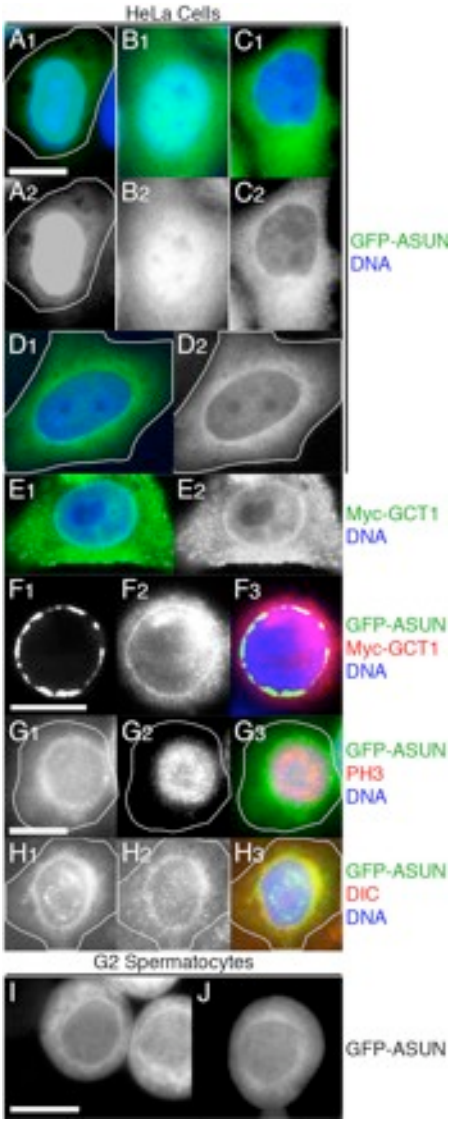

Figure 2.15. Perinuclear localization of ASUN. (A-H) Fluorescence microscopy of transfected HeLa cells. DNA is in blue. (A-D) Localization of GFP-ASUN (green in A1-D1; grayscale in A2-D2) ranges from predominantly nuclear (A), distributed between the nucleus and cytoplasm (B), and predominantly cytoplasmic (C) with perinuclear enrichment (D) frequently observed. (E) Perinuclear enrichment of Myc-GCT1, the human homolog of ASUN (green in E1; grayscale in E2). (F) Co-localization of GFP-ASUN (F1, green in merge) and Myc-GCT1 (F2, red in merge) at the nuclear surface (F3, merge). (G,H) Nocodazole-treated cells expressing GFP-ASUN. (G) In prophase cells identified by phospho-histone H3 staining (G2, red in merge), GFP-ASUN (G1, green in merge) displayed a perinuclear localization (G3, merge). (H) Co-localization of GFP-ASUN (H1, green in merge) and dynein intermediate chain (H2, red in merge) in cells exhibiting perinuclear dynein localization (H3, merge). (I-J) Perinuclear localization of GFP-ASUN is occasionally observed in late G2 spermatocytes of a *Drosophila* transgenic line with relatively low expression. Bars, 10 μm.

dynein tightly co-localized with GFP-ASUN at the nuclear surface in ~90% of cells displaying perinuclear dynein (Figure 2.15H). These observations suggest that ASUN and dynein-dynactin may functionally interact at the nuclear surface during the G2/prophase transition.

Given our observations of ASUN/GCT1 localization in HeLa cells, we carefully reassessed the localization pattern of GFP-ASUN in transgenic spermatocytes. Using a second transgenic line with relatively low expression of GFP-ASUN, we occasionally detected perinuclear enrichment of GFP-ASUN in G2 primary spermatocytes (Figure 2.15, P and Q; data not shown). The low frequency at which we detected this perinuclear pool of GFP-ASUN may suggest either that it is transient and/or that it is masked by transgenic overexpression. Taken together with our HeLa cell data, these observations are consistent with a model in which perinuclear ASUN recruits and/or retains dynein-dynactin at the nuclear surface of G2 spermatocytes, thereby mediating nucleus-centrosome coupling at M-phase entry that helps to ensure fidelity of the meiotic divisions.

ASUN contains a nuclear localization sequence

Given the appearance of ASUN in the nucleus of early G2 spermatocytes, we questioned whether sequences within ASUN were responsible for promoting its nuclear localization. Our database searches revealed a putative nuclear localization sequence at the C-terminal region of ASUN (Figure 2.16) (Cokol et al., 2000). To determine if this sequence was required for the nuclear localization of ASUN, we generated a recombinant form of ASUN in which three of the positively charged residues were converted to

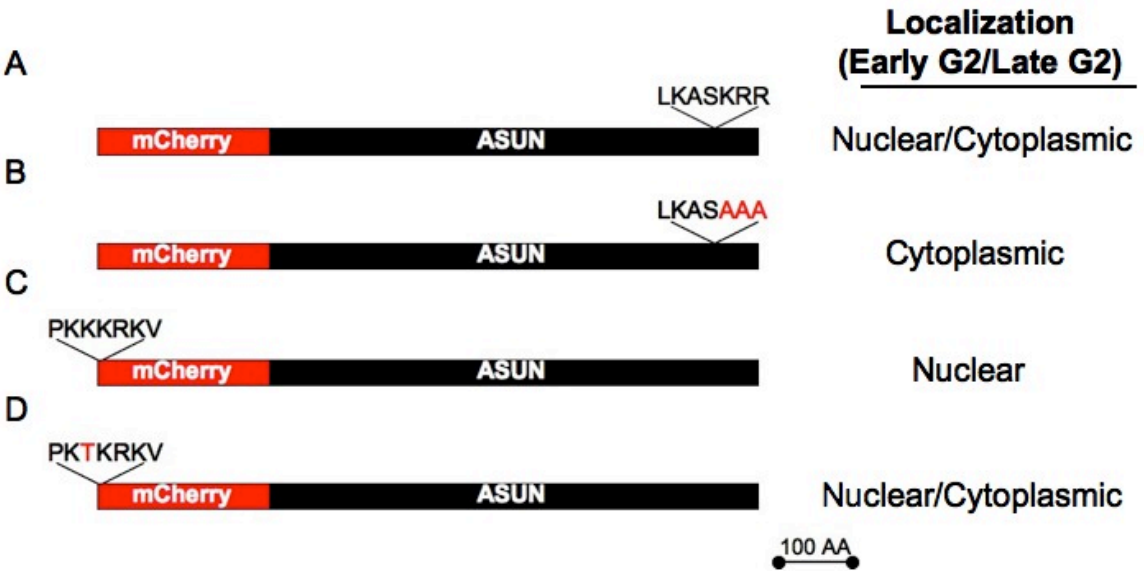

Figure 2.16. Generation of cytoplasmic and nuclear forms of ASUN. Schematic diagram of mCherry-ASUN fusion proteins expressed in the male germline. (A) ASUN possesses a predicted nuclear localization sequence within its C-terminal region and displays nuclear (early) and nuclear/cytoplasmic (late) localizations in G2 spermatocytes. (B) Inactivation of this nuclear localization sequence (through mutation of the last three positively charged residues to alanines) inhibits the nuclear localization of ASUN. (C) A strictly nuclear form of ASUN was generated by addition of a strong nuclear localization sequence from the SV40 T-antigen to the N-terminal region of the Cherry tag (Kalderon et al., 1984). (D) Inactivation of this strong nuclear localization sequence restores the cytoplasmic localization of recombinant ASUN in late G2 spermatocytes.

alanines (Figure 2.16B). We generated transgenic lines that express this mutant form of ASUN in the male germline. We found that this form of ASUN was restricted to the cytoplasm of primary spermatocytes throughout G2 (data not shown), thus demonstrating that the putative nuclear localization sequence identified in our database search was, indeed, required for ASUN's nuclear localization.

Discussion

Here we report that *asun* is a critical regulator of spermatogenesis in *Drosophila*. We have shown that primary spermatocytes lacking *asun* exhibit failure of nucleus-centrosome coupling, which normally occurs upon M-phase entry, with subsequent defects in spindle assembly and chromosome segregation. The normal attachment between the nucleus and another centriole-based structure, the basal body, is similarly lost in *asun* postmeiotic spermatids. Furthermore, we have shown that dynein-dynactin complexes, which mediate nucleus-centrosome/basal body interactions, fail to localize to the nuclear surface in both *asun* spermatocytes and spermatids (Gonczy et al., 1999; Malone et al., 2003; Robinson et al., 1999; Salina et al., 2002).

We propose the following model to describe the role of ASUN in promoting nucleus-centrosome coupling during male meiosis. In early G2 spermatocytes, ASUN is largely sequestered in the nucleus, and dynein-dynactin localizes diffusely throughout the cytoplasm. In late G2, a pool of ASUN is released from the nucleus into the cytoplasm where it promotes accumulation of dynein-dynactin at the nuclear periphery. Perinuclear dynein-dynactin captures astral microtubules emanating from cortical centrosomes. Due to the minus-end-directed motor activity of dynein, interaction between astral

microtubules and anchored dynein-dynactin results in movement of centrosomes toward the nucleus; stable linkage between the nucleus and centrosomes, a prerequisite for fidelity of meiotic divisions, is then established.

Dynein-dynactin-mediated interactions between centrosomes and the nucleus have been shown to be important in a variety of biological processes, including nuclear positioning, nuclear migration, and nuclear envelope breakdown (Morris, 2000; Reinsch and Gonczy, 1998; Salina et al., 2002). Although it is generally assumed that dynein-dynactin on the nuclear envelope interacts with centrosomes via astral microtubules that they nucleate, the mechanism by which dynein-dynactin is anchored to the nucleus remains unclear. The *C. elegans* Hook protein ZYG-12, which localizes to the nuclear periphery, tethers dynein to this site in embryos; a similar role for Hook proteins in other species, however, has not been reported (Gonczy, 2004; Malone et al., 2003). Nuclear pore complexes have been proposed as likely candidates for sites of dynein-dynactin attachment as they are unique to the nuclear envelope and span both outer and inner nuclear membranes (Salina et al., 2002). In support of this model, dynein-dynactin has been found to physically interact with nuclear pore complex components in bovine zygotes and oocytes (Payne et al., 2003).

Dynein-dynactin accumulation at the nuclear envelope occurs in late G2 in dividing mammalian cells; we have observed a similar pattern of timing during *Drosophila* male meiosis (Salina et al., 2002). The mechanisms underlying this cell cycle-dependent localization of dynein-dynactin remain to be determined. The coincident timing of ASUN's release to the cytoplasm and accumulation of dynein-dynactin on the

nucleus, however, raises the intriguing possibility that ASUN plays a key role in mediating this event.

We have observed a striking perinuclear localization of fluorescently tagged versions of *Drosophila* ASUN and its candidate human homolog, GCT1, in transfected HeLa cells at the G2/prophase transition that significantly overlaps with that of dynein intermediate chain. Similarly, we have occasionally observed weak perinuclear enrichment of fluorescently tagged ASUN in G2 spermatocytes of transgenic flies. Based on these findings, we propose that this perinuclear pool of ASUN directly promotes dynein-dynactin recruitment and/or retention at the nuclear surface, a prerequisite for nucleus-centrosome coupling. In contrast, dynein-dynactin localization to kinetochores and the Nebenkern appears to be independent of ASUN, suggesting that ASUN mediates localization of a subset of cellular pools of dynein-dynactin. We have been unable to detect physical interactions between ASUN and dynein-dynactin (our unpublished observations). Dynein-dynactin localization and its interactions with molecular cargos depends on several factors, including the presence of adaptors and phosphorylation state of its subunits, thus providing many levels at which it may be regulated by ASUN (Farshori and Holzbaur, 1997; Tai et al., 2001).

In addition to defects in nucleus-centrosome coupling in *asun* spermatocytes, the centriole-derived basal bodies fail to form stable attachments to the nuclei of *asun* spermatids. Functional basal bodies, which organize the sperm axoneme, appear to be required for positioning of nuclei within sperm bundles and nuclear shaping during spermatid elongation (Texada et al., 2008; Vogt et al., 2006). Dynein-dynactin localizes to a hemispherical cap on the nuclei of onion-stage spermatids, and the site of nucleus-

basal body attachment lies in the middle of this region ((Li et al., 2004) and this report). Furthermore, spermatids of males lacking *tctex-1*, which encodes a dynein light chain, exhibit defects in nucleus-basal body coupling similar to what we observe in *asun* males (Li et al., 2004). We propose that disruption of nucleus-basal body interactions in *asun* spermatids is due to loss of perinuclear dynein-dynactin.

Our database searches have revealed putative *asun* homologs in organisms ranging from *C. elegans* to humans. The human gene, *GCT1*, resides in a chromosomal region (12p11-p12) that is both amplified and overexpressed in testicular seminomas (Bourdon *et al.*, 2002; Rodriguez *et al.*, 2003). In contrast to the germline-specific expression of *asun* in *Drosophila*, *GCT1* is broadly expressed in human tissues, suggesting that it may have functions in somatic cells (Bourdon et al., 2002). We previously showed that downregulation of *GCT1* in HeLa cells resulted in a multinucleated phenotype (Lee et al., 2005). Further experiments will be needed to determine if human *GCT1* coordinates mitosis by regulating dynein-dynactin localization.

Future Directions

What is the consequence of ASUN's subcellular localization?

We have shown that ASUN is restricted to the nucleus of early G2 primary spermatocytes, suggesting that ASUN is actively sequestered in the nucleus before entry into late G2/prophase. In support of this, we have recently identified a putative nuclear localization sequence in the C-terminal region of ASUN based on sequence homology (Cokol et al., 2000). The importance of ASUN's nuclear localization, however, is

unclear. The enrichment of dynein-dynactin at the nuclear surface of primary spermatocytes tightly coincides with the cytoplasmic accumulation of ASUN at the end of the G2 growth phase, suggesting that cytoplasmic ASUN directly stimulates dynein-dynactin's recruitment to the nuclear surface. The nuclear partitioning and release of ASUN during the meiotic cycle may therefore represent a mechanism of control over ASUN's cytoplasmic activities. Alternatively, ASUN may serve dual roles in the nucleus and the cytoplasm.

To investigate these possibilities, we have generated transgenic forms of fluorescently tagged ASUN that are restricted to either the cytoplasm or the nucleus during male meiosis (Figure 2.16, B and C; data not shown). We are currently working toward expressing these forms of ASUN in an $asun^{null}$ background (described in Chapter IV). By evaluating the ability of these forms of ASUN to influence dynein's localization and to rescue the $asun^{null}$ phenotype, we hope to gain insight into ASUN's role in perinuclear recruitment of cytoplasmic dynein and to establish whether ASUN serves an essential role in the nucleus.

Is *asun's* role conserved?

We have shown that *Drosophila* ASUN colocalizes with its human homolog, GCT1, when coexpressed in cultured human (HeLa) cells. Furthermore, we have demonstrated that ASUN localizes with dynein at the nuclear surface in nocodazole-treated HeLa cells. These results suggest that ASUN's functions are likely conserved in vertebrates. While the expression of *asun* in *Drosophila* is restricted to the testis and ovary, *GCT1* is widely expressed in human tissues (Bourdon et al., 2002). This raises the

intriguing possibility that GCT1 may serve as a regulator of dynein-dynactin in mitotically dividing cells. We are currently utilizing an RNAi-based approach to examine the role of GCT1 in the regulation of dynein-dynactin in cultured cell systems.

How does ASUN interact with dynein-dynactin?

While we have found that ASUN colocalizes with dynein-dynactin at the nuclear surface of HeLa cells, we have been unable to detect a direct interaction between ASUN and dynein-dynactin through our immunoprecipitation experiments. While this may suggest that interactions between ASUN and dynein-dynactin are transient, it is also possible that ASUN may act on intermediary components of the dynein-dynactin pathway. Current efforts are underway to identify proteins that physically interact with ASUN through a yeast two-hybrid assay. The identification of these proteins should serve to aid in our elucidation of ASUN's mechanism.

CHAPTER III

Lis-1 AND *asunder* COOPERATIVELY REGULATE DYNEIN-DYNACTIN FUNCTION DURING DROSOPHILA SPERMATOGENESIS

Introduction

Nuclear positioning and migration are essential for a number of cell cycle and developmental processes. For example, in yeast, migration of the nucleus to the bud neck ensures equal partitioning of chromatin to daughter cells during mitosis (Bloom, 2001). During *Drosophila* oogenesis, nuclear migration is required to establish polarity in the developing oocyte (Gonzalez-Reyes et al., 1995; Roth et al., 1995). In zebrafish neuroepithelial progenitor cells, the position of the nucleus during mitosis influences daughter cell fates (Baye and Link, 2007; Del Bene et al., 2008). During vertebrate brain development, nuclear movements are critical for neuronal migration (Hatten, 2002).

Nuclear positioning and migration are dependent on interactions between the nucleus and cytoskeletal elements, and often involves the coupling of the nucleus to microtubule organizing centers via microtubules (Reinsch and Gonczy, 1998; Tsai and Gleeson, 2005). These interactions are dependent on the function of the microtubule motor protein dynein. Dynein's function in nuclear migration and positioning is, in turn, dependent on the presence of its regulatory factor Lis-1 (Geiser et al., 1997; Lei and Warrior, 2000; Liu et al., 1999; Swan et al., 1999; Willins et al., 1997; Xiang et al., 1995).

Lis-1 is also essential for dynein's cell cycle functions. In *Drosophila* neuroblasts, disruption of *Lis-1* during mitosis results in defects in centrosome migration, bipolar

spindle assembly, attachment of the centrosomes to the spindle, and spindle checkpoint function, all presumably due to a loss of dynein activity (Siller and Doe, 2008; Siller et al., 2005). Lis-1 directly binds dynein and dynactin components involved in the regulation of dynein's cargo binding and motor activity; however, the mechanism by which Lis-1 regulates dynein's function remains unclear (Faulkner et al., 2000; Mesngon et al., 2006; Sasaki et al., 2000; Smith et al., 2000; Tai et al., 2002).

To gain insight into Lis-1's *in vivo* functions, we analyzed the role of *Lis-1* during *Drosophila* spermatogenesis using a male sterile allele of *Lis-1*. In addition, we examined Lis-1's subcellular localization within spermatocytes and spermatids of the *Drosophila* testis. We found that *Lis-1* spermatocytes display defects in nucleus-centrosome coupling at meiotic prophase, and that nucleus-basal body coupling is similarly disrupted in postmeiotic spermatids of *Lis-1* testes. In addition, we found that Lis-1 localizes with dynein at the nuclear surface, spindle poles, and kinetochores of dividing spermatocytes. We report here that *Lis-1* is required for the recruitment of dynein to these sites, and present evidence that *Lis-1* may cooperate with *asunder* (*asun*) in the regulation of *Drosophila* spermatogenesis.

Methods and Materials

Drosophila stocks

y w was used as the "wild-type" stock. *Lis-1*^{K11702} and *Df(2R)JP5* flies were obtained from Bloomington Stock Center. The *PACT-GFP* flies were a gift from Jordan Raff. *β-tubulin-GFP* flies were a gift from H. Oda and Y. Akiyama-Oda. The *Dmn-GFP*

stock has been previously described (Wojcik et al., 2001). *piggyBac* insertion line *f02815* was from the Exelixis Collection (Harvard Medical School). *asun*^{null} flies are described in Chapter IV.

DNA clones and transgenics

cDNA clone LD11219 encoding Lis-1 was from the *Drosophila* Gene Collection. For male germline expression of fluorescently tagged Lis-1, cDNA encoding Lis-1 with an N-terminal Cherry tag was subcloned into testis expression vector tv3 (gift from J. Brill) (Wong et al., 2005). Transgenic lines were generated by *P*-element-mediated transformation via embryo injection (Rubin and Spradling, 1982)

Cytological analysis of live and fixed testes

Live testes cells were prepared for examination by phase contrast or fluorescent microscopy as described (Kemphues et al., 1980). Formaldehyde fixation was performed as described (Gunsalus et al., 1995). Actin individualization cones were stained with Alexa Fluor 594 phalloidin (1:100, Invitrogen). Primary antibodies were used as follows: mouse anti-γTubulin (GTU-88, 1:100, Sigma) and rabbit anti-D-PLP (1:250, gift from Jordan Raff). Cy2- and Cy3-conjugated secondary antibodies were used at 1:800. Fixed samples were mounted in phosphate-buffered saline with DAPI (0.2 μg/ml) to visualize DNA.

Fluorescent images were obtained using one of two microscopes: Nikon Eclipse 80i with Plan-Apo 60x and Plan-Fluor 40x objectives or Zeiss Axiophot with Neo-Fluor Ph2 40x objective. Bright field images of whole testes were obtained using a Zeiss Stemi

2000-CS stereoscope. Phase contrast images were captured using Zeiss Axiophot with Neo-Fluor Ph2 40x objective.

Results

Lis-1 is required for male fertility

In the female germline of *Drosophila*, *Lis-1* has been found to play multiple roles, including germ cell division, oocyte differentiation, and nuclear migration, presumably through interactions with dynein-dynactin (Lei and Warrior, 2000; Liu et al., 1999). To analyze the role of *Lis-1* in *Drosophila* spermatogenesis, we obtained a reported male sterile allele of *Lis-1*, *Lis-1*^{k11702}, hereafter referred to as simply as "*Lis-1*" (Lei and Warrior, 2000). We began our characterization of the male *Lis-1* phenotype by reassessing the fertility of *Lis-1* males. In our fecundity tests, we found that all males tested (25/25) failed to produce a single progeny. Identical results were obtained when we placed *Lis-1* over a deficiency that uncovers the *Lis-1* gene region, suggesting that infertility of *Lis-1* males is in fact due to disruption of *Lis-1*.

To determine if *Lis-1* males are capable of producing functional sperm, we examined the seminal vesicles of *Lis-1* males for the presence of sperm. We found that although the size and shape of *Lis-1* testes appeared normal, their seminal vesicles were empty (Figure 3.1), strongly suggesting that infertility of *Lis-1* males results from a disruption in spermatogenesis. In order to determine the developmental stage at which spermatogenesis is disrupted in *Lis-1* males, we examined the different populations of

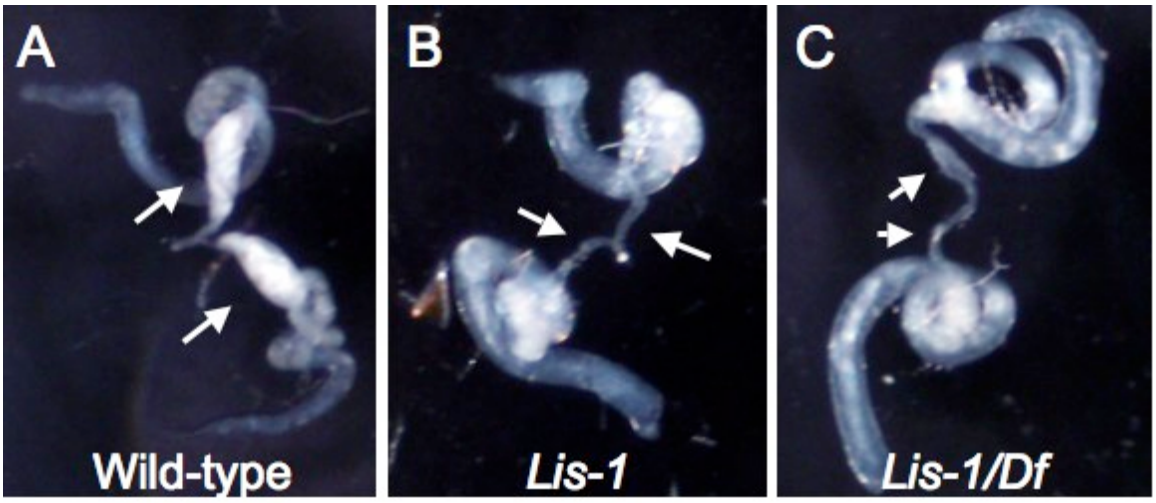

Figure 3.1. *Lis-1* males are sterile. (A-C) Testes of males separated from females for six days. Arrows, seminal vesicles. (A) Wild-type seminal vesicles are filled with mature sperm. Seminal vesicles of *Lis-1* (B) and *Lis-1/Df* (C) males are empty, indicating an absence of mature sperm.

sperm precursor cells within *Lis-1* testes for abnormalities. Our initial characterization revealed that spermatocyte and spermatid cysts contained the appropriate number of cells (16 and 64 respectively; data not shown), suggesting normal progression through mitosis and meiosis. When we examined the centrosomes and spindles of the meiotic primary spermatocytes, however, we observed profound defects in centrosome migration and spindle assembly.

Defective centrosome migration and attachment to meiotic spindles of *Lis-1* spermatocytes

In wild-type primary spermatocytes, centrosomes undergo migration to the cell cortex during the G2 growth phase. At the G2/prophase transition, the centrosomes at the cortex nucleate astral microtubules and travel back to the nucleus (Figure 3.2A). Once stably reattached to the nuclear surface, the asters (centrosomes with astral microtubules) migrate to opposite poles and direct formation of the meiotic spindles (Figure 3.2B). In *Lis-1* spermatocytes however, we observed that the centrosomes failed to break their associations with the cell cortex, and instead formed prominent asters at the cell periphery in approximately 95% of the cells (Figure 3.2E). These asters were still observed to migrate to opposite poles of the cells at prophase (Figure 3.2E). Although the asters of *Lis-1* spermatocytes were found to remain at the cell cortex throughout meiosis, we found that *Lis-1* spermatocytes still formed meiotic spindles during prometaphase/metaphase (Figure 3.2, F and G). The meiotic spindles of *Lis-1* spermatocytes, however, were often observed to be long and wavy compared to those of wild-type spermatocytes (Compare Figures 3.2, F and B). In addition, the centrosomes

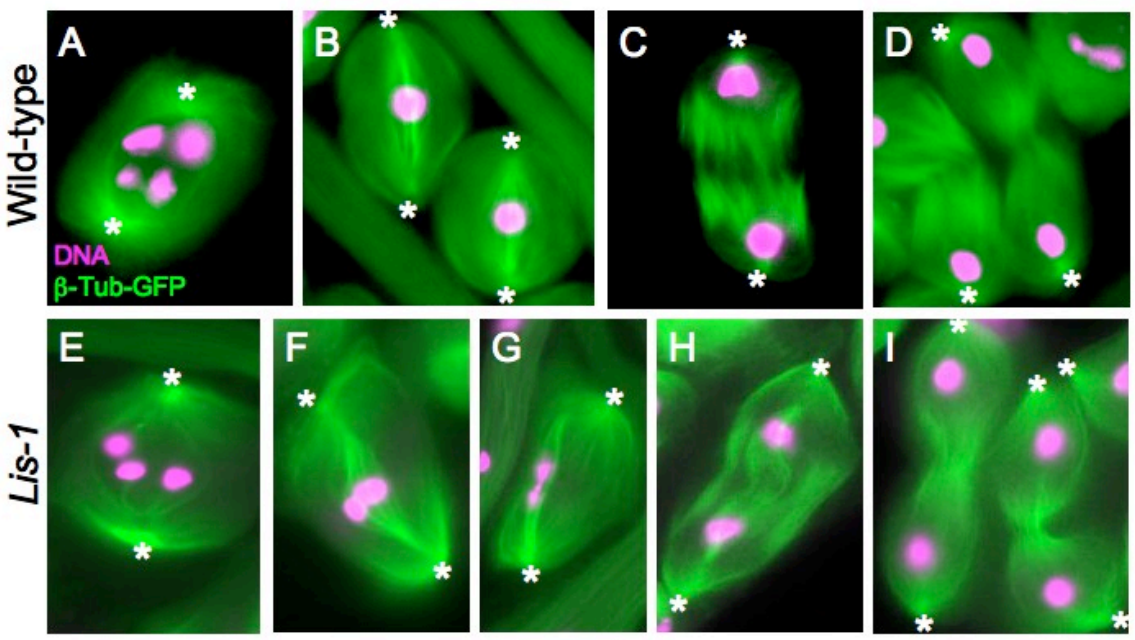

Figure 3.2. Defective centrosome migration and attachment to meiotic spindles in *Lis-1* spermatocytes. (A-I) Meiotic primary spermatocytes from wild-type (A-D) or *Lis-1* (E-I) males expressing β-Tubulin-GFP (green), stained for DNA (magenta). Centrosomes (asterisks) of wild-type spermatocytes migrate to the nucleus at entry into prophase (A). Wild-type centrosomes are tightly coupled to the meiotic spindle at metaphase (B), and are associated with both the spindle poles and chromatin masses at late anaphase (C) and telophase (D). Centrosomes of Lis-1 spermatocytes fail to migrate to the nuclear surface at prophase (E), and remain at the cortex throughout meiosis I (E-I). Spindles of *Lis-1* spermatocytes often appear long and wavy (F), and the centrosomes are frequently found uncoupled from the spindle (G). At anaphase (H) and telophase (I), centrosomes of *Lis-1* spermatocytes are only loosely associated with the spindle poles and chromatin masses.

were frequently detached from the spindle (Figure 3.2G). At anaphase and telophase, the centrosomes, if attached, appeared to be positioned at an increased distance from the chromatin masses (Figure 3.2, H and I), suggesting that the centrosomes of *Lis-1* spermatocytes are only loosely associated with the meiotic spindle.

In addition to the observed defects in spindle assembly in *Lis-1* spermatocytes, we noticed a sharp increase in the percentage of dividing cells at prometaphase of meiosis I (data not shown) suggesting that *Lis-1* spermatocytes undergo a transient delay at this stage. Despite the defects that we observed in centrosome migration and spindle assembly, cytokinesis of *Lis-1* spermatocytes appeared to progress normally, as multinucleated spermatids were not observed.

Lis-1 spermatids exhibit defects in attachments between the nucleus, Nebenkern, and basal body

Although cytokinesis appears to proceed normally in *Lis-1* spermatocytes, we found that the early, round postmeiotic spermatids possessed an abnormal morphology. Round spermatids of wild-type testes possess a highly characteristic appearance when viewed through phase-contrast optics in that they contain a light nucleus associated with a dark mitochondrial aggregate, known as the Nebenkern, which is of roughly the same size. In wild-type spermatids, the association between the nucleus and Nebenkern appeared fairly robust, as they were found tightly linked in approximately 84% of the cells (Figure 3.3, A and D). In *Lis-1* spermatids, however, we found that the nuclei and Nebenkern were dissociated in more than 70% of the cells (Figure 3.3, B, E and F).

Both the nucleus and Nebenkern of round spermatids are associated with the centriole-derived basal body, which embeds in the nucleus at the site of nucleus-

Nebenkern linkage (Figure 3.3D) (Fuller, 1993). Based on the observed loss of nucleus-centrosome coupling in *Lis-1* meiotic spermatocytes, we questioned whether the dissociation of the nucleus from the Nebenkern in *Lis-1* spermatids stemmed from a disruption in nucleus-basal body coupling. To examine this possibility, we examined the position of the basal body within living spermatids expressing fluorescently tagged Pericentrin/AKAP450 centrosomal targeting (PACT) domain, which labels the basal bodies (Martinez-Campos et al., 2004). We found that indeed, nucleus-basal body coupling was disrupted in more that 90% of *Lis-1* spermatids (Figure 3.3, E and F). Furthermore, we found that Nebenkern-basal body coupling was similarly disrupted in approximately 40% of *Lis-1* spermatids (Figure 3.3F). These results suggest that *Lis-1* is required to maintain linkage of the basal body with both the nucleus and the Nebenkern.

While examining the linkage between the basal body, nucleus, and Nebenkern of the early round spermatids, we observed that the morphology of the Nebenkern in *Lis-1* spermatids was often abnormal. When viewed through phase contrast optics, the Nebenkern of wild-type spermatids appeared round and uniform in shape (Figure 3.3A). In *Lis-1* spermatids, however, we found that the Nebenkern frequently exhibited blebbing (Figure 3.3B). In addition, we occasionally observed spermatids from *Lis-1* males to contain multiple, irregularly sized Nebenken (Figure 3.3C). Thus, *Lis-1* appears to be required for the proper morphogenesis of the Nebenkern.

During spermatid elongation in wild-type testes, the Nebenkern elongates down the length of the axoneme. The Nebenkern will eventually serve to provide energy that

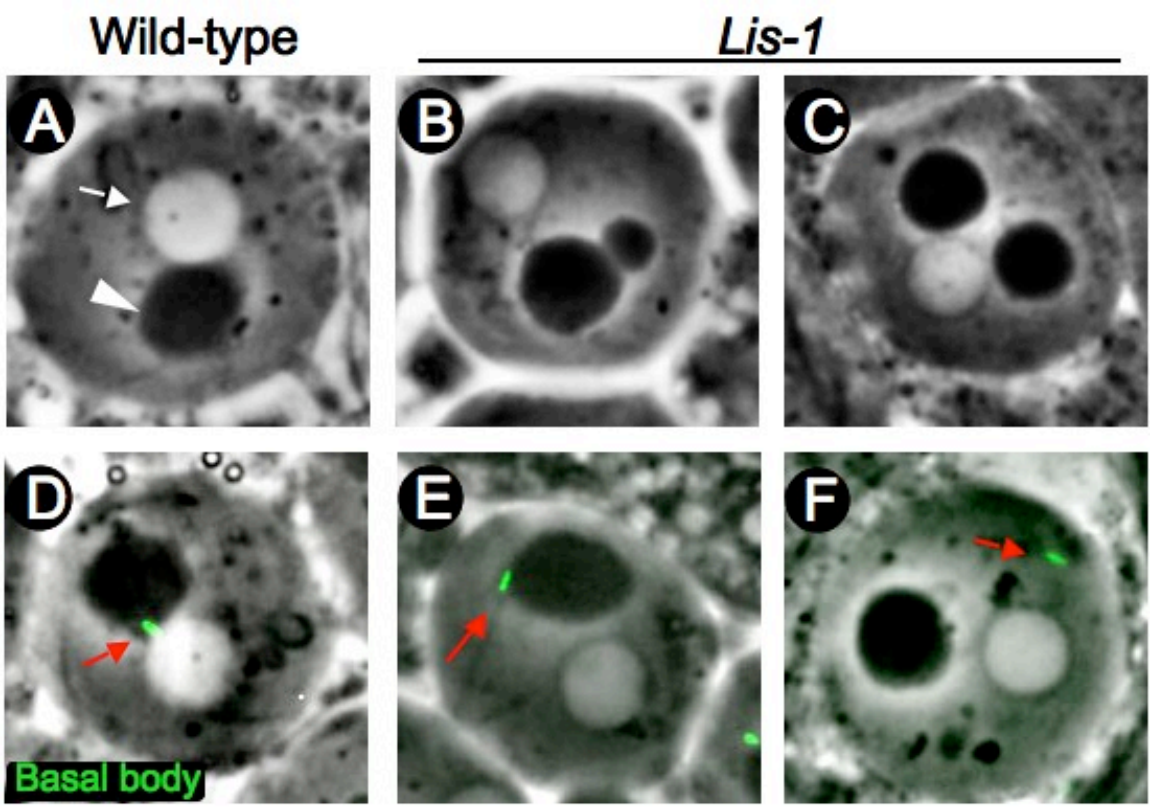

Figure 3.3. Aberrant Nebenkern formation and disruption of nucleus-basal body-Nebenkern coupling in *Lis-1* round spermatids. (A-C) Phase-contrast micrographs of wild-type (A) or *Lis-1* (B and C) round spermatids. In wild-type spermatids (A), the phase-dark Nebenkern (arrowhead) is uniformly round in shape, and closely associated with the phase-light nucleus (arrow). Nebenkerne of *Lis-1* spermatids frequently appear blebbed (B). In addition, *Lis-1* spermatids occasionally possess multiple Nebenkerne (C). (D-F) Merged phase-contrast and fluorescent micrographs of wild-type (D) and *Lis-1* (E and F) round spermatids expressing PACT-GFP to label basal bodies (green, red arrows). Basal bodies of wild-type spermatids (D) are found tightly associated with both the nucleus and the Nebenkern at the junction between these two structures (D). Basal bodies of *Lis-1* spermatids (E and F) are rarely associated with the nucleus; although most maintain attachments with the Nebenkern (E), ~40% of basal bodies lose this association and may be connected instead with the cell cortex (F).

powers the beating of the flagella in mature sperm. Because the axoneme nucleates from the basal body, we set out to determine how changes in Nebenkern and basal body linkage may affect the association of the Nebenkern with the sperm axoneme in *Lis-1* spermatids. Using a combination of fluorescent and phase contrast microscopy, we examined the association of the Nebenkern with the sperm axoneme (labeled with β–Tubulin-GFP) in early elongating spermatids (Inoue et al., 2004; Anderson et al., 2009). We found that the Nebenkern properly associated with the axoneme in early elongating *Lis-1* spermatids (Figure 3.4), suggesting that Nebenkern-basal body coupling is not essential for this process.

Lis-1 is required for late stages of spermatogenesis

Postmeiotic spermatids must undergo elongation and individualization to form functional sperm. During these processes in wild-type individuals, the nuclei and associated basal bodies are uniformly positioned at the proximal tips of growing sperm bundles (Figure 3.5A). As the spermatids elongate, the shape of the nuclei changes from round to needle like (Figure 3.5A). During individualization, actin investment cones travel the length of the axoneme as a cohesive unit (Figure 3.5C), pushing out excess cytoplasm and resolving the cytoplasmic bridges that connect individual spermatids formed within a common cyst. In *Lis-1* males, however, we found that while the basal bodies often appeared to be loosely situated at the proximal tip of elongating bundles (data not shown), the nuclei were randomly oriented along the lengths of the bundles and remained round (Figure 3.5B). In addition, we found that the actin investment cones were likewise randomly distributed down the length of *Lis-1* spermatid bundles (Figure

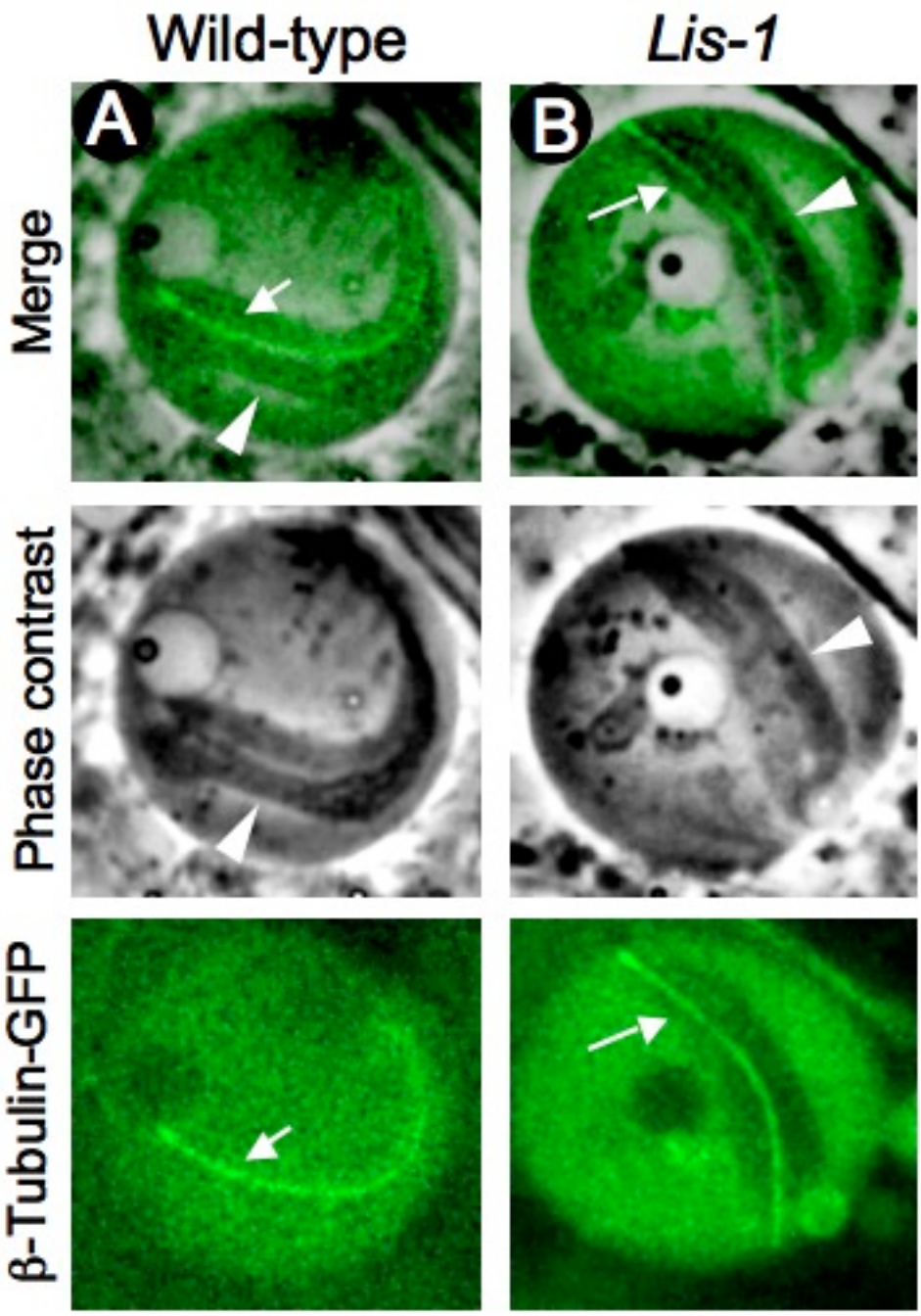

Figure 3.4. Nebenkern-axoneme associations in *Lis-1* spermatids. (A and B) Merged phase-contrast and fluorescent micrographs of wild-type (A) and *Lis-1* (B) early elongating spermatids. Matched phase-contrast and fluorescent micrographs are shown below merged images. During elongation in wild-type spermatids (A), the phase-dark Nebenkern (arrowhead) spreads down the developing sperm axoneme (green, arrow). The Nebenkerne of *Lis-1* spermatids (B) are also observed to spread down the sperm axonemes during elongation, despite frequent dissociation from the basal body.

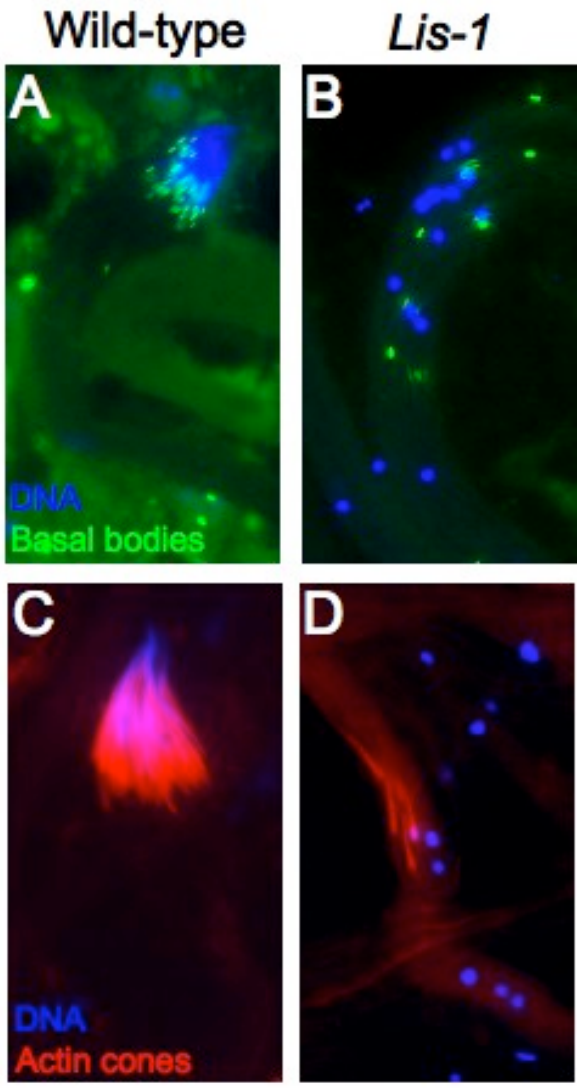

Figure 3.5. Disrupted nuclear positioning and individualization in *Lis-1* spermatids. (A and B) Elongating spermatids of wild-type (A) and *Lis-1* (B) testes expressing PACT-GFP to label basal bodies (green), stained for DNA to label nuclei (blue). (A) Nuclei of wild-type spermatids remain tightly positioned with their associated basal bodies at the proximal tip of elongating sperm bundles and change their morphology from round to needle shaped. (B) Nuclei of *Lis-1* spermatids fail to associate with the basal bodies and are found randomly distributed along the lengths of elongating sperm bundles. In addition, the nuclei of *Lis-1* spermatids remain round. (C and D) Developing spermatids of wild-type (C) and *Lis-1* (D) testes stained for actin (red) and DNA (blue) to label actin investment cones and nuclei. During individualization in wild-type testes (C), actin investment cones travel the length of the spermatid bundle as a cohesive unit. In *Lis-1* spermatids (D), the actin cones are found dispersed along the length of the sperm bundles.

3.5D). These results demonstrate that *Lis-1* is required for maintaining the position of spermatid nuclei within growing sperm bundles. The random distribution of the investment cones observed in elongating *Lis-1* spermatid bundles may reflect the loss of nuclear positioning within *Lis-1* spermatids, as investment cones are thought to originate at the nuclear surface (Texada et al., 2008).

Localization of Lis-1 during *Drosophila* spermatogenesis

Our results suggested roles for *Lis-1* in centrosome migration, spindle assembly, nucleus-basal body coupling, Nebenkern morphogenesis, and nuclear positioning. To gain insight into how *Lis-1* may be impacting these processes, we examined Lis-1's subcellular localization in spermatocytes and spermatids. We generated transgenic lines that express a fluorescently tagged form of Lis-1 under the control of the testes-specific *β2-Tubulin* promoter (Wong et al., 2005). Using these lines, we found that Lis-1 displays a dynamic localization in meiotic spermatocytes and postmeiotic spermatids similar to what has been reported in other systems (Cockell et al., 2004; Coquelle et al., 2002; Faulkner et al., 2000; Li et al., 2005; Tai et al., 2002). In early G2 primary spermatocytes, we observed a weak accumulation of Lis-1 at the cell cortex (data not shown). During late G2, immediately prior to entry into prophase, we observed an accumulation of Lis-1 at the nuclear surface (Figures 3.6A and 3.7A). During prophase, we found that Lis-1 localized to the attached asters (Figure 3.6B). In secondary spermatocytes, we found Lis-1 to be evenly distributed around the nuclear surface at prophase II (Figures 3.6D and 3.7B). At prometaphase, we observed an accumulation of Lis-1 at the spindle poles and kinetochores (Figure 3.6E and 3.7C). Lis-1 remained concentrated at the spindle poles

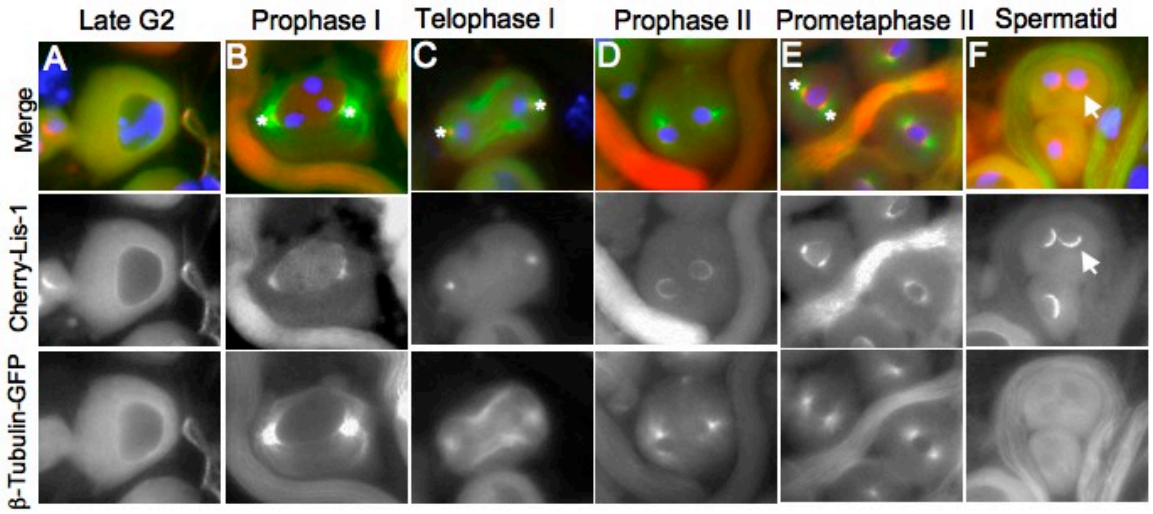

Figure 3.6. Lis-1 localization in primary spermatocytes and round spermatids. (A-F) Fluorescence microscopy of spermatocytes and spermatids co-expressing Cherry-Lis-1 (red) and β-Tubulin-GFP (green). DNA is in blue. Asterisks mark centrosomes/spindle poles. Matched fluorescent micrographs are shown in grayscale below merged images. Lis-1 localizes to the nuclear surface of late G2 spermatocytes (A). During prophase I, Lis-1 begins to accumulate at the attached centrosomes (B). At telophase I, Lis-1 is localized to the spindle poles (C). During prophase of meiosis II, Lis-1 is observed dispersed around the nuclear surface (D). At prometaphase II, Lis-1 is present at the nuclear surface and spindle poles (E). In round spermatids, Lis-1 localizes to a hemispherical cap (arrow) on the surface of the nucleus (F).

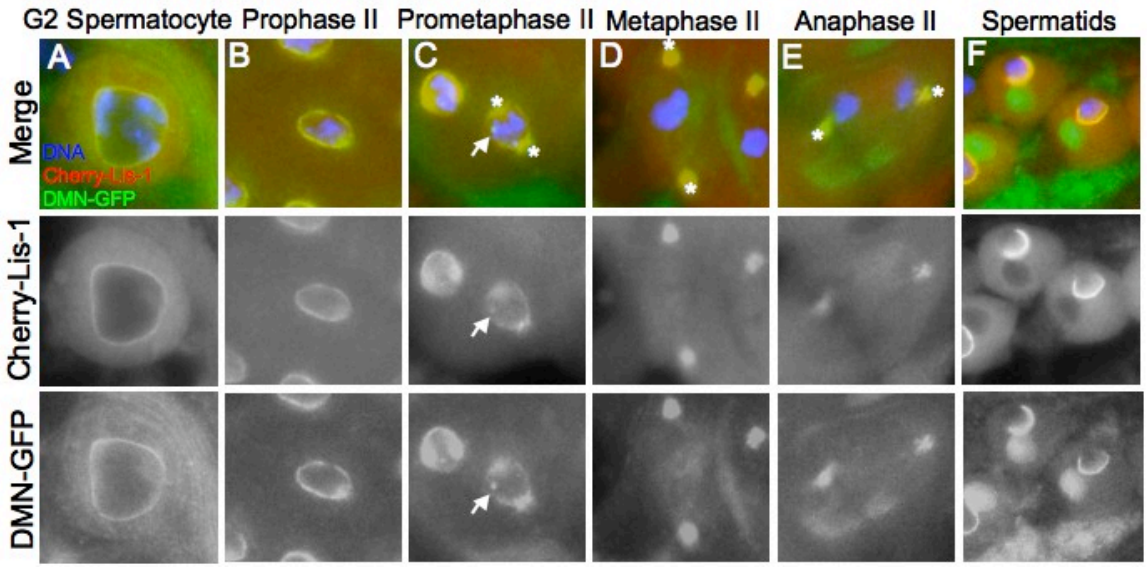

Figure 3.7. Lis-1 colocalizes with dynactin during *Drosophila* spermatogenesis. (A-F) Fluorescence microscopy of spermatocytes and spermatids co-expressing Cherry-Lis-1 (red) and DMN-GFP (green). DNA is in blue. Matched fluorescent micrographs are shown below merged images. (A) Cherry-Lis-1 colocalizes with DMN-GFP at the nuclear surface of late G2 primary spermatocytes. (B-E) During meiosis II, Cherry-Lis-1 and DMN-GFP colocalize at the nuclear surface of prophase spermatocytes (B), at the kinetochores (arrow) and spindle poles (asterisks) of prometaphase spermatocytes (C), and at the spindle poles of metaphase (D) and anaphase (E) spermatocytes. In postmeiotic spermatids (F), Cherry-Lis-1 and DMN-GFP colocalize at a hemispherical cap on the nuclear surface.

Through metaphase and anaphase II (Figure 3.7, D and E). In early postmeiotic spermatids, Lis-1 localized to a hemispherical cap on the nuclear surface (Figures 3.6F and 3.7F).

These localization patterns are strikingly similar to what we, and others, have previously reported for dynein-dynactin, suggesting that Lis-1 may colocalize with dynein-dynactin at these sites (Anderson et al., 2009; Li et al., 2004). To determine if this was in fact the case, we examined spermatocytes and spermatids expressing both Cherry-Lis-1 and a GFP-tagged version of Dynamitin (DMN), the p50 subunit of dynactin (McGrail and Hays, 1997; Wojcik et al., 2001). We found that Lis-1 tightly colocalized with dynein at the nuclear surface of spermatocytes and spermatids (Figure 3.7, A and F). Furthermore, in meiotic secondary spermatocytes, we found that Lis-1 colocalized with dynein at the nuclear surface, kinetochores, and spindle poles (Figure 3.7, B-E). These results are consistent with a tight association between Lis-1 and dynein-dynactin during *Drosophila* spermatogenesis, as has been reported in other systems.

Lis-1 **is required for normal dynein-dynactin localization in spermatocytes and spermatids**

Although *Lis-1* is an established regulator of dynein-dynactin, it is currently unclear how *Lis-1* regulates dynein-dynactin activity. There are conflicting reports as to whether or not *Lis-1* is required for dynein-dynactin localization; however, a recent report has suggested that *Lis-1* is required for accumulation of dynein-dynactin on the nuclear surface during the mitotic cell cycle (Hebbar et al., 2008). We therefore examined dynein-dynactin's localization in *Lis-1* spermatocytes and spermatids to determine if Lis-1 contributes to dynein-dynactin's localization during *Drosophila* spermatogenesis. We

found that the localization of dynein-dynactin to the nuclear surface of late G2 spermatocytes and round spermatids was significantly reduced in *Lis-1* testes (Figure 3.8, E and H). Furthermore, dynein-dynactin failed to localize to the spindle poles of meiotic spermatocytes (Figure 3.8, F and G). These results suggest that Lis-1 is at least partially required for the localization of dynein-dynactin during *Drosophila* male meiosis. Interestingly, we found that the low level of dynein-dynactin present at the nuclear surface of *Lis-1* spermatids was not concentrated to one hemisphere as is seen in wild-type spermatids, but was instead often found to be distributed evenly around the entire periphery of the nucleus (Figure 3.8H). The expansion of dynein-dynactin's localization in *Lis-1* spermatids could be reflective of the loss of nucleus-basal body coupling, as we have previously observed similar expansions of dynein-dynactin's localization at the nuclear surface in *abnormal spindle* and *βTub85D* spermatids, in which nucleus-basal body coupling is commonly disrupted (Anderson et al., 2009).

Lis-1 and *asun* cooperatively regulate spermatogenesis

As described in Chapter II, we identified *asunder* (*asun*) as a critical regulator of dynein-dynactin localization during *Drosophila* spermatogenesis (Anderson et al., 2009). Because we found *Lis-1* to also contribute to dynein-dynactin's localization, we questioned whether they could cooperate in this process. To answer this question, we examined the ability of *Lis-1* to modify the *asun* phenotype, using a hypomorphic allele of *asun* ($asun^{f02815}$). We found that the introduction of a single copy of *Lis-1* into the $asun^{f02815}$ background strongly enhanced the *asun* phenotype. $asun^{f02815}$ males harboring a

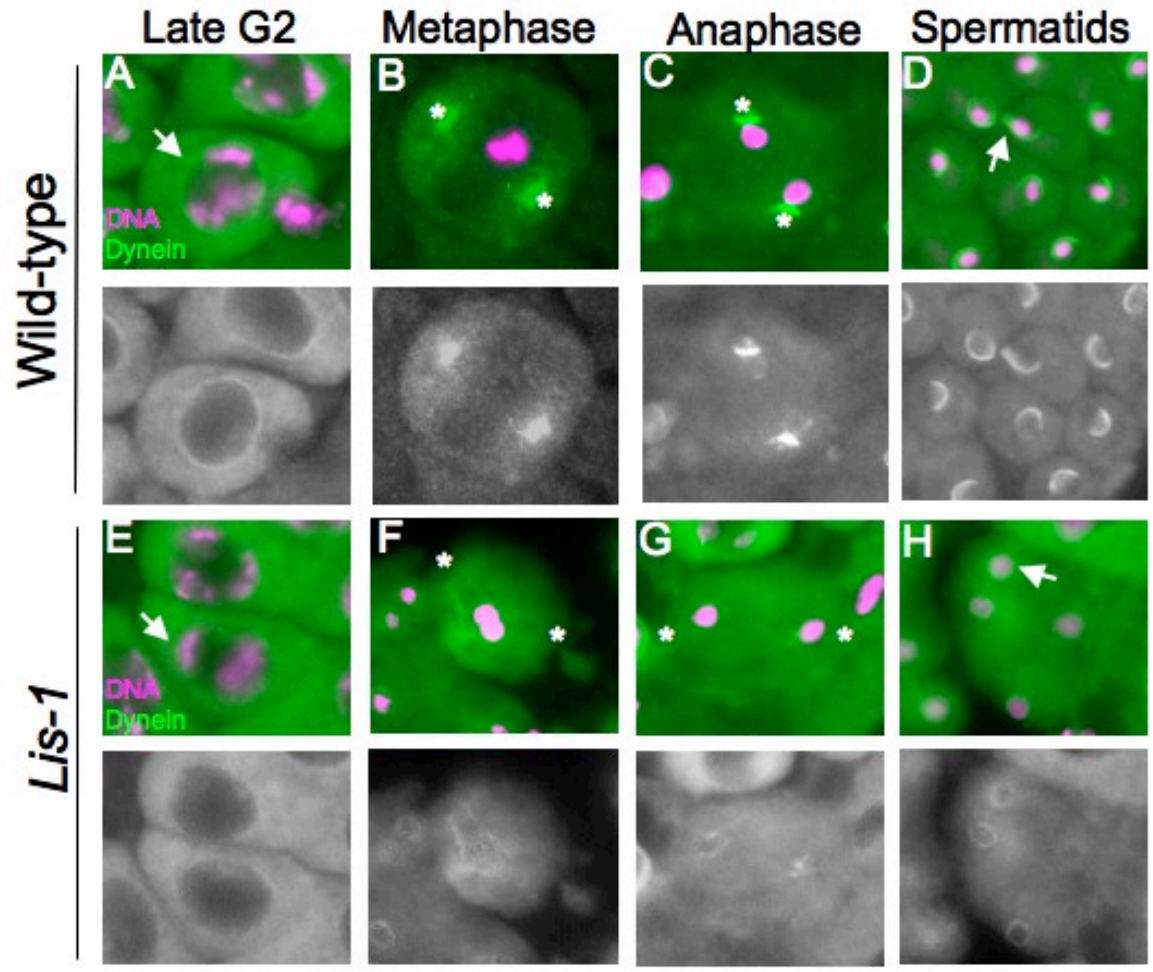

Figure 3.8. Dynein localization is disrupted in *Lis-1* spermatocytes and spermatids. (A-H) Fluorescence microscopy of wild-type (A-D) and *Lis-1* (E-H) spermatocytes and spermatids stained for dynein (green) and DNA (magenta). Arrows mark the nuclear surface. Asterisks mark spindle poles. Matched fluorescent micrographs of dynein staining are shown in grayscale below merged images. (A-D) Normal localization of dynein in wild-type spermatocytes and spermatids. Dynein localizes to the nuclear surface of late G2 spermatocytes (A). At metaphase (B) and anaphase (C) dynein stains intensely at the spindle poles. In postmeiotic spermatids, dynein accumulates at a hemispherical cap on the nuclear surface (D). (E-H) Disrupted localization of dynein in *Lis-1* spermatocytes and spermatids. (E) Dynein fails to accumulate normally on the nuclear surface of late G2 spermatocytes. Dynein is also absent from the spindle poles at metaphase (F) and anaphase (G). In postmeiotic spermatids, low levels of dynein are frequently found distributed around the entire nuclear surface (H).

single copy of *Lis-1* were found to possess testes that were drastically reduced in size, even when compared to those of $asun^{null}$ males (Figure 3.9). These results suggest that *Lis-1* and *asun* cooperate in the regulation of *Drosophila* spermatogenesis.

Discussion and Future Directions

Our analysis of a male sterile allele of *Lis-1* has revealed that *Lis-1* plays essential roles in both male meiosis and spermatid development during *Drosophila* spermatogenesis. We have shown that during male meiosis, the centrosomes fail to migrate to the nuclear surface at entry into prophase in *Lis-1* spermatocytes. Although *Lis-1* spermatocytes are capable of forming meiotic spindles, the centrosomes/asters are only loosely associated with the spindles and are frequently found to be detached. We also demonstrated that coupling between the nucleus and the centriole-derived basal body is lost in postmeiotic spermatids, and that the position of spermatid nuclei within elongating bundles is disrupted in *Lis-1* testes. Furthermore, we have shown that *Lis-1* colocalizes with dynein-dynactin at the nucleus and spindle poles, and that the localization of dynein-dynactin to the nuclear surface and spindle poles is severely impaired in *Lis-1* spermatocytes and spermatids. Dynein-dynactin at the nuclear surface has previously been shown to mediate interactions between the nucleus and the centrosomes during mitotic and meiotic cell cycles (Anderson et al., 2009; Gonczy et al., 1999; Li et al., 2004; Malone et al., 2003; Robinson et al., 1999; Salina et al., 2002). We therefore propose that the defects in nucleus-centrosome coupling that we have observed in *Lis-1* spermatocytes and spermatids stem from a disruption in the localization of dynein-dynactin to the nuclear surface.

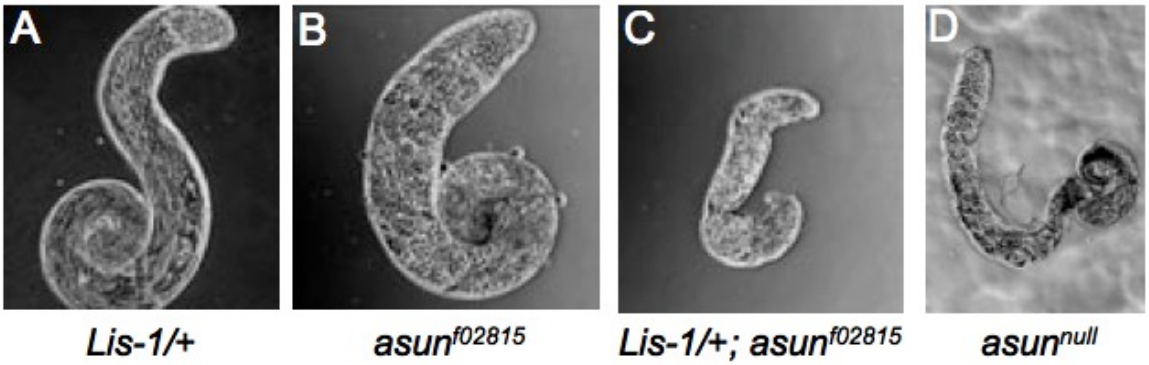

Figure 3.9. *Lis-1* enhances the *asun*^{f02815} phenotype. (A-D) Bright-field micrographs of testes from *Lis-1*/+ (A), *asun*^{f02815} (B), *Lis-1*/+; *asun*^{f02815} (C), and *asun*^{null} (D) males. Testes from *Lis-1*/+; *asun*^{f02815} males (C) are drastically reduced in sized compared to those of *Lis-1*/+ (A) and *asun*^{f02815} (B) males.

Previous studies concerning the role of *Lis-1* in the recruitment of dynein-dynactin to the nuclear surface in other systems have yielded conflicting results. In the *C. elegans* embryo, dynein-dynactin was observed to localize to the nuclear surface and spindle poles in the absence of *Lis-1* (Cockell et al., 2004). In mammalian neural stem cells, however, *Lis-1* was shown to be required for the recruitment of dynein to the nuclear surface at entry into mitotic prophase (Hebbar et al., 2008). These studies suggest that dynein-dynactin may localize to the nuclear surface through multiple pathways.

We previously identified *asun* as a critical regulator of dynein-dynactin localization during *Drosophila* spermatogenesis (Anderson et al., 2009). Our results demonstrating a genetic interaction between *Lis-1* and *asun* suggest that they may cooperate in the regulation of dynein-dynactin's localization. In *asun* testes, dynein-dynactin fails to accumulate on the nuclear surface of spermatocytes and spermatids. A similar requirement for *asun* in the recruitment of Lis-1 to the nuclear surface, however, has not yet been determined.

We have shown that the cytoplasmic accumulation of ASUN in late G2 spermatocytes coincides with the appearance of dynein-dynactin at the nuclear surface, suggesting that cytoplasmic ASUN may directly regulate dynein-dynactin's localization. Given our observation that dynein-dynactin is mislocalized in *Lis-1* spermatocytes and spermatids, one possible function for ASUN may be to promote interactions between Lis-1 and dynein-dynactin. Future experiments concerning the interactions between ASUN and Lis-1 should aid in the elucidation of the mechanism by which dynein-dynactin is recruited to the nuclear surface.

The finding that *asun* testes were drastically reduced in size after the introduction of a single copy of *Lis-1* suggests potential roles for *Lis-1* and *asun* in the regulation of stem cell divisions of *Drosophila* testes, as a reduction in testes size is associated with a loss of cell proliferation (Castrillon et al., 1993). In the *Drosophila* testis, approximately seven to eight germline stem cells are maintained at a structure known as the hub (Fuller, 1993). During stem cell division, the cleavage plane of dividing cells must be oriented so that daughter cells are released away from the hub to prevent the displacement of neighboring stem cells (Yamashita et al., 2003). The orientation of the cleavage plane is dependent on the proper migration of the centrosomes along the nuclear surface at entry into prophase, and misorientation of the centrosomes has been shown to lead to loss of stem cells in the *Drosophila* testes (Cheng et al., 2008; Yamashita et al., 2003; Yamashita et al., 2007). Given the importance of *Lis-1* and *asun* in mediating nucleus-centrosome coupling in Drosophila spermatocytes, it is possible that *Lis-1* and *asun* may also cooperate in the regulation of centrosome migration during stem cell divisions. Experiments are currently underway to test this possibility.

Our observations of *Lis-1* spermatids suggest that in addition to its role in maintaining nucleus-basal body coupling, *Lis-1* is required both for the morphogenesis of the Nebenkern and for its association with the nucleus and basal body. The Nebenkern is generated through the fusion of mitochondria that aggregate immediately following completion of male meiosis during *Drosophila* spermatogenesis (Fuller, 1993). The appearance of multiple Nebenkerne in spermatids of *Lis-1* testes suggests that *Lis-1* may be involved in the aggregation of mitochondria during spermatid differentiation. In addition, we have found that the Nebenkern tightly associates with the basal body of

wild-type spermatids and that these associations are lost in *Lis-1* spermatids. It is possible that associations between the Nebenkern and basal body facilitate spreading of the Nebenkern down the axoneme during spermatid differentiation; however, the Nebenkerne of *Lis-1* spermatids properly associate with the sperm axoneme during elongation, suggesting that coupling between the Nebenkern and basal body is not essential for Nebenkern-axoneme interactions.

We have previously found that dynein-dynactin localizes to the surface of the Nebenkern (Anderson et al., 2009). In the *Drosophila* ovary, the adaptor protein Milton has been suggested to physically couple dynein to the surface of mitochondria during oogenesis (Cox and Spradling, 2006). Intriguingly, *Drosophila* spermatids lacking Milton display defects in nucleus-Nebenkern associations similar to what we have observed in *Lis-1* testes (Aldridge et al., 2007). The defects in Nebenkern morphogenesis and basal body coupling in *Lis-1* spermatids that we have reported herein may therefore stem from a loss of dynein-dynactin activity at the Nebenkern. Future experiments will be directed toward determining the role of *Lis-1* and dynein-dynactin during Nebenkern morphogenesis.

CHAPTER IV

THE ROLE OF *asunder* IN THE FEMALE GERMLINE OF *DROSOPHILA*

Introduction

Expression of *asun* in adult flies appears to be limited to the male and female germ lines (Stebbings et al., 1998). We previously identified ASUN as an *in vitro* substrate of PNG kinase (Lee et al., 2005). *png* expression, which appears to be limited to the female germ line with maternal deposition in the egg, is required for cell-cycle progression during syncytial embryogenesis (Fenger et al., 2000; Lee et al., 2005). Embryos derived from *png* females undergo repeated rounds of DNA replication in the complete absence of mitosis, resulting in the formation of giant, polyploid nuclei (Fenger et al., 2000). While we previously found that *asun* is essential for gametogenesis in males, we observed only a slight reduction in egg-laying rates of *asun* females and normal development of their embryos (Anderson et al., 2009). The lack of defects in *asun*-derived embryos in our previous report may be due to the hypomorphic nature of the *f02815* allele.

To further explore the role of *asun* in the female germline and its potential involvement in the *png* pathway, we have generated a deletion allele of *asun*. Our preliminary characterization of the *asun* null phenotype has revealed that females display profound defects in oogenesis. Embryos deposited by *asun* null females often appear short and round, and they possess malformed dorsal appendages, similar to the phenotype associated with loss of dynein-dynactin function. Despite these abnormalities, almost half

of the embryos laid by *asun* null females to developed normally, suggesting that *asun* is primarily required during oogenesis.

Materials and Methods

Drosophila stocks

y w was used as the "wild-type" stock. *piggyBac* insertion lines *f02815* and *f01662* were from the Exelixis Collection (Harvard Medical School). *piggyBac* transposase and *NGT40-Gal4* flies were obtained from the Bloomington Stock Center.

Generation of a null allele

A deletion allele of *asun* was generated using *piggyBac* insertion lines *f02815* and *f01662* according to an established protocol (Parks et al., 2004; Figure 4.1 A and B).

Transgenics

A 4-kb genomic fragment containing *belphegor* and flanking regions (Figure 4.1C) was PCR-amplified from BAC clone BACR05P04 (Drosophila Genomics Resource Center) and subcloned into pCaSpeR4. A stop codon was introduced into the 5'-end of the coding region of *asun*. A transgenic line carrying *pCaSpeR4-belphegor* was generated by *P*-element-mediated transformation via embryo injection (Rubin and Spradling, 1982).

Cytological analysis of fixed ovaries

Ovaries were dissected in Grace's insect medium (Life Technologies) and fixed in 4% formaldehyde in PBST (PBS with 0.1% Tween 20) for 13 minutes. Ovaries were then washed in PBST and processed for immunostaining and/or incubated in 0.5 μg/ml DAPI for 10 minutes for visualization of DNA. Samples were mounted in Vectashield (Vector Laboratories). Immunostaining was performed using mouse anti-Gurken antibodies (1D12, 1:100, Developmental Studies Hybridoma Bank). A Cy2-conjugated goat anti-mouse secondary antibody was used at 1:800. Fluorescent images were obtained using a Nikon Eclipse 80i microscope with Plan-Apo 100x, Plan-Fluor60x, and Plan-Fluor 40x objectives.

Results

To aid in our investigation of *asun*'s role in female gametogenesis, we generated a small, two-gene deletion that removed the majority of *asun*'s coding region and all of its neighboring gene, *belphegor* (*bor*) (Figure 4.1, A and B). *bor* is a novel gene predicted to encode an AAA ATPase domain protein of unknown function. Although this deletion was lethal in homozygous individuals, we were able to rescue lethality using a *bor* genomic rescue construct (Figure 4.1C), thus demonstrating that *asun* is not essential for viability.

Before examining the female phenotype, we first examined the male phenotype to confirm the loss of *asun* function. We found that *bor, asun, P{bor (w+)}* (referred to hereafter simply as "$asun^{null}$") males were completely sterile (18/18 males examined). Furthermore, we found that greater than 99% of spermatids within $asun^{null}$ testes

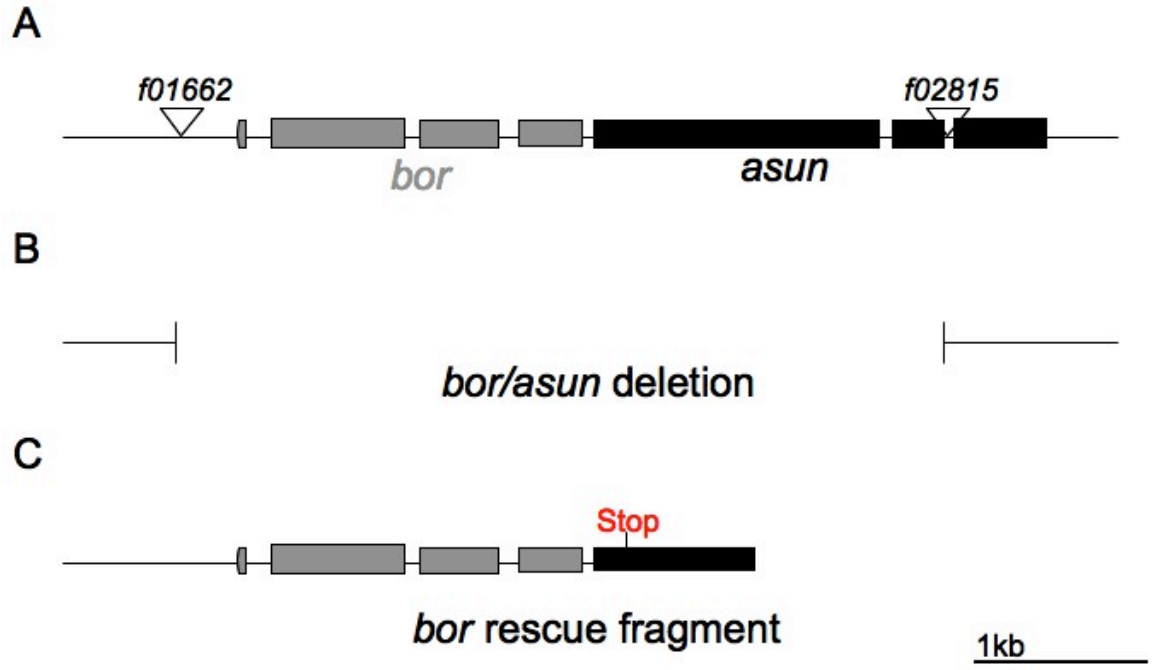

Figure 4.1. Generation of a null allele of *asun*. (A) Schematic diagram of the *bor*/*asun* gene region. Coding regions plus UTRs are represented as shaded boxes, respectively, introns as thin lines, and *piggyBac* transposons *f01662* and *f02815* as triangles. A deletion allele was generated through FLP-mediated recombination of *FRT* sites within *piggyBac* transposons *f01662* and *f02815* (Parks et al., 2004). The breakpoints of this allele are illustrated (B). (C) Schematic diagram of the *bor* rescue construct. Note the introduction of a stop codon (red) in the 5'-end of the *asun* coding region to prevent production of a truncated ASUN protein that might have partial activity.

contained multiple nuclei (199/201 cells scored), which indicates a severe defect during cytokinesis. Importantly, we found that we could rescue these phenotypes through male germline-specific expression of GFP-tagged ASUN (described in Chapter II; data not shown), demonstrating that these defects were due to the loss of *asun*.

We next turned our focus to $asun^{null}$ females. We found that the egg-laying rates of $asun^{null}$ females were sharply reduced compared to those of wild type (Table 4.1). In addition, we found that the eggs of $asun^{null}$ females often appeared round and displayed short, fused dorsal appendages, suggestive of defects in egg shell formation (Figure 4.2B, Table 4.1). Despite these abnormalities, we found that approximately 45% of embryos deposited by $asun^{null}$ females hatched into larvae (Table 4.1).

Based on the severe reduction in egg laying rates, we decided to examine the egg chambers of $asun^{null}$ ovaries. We found that $asun^{null}$ ovaries commonly possessed fused egg chambers, containing 30 nurse cells and 2 oocytes (Figure 4.3B). In addition, we often observed degenerating egg chambers (Figure 4.3D) within $asun^{null}$ ovaries. To determine if these defects were due to loss of *asun*, we attempted to rescue the $asun^{null}$ phenotype through germline expression of Myc-tagged ASUN using the NGT40-Gal4 driver. We found that while expression of this transgene did not significantly affect egg-laying rates (Table 4.1), it fully rescued the morphological defects of $asun^{null}$-derived eggs, suggesting that *asun* is required in the female germ line for formation of the dorsal appendages.

Intriguingly, defects in the formation and location of dorsal appendages have been reported following germline-specific knockdown of two dynein regulatory factors, *Lis-1* and *Bicaudal-D* (Lei and Warrior, 2000; Swan and Suter, 1996). The dorsal

Table 4.1. Quantification of egg laying, hatching, and dorsal appendage defects

Genotype	Egg Laying Rate (% WT)	Hatch Rate (%WT)	% Embryos with Dorsal Appendage Defects
Wild-type	100	77	0
asun^{null}/TM3	73	91	0
asun^{null}	6	45	34
UASp-myc-asun; NGT40-Gal4/ +; asun^{null}	11	65	5

Courtesy of Julie Merkle

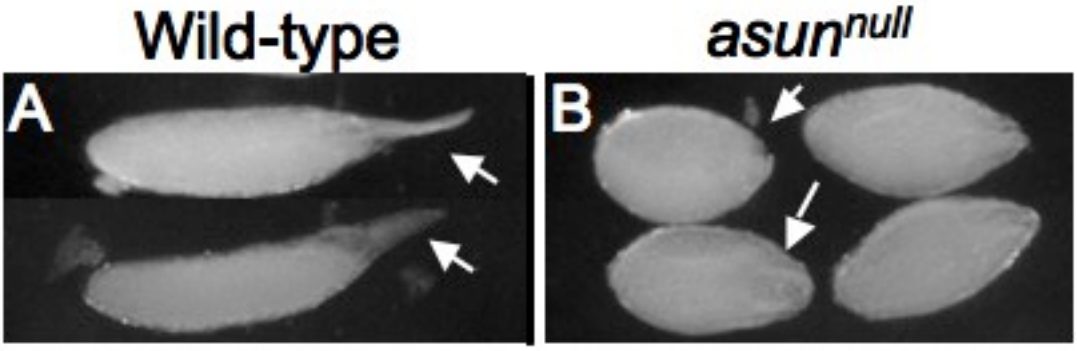

Figure 4.2. Aberrant morphology of eggs derived from *asun*^{null} females. Stage 14 eggs from wild-type (A) and *asun*^{null} (B) females. Arrows mark dorsal appendages. Eggs from *asun*^{null} females (B) appear short and round compared to those of wild-type (A) and possess short, fused dorsal appendages.

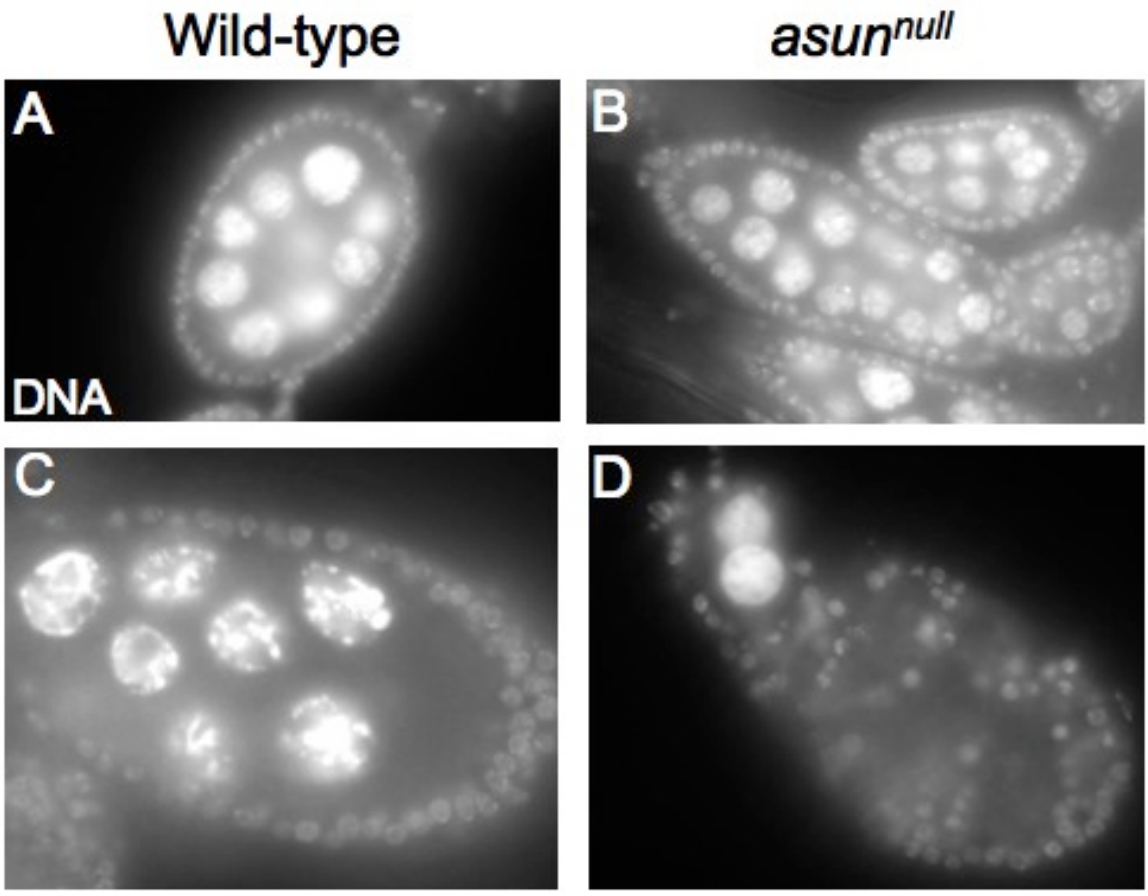

Figure 4.3. Defective egg chamber formation in *asun*^{null} ovaries. Egg chambers stained with DAPI to visualize DNA. (A and C) Wild-type egg chambers containing 15 nurse cells and one oocyte. (B) *asun*^{null} egg chamber containing 30 nurse cells and two oocytes. (D) *asun*^{null} egg chamber containing pyknotic nuclei. Images courtesy of Julie Merkle.

appendage defects of *Lis-1* and *Bicaudal-D*-derived embryos are attributed to the disruption of dynein-mediated transport of the morphogen, Gurken, to the dorsal-anterior region (Lei and Warrior, 2000; Swan and Suter, 1996). We therefore examined Gurken localization in $asun^{null}$ egg chambers. We found that Gurken protein appears to localize normally at the dorsal-anterior region of the oocyte (Figure 4.4) in $asun^{null}$ egg chambers. We have not, however, directly compared levels of Gurken at this site between wild-type and $asun^{null}$ oocytes, so a subtle disruption in Gurken accumulation in $asun^{null}$ oocytes cannot be ruled out.

Discussion and Future Directions

Our preliminary characterization of the $asun^{null}$ female phenotype suggests a role for *asun* in oogenesis. Although the defects in dorsal appendage formation that we have observed in $asun^{null}$-derived eggs are reminiscent of a disruption in dynein-dynactin activity, *asun's* role in the regulation of dynein-dynactin during *Drosophila* oogenesis remains to be determined. In the Drosophila ovary, dynein-dynactin has been shown to localize to the nuclear surface of the oocyte within developing egg chambers (Li et al., 1994). Localization of dynein-dynactin to this site appears to be important for nuclear migration and the recruitment of morphogens such as Gurken (Lei and Warrior, 2000). We have previously shown that ASUN is required for the perinuclear localization of dynein-dynactin in the male germline (Anderson et al., 2009). Efforts are currently underway to determine if a similar role for ASUN exists in the female germline.

High levels of *asun* transcript have previously been observed in both the germline and follicle cells of the *Drosophila* ovary. The inability to rescue egg-laying rates of

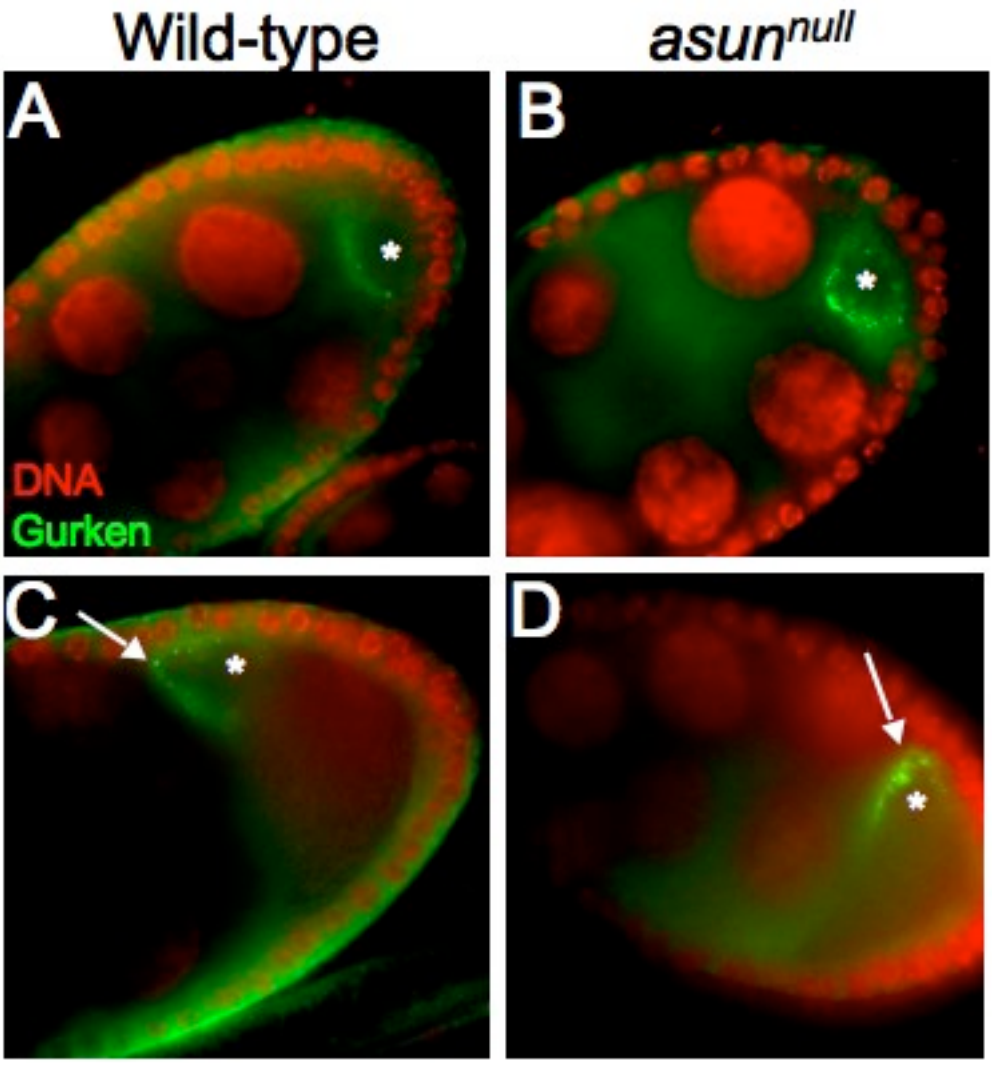

Figure 4.4. Gurken localization in *asun*^{null} oocytes. (A-D) Egg chambers of ovaries stained for Gurken (green) and DNA (red). Asterisks mark oocyte nuclei. Arrows mark dorsal-anterior region. (A and C) Wild-type egg chambers. During early oogenesis, Gurken protein is distributed around the oocyte nucleus (A). At later stages of oogenesis, Gurken accumulates at the dorsal-anterior region of the oocyte (B). (B and D) *asun*^{null} egg chambers. Gurken localizaton appears normal in *asun*^{null} egg chambers (compare A and B; C and D). Images courtesy of Julie Merkle.

asun^{null} females through germline-specific expression of Myc-tagged ASUN may indicate essential roles for *asun* in the follicle cells, as the germline and follicle cells are intimately connected in oogenesis. It is also possible that low egg-laying rates stem from an incomplete rescue of *asun's* neighboring gene, *bor*. Efforts are currently underway to generate an *asun* genomic rescue construct so that potential roles for *asun* in the female germline and follicles cells may be more fully explored.

In stark contrast to *png*, we found that almost half of the embryos deposited by *asun*^{null} females developed to larval stages, suggesting that *asun* is not essential for embryonic development. In addition, we have not observed disruption of mitosis during the syncytial divisions of *asun*-derived embryos (our unpublished results). *png* is required for the translation of Cyclin A and Cyclin B in *Drosophila* ovaries and embryos (Fenger et al., 2000; Vardy and Orr-Weaver, 2007; Vardy et al., 2009). While we have not yet examined Cyclin A and Cyclin B levels in embryos derived from *asun*^{null} females, our previous observation of elevated Cyclin A and Cyclin B levels in *asun* testes suggests that *asun* is not involved in this process (Anderson et al., 2009). These results suggest that *asun* is not an essential component of the *png* pathway.

CHAPTER V

ACETYLATION OF MICROTUBULES DURING *DROSOPHILA* SPERMATOGENESIS

Introduction

The microtubule cytoskeleton is a highly dynamic structure that is capable of undergoing dramatic changes in its organization to meet the needs of the cell. The architecture of the microtubule cytoskeleton is controlled through the activity of a host of microtubule-associated proteins, microtubule-severing factors, and microtubule catastrophe factors, all of which regulate the stability of microtubules (Drewes et al., 1998; Garrett and Kapoor, 2003; Quarmby and Lohret, 1999). The structure and function of microtubules can also be regulated through post-translational modifications to polymerized microtubules (Hammond et al., 2008). For example, glycylation and glutamylation of microtubules is required for the assembly of axonemal structures, while detyrosination and acetylation of microtubles regulates the affinity of microtubules for microtubule motors (Hammond et al., 2008).

During mitosis, the highly organized microtubule arrays of interphase cells are dismantled to allow for assembly of the mitotic spindles at entry into M phase. During this transition, microtubule stability is dramatically reduced (Rusan et al., 2001). Subsets of stable cytoplasmic microtubules, however, are actively transported toward the nuclear envelope and centrosomes at entry into prophase in a dynein-dependent manner (Rusan et al., 2002; Tulu et al., 2003). These stable microtubules are incorporated into the mitotic spindle along with newly polymerized microtubules emanating from the microtubule

organizing centers, chromatin, and nuclear envelope (Tulu et al., 2003). The importance of cytoplasmic microtubules in spindle assembly and the mechanism by which they are recruited are currently unclear.

Through a chance observation, we have found that microtubules present at the nuclear surface of *Drosophila* primary spermatocytes during prophase are heavily acetylated. We have not observed a similar phenomenon in *asunder (asun)* primary spermatocytes, which fail to recruit dynein-dynactin to the nuclear surface during meiosis, suggesting that dynein-dynactin may be required for this process (Anderson et al., 2009). Current efforts are underway to determine the origin of these microtubules and the functional consequence of their acetylation.

Methods and Materials

Drosophila stocks

y w was used as the "wild-type" stock. *β-tubulin-GFP* flies were a gift from H. Oda and Y. Akiyama-Oda. *piggyBac* insertion line *f02815* was from the Exelixis Collection (Harvard Medical School).

Cytological analyses of live and fixed testes

Live testes cells were prepared for examination by phase contrast or fluorescence microscopy as described (Kemphues et al., 1980). Preparations were fixed in either methanol or formaldehyde. Methanol fixation was performed as follows: slides of squashed testes were snap-frozen, immersed in methanol for 10 minutes at -20˚C after

coverslip removal, and washed twice in phosphate-buffered saline. Formaldehyde fixation was performed as described (Gunsalus et al., 1995).

Primary antibodies were used as follows: mouse anti-acetylated-Tubulin (6-B11-1, 1:50, Sigma) and rat anti-α-tubulin (Mca77G, 1:500, Accurate Chemical & Scientific Corp.). Cy2- and Cy3-conjugated secondary antibodies were used at 1:800. Fixed samples were mounted in phosphate-buffered saline with DAPI (0.2 μg/ml) to visualize DNA.

Fluorescent images were obtained using one of two microscopes: Nikon Eclipse 80i with Plan-Apo 100x and Plan-Fluor 40x objectives or Zeiss Axiophot with Neo-Fluor Ph2 40x objective.

Immunoblots

Protein extracts were prepared by homogenizing dissected testes from newly eclosed males in non-denaturing lysis buffer. 20 μg of protein was loaded in each lane. Proteins were transferred to nitrocellulose for immunoblotting using standard techniques. Primary antibodies were used as follows: mouse anti-acetylated-tubulin (6-11B-1, 1:5000, Sigma) and mouse anti-tubulin (DM1α, 1:7000). HRP-conjugated secondary antibodies and chemiluminescence were used to detect primary antibodies.

Results

While immunostaining primary cilia of *Drosophila* spermatocytes with an antibody that recognizes acetylated microtubules, we observed an unexpected enrichment of acetylated microtubules at the nuclear surface of dividing meiotic spermatocytes

(Figure 5.1). Upon closer examination, we found that acetylated microtubules first appeared at the nuclear surface at entry into prophase (Figures 5.1A and 5.2A). During metaphase, anaphase, and telophase, acetylated microtubules were found to remain in association with what appeared to be the remnants of the nuclear envelope (Figure 5.1B), which does not fully break down during *Drosophila* male meiosis (Fuller, 1993). In addition, we observed acetylated microtubules to be present at the kinetochores and spindle poles during male meiosis (Figure 5.1B).

Recruitment of microtubules to the nuclear surface is largely dependent on dynein-dynactin (Rusan et al., 2002; Salina et al., 2002). To determine if dynein-dynactin is required for the perinuclear accumulation of acetylated microtubules, we examined prophase spermatocytes of *asun* testes, which fail to recruit dynein-dynactin to the nuclear surface (Anderson et al., 2009). We found that acetylated microtubules failed to localize to the nuclear surface of *asun* spermatocytes at prophase (Figure 5.2B). When we compared levels of acetylated microtubules between wild type and *asun* testes, we found that they were identical (Figure 5.3) suggesting that the loss of acetylated microtubules at the nuclear surface of *asun* spermatocytes is not due to a global reduction of microtubule acetylation in testes. These results suggest that dynein-dynactin may play a role in the recruitment of acetylated microtubules to the nuclear surface.

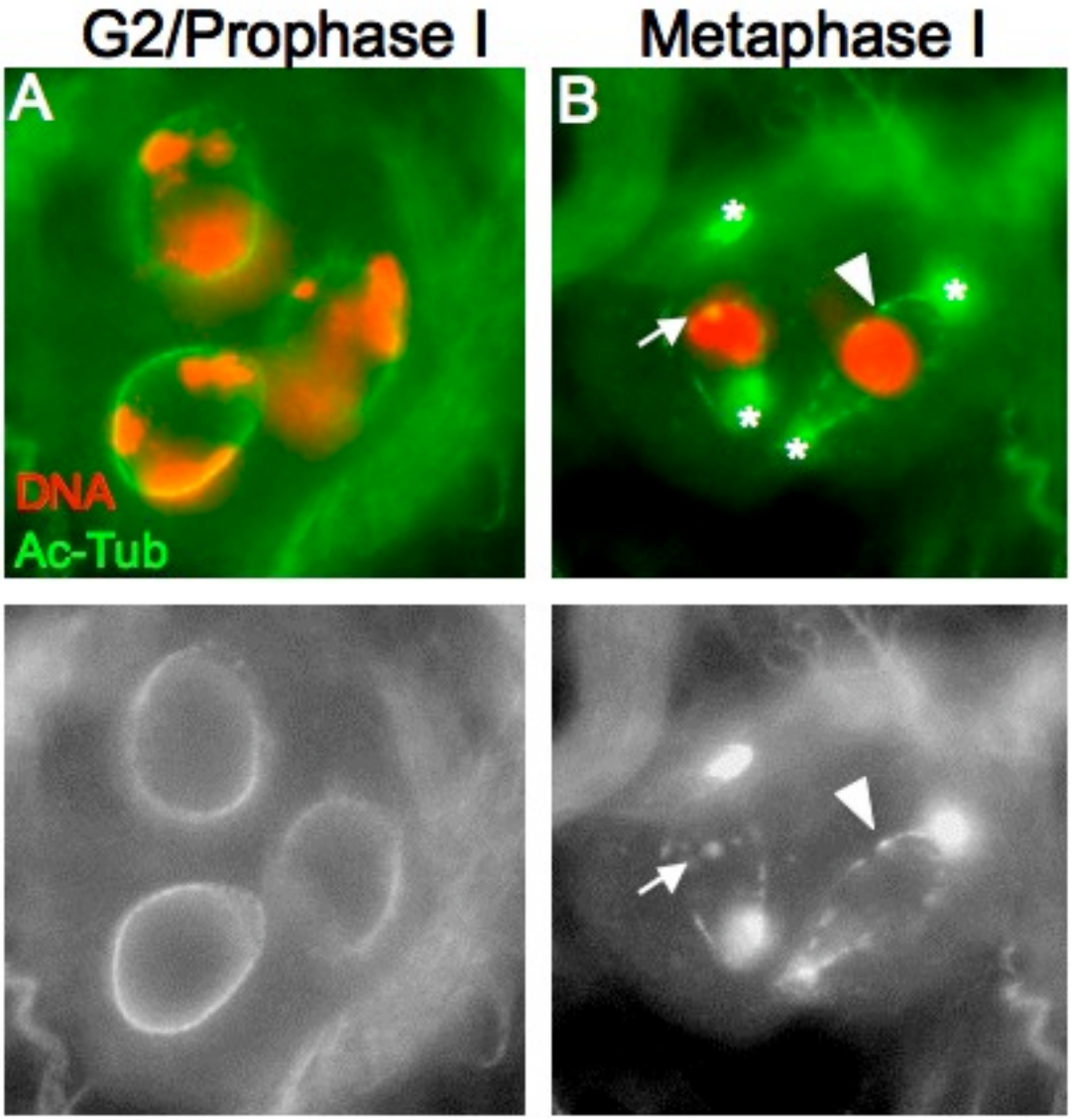

Figure 5.1. Localization of acetylated microtubules during *Drosophila* male meiosis. (A and B) Fluorescent micrographs of G2/prophase (A) and metaphase (B) primary spermatocytes stained for acetylated tubulin (green) and DNA (red). Matched fluorescent micrographs of acetylated tubulin are shown in grayscale below merged images. (A) Acetylated microtubules accumulate at the nuclear surface during G2/prophase. (B) At metaphase, acetylated microtubules are present at the kinetochores (arrow), spindle poles (asterisks), and the remnants of the nuclear envelope (arrowhead).

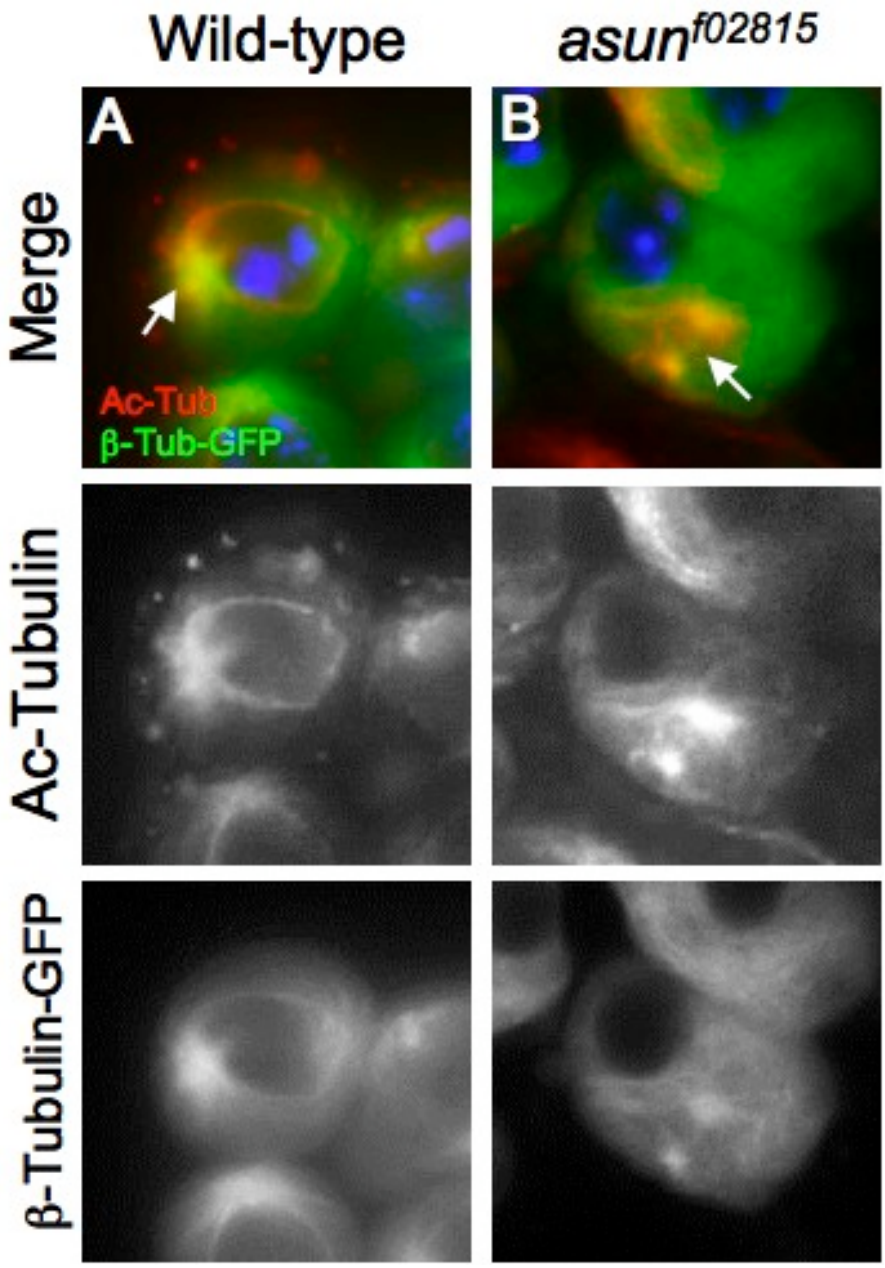

Figure 5.2. Aberrant localization of acetylated microtubules in *asun*^{f02815} spermatocytes at prophase I. (A and B) Fluorescent micrographs of wild-type (A) and *asun*^{f02815} (B) spermatocytes at prophase, expressing β-Tubulin-GFP (green) and stained for acetylated tubulin (red). DNA is shown in blue. Matched fluorescent micrographs of β-Tubulin-GFP and acetylated tubulin are shown in grayscale below merged images. During prophase in wild-type primary spermatocytes (A), acetylated tubulin is observed at the nuclear surface and centrosomes (arrow). In *asun*^{f02815} spermatocytes undergoing prophase (B), acetylated tubulin is present at the free centrosomes (arrow), but is absent from the nuclear surface.

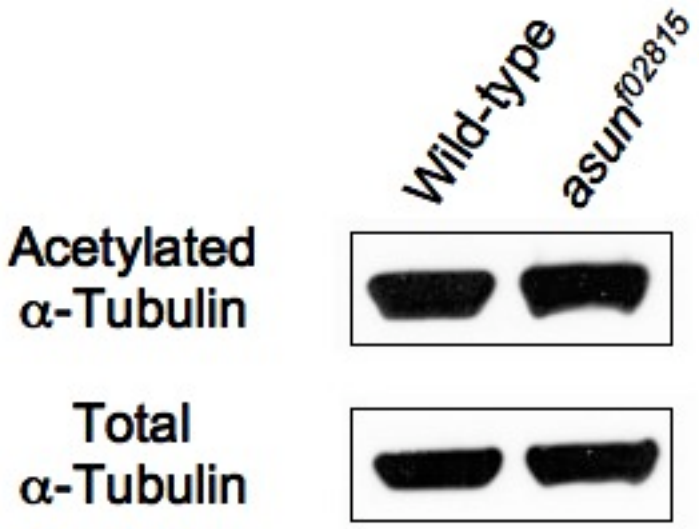

Figure 5.3. Normal levels of acetylated tubulin in *asun*^{f02815} testes. Acetylated tubulin and α-tubulin immunoblots. Levels of acetylated tubulin are equivalent between wild-type and *asun*^{f02815} testes.

Discussion and Future Directions

We showed that acetylated microtubules localize to the nuclear surface during *Drosophila* male meiosis. Furthermore, we found that this localization may depend on dynein-dynactin. The origin and function of acetylated microtubules at the nuclear surface is currently unclear.

Acetylation is a fairly common modification of stable microtubules, raising the possibility that the acetylated microtubules that we have observed at the nuclear surface of prophase spermatocytes are stable remnants of the interphase microtubule array (Hammond et al., 2008; Rusan et al., 2002; Tulu et al., 2003). Astral microtubules, however, are also acetylated during the mitotic cycle, preventing their contribution from being ruled out. To determine if acetylated microtubules at the nuclear surface emanate from the centrosomes, or are derived from another source, we are working toward analyzing the localization of acetylated microtubules in *abnormal spindle* spermatocytes. Because centrosomes of *abnormal spindle* spermatocytes do not nucleate astral microtubules, migrate to the nuclear surface, or contribute to the assembly of the meiotic spindle, the use of this line should allow us to preclude the involvement of centrosomal microtubules (Rebollo et al., 2004).

Interactions between dynein-dynactin, anchored to the nuclear surface during prophase, and perinuclear microtubules have previously been shown to facilitate tearing of the nuclear lamina during nuclear envelope breakdown (Salina et al., 2002). Intriguingly, acetylation of microtubules has been shown to enhance dynein-dynactin activity, suggesting that recruitment of acetylated microtubules to the nuclear surface may stimulate nuclear envelope breakdown (Dompierre et al., 2007; Reed et al., 2006).

To investigate the role of microtubule acetylation during *Drosophila* male meiosis, we are currently working toward generating *Drosophila* lines that express either non-acetylatable or acetylation-mimic forms of α-Tubulin specifically in the male germline. The analysis of these lines should provide valuable insight into the cell-cycle and developmental roles of microtubule acetylation.

CHAPTER VI

CONCLUDING REMARKS

It has now become clear that dynein's activity is controlled at multiple levels ranging from the composition and phosphorylation state of its subunits to its interactions with regulatory factors, microtubules, and cargos. While great progress has been made in discerning the structure and functional roles of dynein, the mechanisms underlying its regulation still remain poorly understood.

I have demonstrated herein an essential role for a novel gene, *asunder* (*asun*), in promoting the perinuclear localization of dynein-dynactin during *Drosophila* spermatogenesis. Furthermore, I have shown that ASUN colocalizes to the nuclear surface of HeLa cells with its human homolog, GCT1, and dynein, suggesting that the function of *asun* in the regulation of dynein-dynactin localization may be conserved in higher vertebrates. Finally, I have provided evidence that *asun* cooperates with *Lis-1* in the regulation of *Drosophila* spermatogenesis.

Nucleus-centrosome coupling is essential for the migration of neurons during vertebrate brain development, and dynein-dynactin at the nuclear surface plays a critical role in maintaining nucleus-centrosome interactions during this process. The loss of dynein-dynactin activity during neuronal migration prevents the movement of nuclei within neurons, thus blocking the relocation of neurons to their final position within the developing brain. The disruption of neuronal migration results in a severe developmental defect known as lissencephaly, or smooth brain. The discovery of *asun* as a novel

regulator of dynein-dynactin's localization to the nuclear surface may provide new insights into the mechanisms underlying dynein-dynactin's regulation during neuronal migration and have broader implications for human health.

The work that I have presented herein should serve as a frame for future studies concerning the molecular mechanism of *asun*. Given the conserved nature of *asun*, the identification of such a mechanism may provide broad insight into the regulation of dynein's subcellular localization in a variety of systems.

REFERENCES

Afshar, G. and Murnane, J. P. (1999). Characterization of a human gene with sequence homology to Saccharomyces cerevisiae SIR2. *Gene* **234**, 161-8.

Ahn, C. and Morris, N. R. (2001). Nudf, a fungal homolog of the human LIS1 protein, functions as a dimer in vivo. *J Biol Chem* **276**, 9903-9.

Aldridge, A. C., Benson, L. P., Siegenthaler, M. M., Whigham, B. T., Stowers, R. S. and Hales, K. G. (2007). Roles for Drp1, a dynamin-related protein, and milton, a kinesin-associated protein, in mitochondrial segregation, unfurling and elongation during Drosophila spermatogenesis. *Fly (Austin)* **1**, 38-46.

Alphey, L., Jimenez, J., White-Cooper, H., Dawson, I., Nurse, P. and Glover, D. M. (1992). twine, a cdc25 homolog that functions in the male and female germline of Drosophila. *Cell* **69**, 977-88.

Anderson, M. A., Jodoin, J. N., Lee, E., Hales, K. G., Hays, T. S. and Lee, L. A. (2009). asunder Is a Critical Regulator of Dynein-Dynactin Localization during Drosophila Spermatogenesis. *Mol Biol Cell*.

Barlow, A. L., van Drunen, C. M., Johnson, C. A., Tweedie, S., Bird, A. and Turner, B. M. (2001). dSIR2 and dHDAC6: two novel, inhibitor-resistant deacetylases in Drosophila melanogaster. *Exp Cell Res* **265**, 90-103.

Basto, R., Lau, J., Vinogradova, T., Gardiol, A., Woods, C. G., Khodjakov, A. and Raff, J. W. (2006). Flies without centrioles. *Cell* **125**, 1375-86.

Baye, L. M. and Link, B. A. (2007). Interkinetic nuclear migration and the selection of neurogenic cell divisions during vertebrate retinogenesis. *J Neurosci* **27**, 10143-52.

Beaudouin, J., Gerlich, D., Daigle, N., Eils, R. and Ellenberg, J. (2002). Nuclear envelope breakdown proceeds by microtubule-induced tearing of the lamina. *Cell* **108**, 83-96.

Bettencourt-Dias, M., Rodrigues-Martins, A., Carpenter, L., Riparbelli, M., Lehmann, L., Gatt, M. K., Carmo, N., Balloux, F., Callaini, G. and Glover, D. M. (2005). SAK/PLK4 is required for centriole duplication and flagella development. *Curr Biol* **15**, 2199-207.

Blangy, A., Arnaud, L. and Nigg, E. A. (1997). Phosphorylation by p34cdc2 protein kinase regulates binding of the kinesin-related motor HsEg5 to the dynactin subunit p150. *J Biol Chem* **272**, 19418-24.

Bloom, K. (2001). Nuclear migration: cortical anchors for cytoplasmic dynein. *Curr Biol* **11**, R326-9.

Bourdon, V., Naef, F., Rao, P. H., Reuter, V., Mok, S. C., Bosl, G. J., Koul, S., Murty, V. V., Kucherlapati, R. S. and Chaganti, R. S. (2002). Genomic and expression analysis of the 12p11-p12 amplicon using EST arrays identifies two novel amplified and overexpressed genes. *Cancer Res* **62**, 6218-23.

Brand, A. H. and Perrimon, N. (1993). Targeted gene expression as a means of altering cell fates and generating dominant phenotypes. *Development* **118**, 401-15.

Brill, J. A., Hime, G. R., Scharer-Schuksz, M. and Fuller, M. T. (2000). A phospholipid kinase regulates actin organization and intercellular bridge formation during germline cytokinesis. *Development* **127**, 3855-64.

Castrillon, D. H., Gonczy, P., Alexander, S., Rawson, R., Eberhart, C. G., Viswanathan, S., DiNardo, S. and Wasserman, S. A. (1993). Toward a molecular genetic analysis of spermatogenesis in Drosophila melanogaster: characterization of male-sterile mutants generated by single P element mutagenesis. *Genetics* **135**, 489-505.

Cenci, G., Bonaccorsi, S., Pisano, C., Verni, F. and Gatti, M. (1994). Chromatin and microtubule organization during premeiotic, meiotic and early postmeiotic stages of Drosophila melanogaster spermatogenesis. *J Cell Sci* **107 (Pt 12)**, 3521-34.

Cheng, J., Turkel, N., Hemati, N., Fuller, M. T., Hunt, A. J. and Yamashita, Y. M. (2008). Centrosome misorientation reduces stem cell division during ageing. *Nature* **456**, 599-604.

Chuang, J. Z., Milner, T. A. and Sung, C. H. (2001). Subunit heterogeneity of cytoplasmic dynein: Differential expression of 14 kDa dynein light chains in rat hippocampus. *J Neurosci* **21**, 5501-12.

Clark, S. W. and Meyer, D. I. (1994). ACT3: a putative centractin homologue in S. cerevisiae is required for proper orientation of the mitotic spindle. *J Cell Biol* **127**, 129-38.

Cockell, M. M., Baumer, K. and Gonczy, P. (2004). lis-1 is required for dynein-dependent cell division processes in C. elegans embryos. *J Cell Sci* **117**, 4571-82.

Cokol, M., Nair, R. and Rost, B. (2000). Finding nuclear localization signals. *EMBO Rep* **1**, 411-5.

Coquelle, F. M., Caspi, M., Cordelieres, F. P., Dompierre, J. P., Dujardin, D. L., Koifman, C., Martin, P., Hoogenraad, C. C., Akhmanova, A., Galjart, N. et al.

(2002). LIS1, CLIP-170's key to the dynein/dynactin pathway. *Mol Cell Biol* **22**, 3089-102.
Cox, R. T. and Spradling, A. C. (2006). Milton controls the early acquisition of mitochondria by Drosophila oocytes. *Development* **133**, 3371-7.

Creppe, C., Malinouskaya, L., Volvert, M. L., Gillard, M., Close, P., Malaise, O., Laguesse, S., Cornez, I., Rahmouni, S., Ormenese, S. et al. (2009). Elongator controls the migration and differentiation of cortical neurons through acetylation of alpha-tubulin. *Cell* **136**, 551-64.

Culver-Hanlon, T. L., Lex, S. A., Stephens, A. D., Quintyne, N. J. and King, S. J. (2006). A microtubule-binding domain in dynactin increases dynein processivity by skating along microtubules. *Nat Cell Biol* **8**, 264-70.

Deacon, S. W., Serpinskaya, A. S., Vaughan, P. S., Lopez Fanarraga, M., Vernos, I., Vaughan, K. T. and Gelfand, V. I. (2003). Dynactin is required for bidirectional organelle transport. *J Cell Biol* **160**, 297-301.

Del Bene, F., Wehman, A. M., Link, B. A. and Baier, H. (2008). Regulation of neurogenesis by interkinetic nuclear migration through an apical-basal notch gradient. *Cell* **134**, 1055-65.

Dix, C. I. and Raff, J. W. (2007). Drosophila Spd-2 recruits PCM to the sperm centriole, but is dispensable for centriole duplication. *Curr Biol* **17**, 1759-64.

Dobyns, W. B. and Truwit, C. L. (1995). Lissencephaly and other malformations of cortical development: 1995 update. *Neuropediatrics* **26**, 132-47.

Dompierre, J. P., Godin, J. D., Charrin, B. C., Cordelieres, F. P., King, S. J., Humbert, S. and Saudou, F. (2007). Histone deacetylase 6 inhibition compensates for the transport deficit in Huntington's disease by increasing tubulin acetylation. *J Neurosci* **27**, 3571-83.

Drewes, G., Ebneth, A. and Mandelkow, E. M. (1998). MAPs, MARKs and microtubule dynamics. *Trends Biochem Sci* **23**, 307-11.

Fabian, L. and Forer, A. (2005). Redundant mechanisms for anaphase chromosome movements: crane-fly spermatocyte spindles normally use actin filaments but also can function without them. *Protoplasma* **225**, 169-84.

Farshori, P. and Holzbaur, E. L. (1997). Dynactin phosphorylation is modulated in response to cellular effectors. *Biochem Biophys Res Commun* **232**, 810-6.

Faulkner, N. E., Dujardin, D. L., Tai, C. Y., Vaughan, K. T., O'Connell, C. B., Wang, Y. and Vallee, R. B. (2000). A role for the lissencephaly gene LIS1 in mitosis and cytoplasmic dynein function. *Nat Cell Biol* **2**, 784-91.

Fenger, D. D., Carminati, J. L., Burney-Sigman, D. L., Kashevsky, H., Dines, J. L., Elfring, L. K. and Orr-Weaver, T. L. (2000). PAN GU: a protein kinase that inhibits S phase and promotes mitosis in early Drosophila development. *Development* **127**, 4763-74.

Fukushige, T., Siddiqui, Z. K., Chou, M., Culotti, J. G., Gogonea, C. B., Siddiqui, S. S. and Hamelin, M. (1999). MEC-12, an alpha-tubulin required for touch sensitivity in C. elegans. *J Cell Sci* **112 (Pt 3)**, 395-403.

Fuller, M. T. (1993). Spermatogenesis. In *The Development of Drosophila melanogaster*, (ed. M. Bate and A. Martinez-Arias), pp. 71-147. Cold Spring Harbor, NY.: Cold Spring Harbor Laboratory Press.

Gaertig, J., Cruz, M. A., Bowen, J., Gu, L., Pennock, D. G. and Gorovsky, M. A. (1995). Acetylation of lysine 40 in alpha-tubulin is not essential in Tetrahymena thermophila. *J Cell Biol* **129**, 1301-10.

Gambello, M. J., Darling, D. L., Yingling, J., Tanaka, T., Gleeson, J. G. and Wynshaw-Boris, A. (2003). Multiple dose-dependent effects of Lis1 on cerebral cortical development. *J Neurosci* **23**, 1719-29.

Garrett, S. and Kapoor, T. M. (2003). Microtubule assembly: catastrophe factors to the rescue. *Curr Biol* **13**, R810-2.

Geiser, J. R., Schott, E. J., Kingsbury, T. J., Cole, N. B., Totis, L. J., Bhattacharyya, G., He, L. and Hoyt, M. A. (1997). Saccharomyces cerevisiae genes required in the absence of the CIN8-encoded spindle motor act in functionally diverse mitotic pathways. *Mol Biol Cell* **8**, 1035-50.

Gepner, J., Li, M., Ludmann, S., Kortas, C., Boylan, K., Iyadurai, S. J., McGrail, M. and Hays, T. S. (1996). Cytoplasmic dynein function is essential in Drosophila melanogaster. *Genetics* **142**, 865-78.

Gergely, F., Karlsson, C., Still, I., Cowell, J., Kilmartin, J. and Raff, J. W. (2000). The TACC domain identifies a family of centrosomal proteins that can interact with microtubules. *Proc Natl Acad Sci U S A* **97**, 14352-7.

Giansanti, M. G., Bonaccorsi, S., Williams, B., Williams, E. V., Santolamazza, C., Goldberg, M. L. and Gatti, M. (1998). Cooperative interactions between the central spindle and the contractile ring during Drosophila cytokinesis. *Genes Dev* **12**, 396-410.

Gill, S. R., Schroer, T. A., Szilak, I., Steuer, E. R., Sheetz, M. P. and Cleveland, D. W. (1991). Dynactin, a conserved, ubiquitously expressed component of an activator of vesicle motility mediated by cytoplasmic dynein. *J Cell Biol* **115**, 1639-50.

Gonczy, P. (2004). Centrosomes: hooked on the nucleus. *Curr Biol* **14**, R268-70.

Gonczy, P., Pichler, S., Kirkham, M. and Hyman, A. A. (1999). Cytoplasmic dynein is required for distinct aspects of MTOC positioning, including centrosome separation, in the one cell stage Caenorhabditis elegans embryo. *J Cell Biol* **147**, 135-50.

Gonzalez, C., Casal, J. and Ripoll, P. (1989). Relationship between chromosome content and nuclear diameter in early spermatids of Drosophila melanogaster. *Genet Res* **54**, 205-12.

Gonzalez-Reyes, A., Elliott, H. and St Johnston, D. (1995). Polarization of both major body axes in Drosophila by gurken-torpedo signalling. *Nature* **375**, 654-8.

Gunsalus, K. C., Bonaccorsi, S., Williams, E., Verni, F., Gatti, M. and Goldberg, M. L. (1995). Mutations in twinstar, a Drosophila gene encoding a cofilin/ADF homologue, result in defects in centrosome migration and cytokinesis. *J Cell Biol* **131**, 1243-59.

Hammond, J. W., Cai, D. and Verhey, K. J. (2008). Tubulin modifications and their cellular functions. *Curr Opin Cell Biol* **20**, 71-6.

Hatten, M. E. (2002). New directions in neuronal migration. *Science* **297**, 1660-3.

Hebbar, S., Mesngon, M. T., Guillotte, A. M., Desai, B., Ayala, R. and Smith, D. S. (2008). Lis1 and Ndel1 influence the timing of nuclear envelope breakdown in neural stem cells. *J Cell Biol* **182**, 1063-71.

Hirotsune, S., Fleck, M. W., Gambello, M. J., Bix, G. J., Chen, A., Clark, G. D., Ledbetter, D. H., McBain, C. J. and Wynshaw-Boris, A. (1998). Graded reduction of Pafah1b1 (Lis1) activity results in neuronal migration defects and early embryonic lethality. *Nat Genet* **19**, 333-9.

Holzbaur, E. L., Hammarback, J. A., Paschal, B. M., Kravit, N. G., Pfister, K. K. and Vallee, R. B. (1991). Homology of a 150K cytoplasmic dynein-associated polypeptide with the Drosophila gene Glued. *Nature* **351**, 579-83.

Hook, P. and Vallee, R. B. (2006). The dynein family at a glance. *J Cell Sci* **119**, 4369-71.

Hubbert, C., Guardiola, A., Shao, R., Kawaguchi, Y., Ito, A., Nixon, A., Yoshida, M., Wang, X. F. and Yao, T. P. (2002). HDAC6 is a microtubule-associated deacetylase. *Nature* **417**, 455-8.

Inoue, Y. H., Savoian, M. S., Suzuki, T., Mathe, E., Yamamoto, M. T. and Glover, D. M. (2004). Mutations in orbit/mast reveal that the central spindle is comprised of two

microtubule populations, those that initiate cleavage and those that propagate furrow ingression. *J Cell Biol* **166**, 49-60.
Kalderon, D., Roberts, B. L., Richardson, W. D. and Smith, A. E. (1984). A short amino acid sequence able to specify nuclear location. *Cell* **39**, 499-509.

Karki, S. and Holzbaur, E. L. (1995). Affinity chromatography demonstrates a direct binding between cytoplasmic dynein and the dynactin complex. *J Biol Chem* **270**, 28806-11.

Kemphues, K. J., Kaufman, T. C., Raff, R. A. and Raff, E. C. (1982). The testis-specific beta-tubulin subunit in Drosophila melanogaster has multiple functions in spermatogenesis. *Cell* **31**, 655-70.

Kemphues, K. J., Raff, E. C., Raff, R. A. and Kaufman, T. C. (1980). Mutation in a testis-specific beta-tubulin in Drosophila: analysis of its effects on meiosis and map location of the gene. *Cell* **21**, 445-51.

Kim, M. H., Cooper, D. R., Oleksy, A., Devedjiev, Y., Derewenda, U., Reiner, O., Otlewski, J. and Derewenda, Z. S. (2004). The structure of the N-terminal domain of the product of the lissencephaly gene Lis1 and its functional implications. *Structure* **12**, 987-98.

King, J. M., Hays, T. S. and Nicklas, R. B. (2000). Dynein is a transient kinetochore component whose binding is regulated by microtubule attachment, not tension. *J Cell Biol* **151**, 739-48.

King, S. J., Brown, C. L., Maier, K. C., Quintyne, N. J. and Schroer, T. A. (2003). Analysis of the dynein-dynactin interaction in vitro and in vivo. *Mol Biol Cell* **14**, 5089-97.

King, S. J. and Schroer, T. A. (2000). Dynactin increases the processivity of the cytoplasmic dynein motor. *Nat Cell Biol* **2**, 20-4.

Kozminski, K. G., Diener, D. R. and Rosenbaum, J. L. (1993). High level expression of nonacetylatable alpha-tubulin in Chlamydomonas reinhardtii. *Cell Motil Cytoskeleton* **25**, 158-70.

Lee, L. A., Lee, E., Anderson, M. A., Vardy, L., Tahinci, E., Ali, S. M., Kashevsky, H., Benasutti, M., Kirschner, M. W. and Orr-Weaver, T. L. (2005). Drosophila genome-scale screen for PAN GU kinase substrates identifies Mat89Bb as a cell cycle regulator. *Dev Cell* **8**, 435-42.

Lei, Y. and Warrior, R. (2000). The Drosophila Lissencephaly1 (DLis1) gene is required for nuclear migration. *Dev Biol* **226**, 57-72.

Li, J., Lee, W. L. and Cooper, J. A. (2005). NudEL targets dynein to microtubule ends through LIS1. *Nat Cell Biol* **7**, 686-90.

Li, M., McGrail, M., Serr, M. and Hays, T. S. (1994). Drosophila cytoplasmic dynein, a microtubule motor that is asymmetrically localized in the oocyte. *J Cell Biol* **126**, 1475-94.

Li, M. G., Serr, M., Newman, E. A. and Hays, T. S. (2004). The Drosophila tctex-1 light chain is dispensable for essential cytoplasmic dynein functions but is required during spermatid differentiation. *Mol Biol Cell* **15**, 3005-14.

Liebrich, W. (1982). The effects of cytochalasin B and colchicine on the morphogenesis of mitochondria in Drosophila hydei during meiosis and early spermiogenesis. An in vitro study. *Cell Tissue Res* **224**, 161-8.

Liu, Z., Xie, T. and Steward, R. (1999). Lis1, the Drosophila homolog of a human lissencephaly disease gene, is required for germline cell division and oocyte differentiation. *Development* **126**, 4477-88.

Malone, C. J., Misner, L., Le Bot, N., Tsai, M. C., Campbell, J. M., Ahringer, J. and White, J. G. (2003). The C. elegans hook protein, ZYG-12, mediates the essential attachment between the centrosome and nucleus. *Cell* **115**, 825-36.

Martinez-Campos, M., Basto, R., Baker, J., Kernan, M. and Raff, J. W. (2004). The Drosophila pericentrin-like protein is essential for cilia/flagella function, but appears to be dispensable for mitosis. *J Cell Biol* **165**, 673-83.

Matsuyama, A., Shimazu, T., Sumida, Y., Saito, A., Yoshimatsu, Y., Seigneurin-Berny, D., Osada, H., Komatsu, Y., Nishino, N., Khochbin, S. et al. (2002). In vivo destabilization of dynamic microtubules by HDAC6-mediated deacetylation. *Embo J* **21**, 6820-31.

McGrail, M., Gepner, J., Silvanovich, A., Ludmann, S., Serr, M. and Hays, T. S. (1995). Regulation of cytoplasmic dynein function in vivo by the Drosophila Glued complex. *J Cell Biol* **131**, 411-25.

McGrail, M. and Hays, T. S. (1997). The microtubule motor cytoplasmic dynein is required for spindle orientation during germline cell divisions and oocyte differentiation in Drosophila. *Development* **124**, 2409-19.

Mesngon, M. T., Tarricone, C., Hebbar, S., Guillotte, A. M., Schmitt, E. W., Lanier, L., Musacchio, A., King, S. J. and Smith, D. S. (2006). Regulation of cytoplasmic dynein ATPase by Lis1. *J Neurosci* **26**, 2132-9.

Mische, S., He, Y., Ma, L., Li, M., Serr, M. and Hays, T. S. (2008). Dynein light intermediate chain: an essential subunit that contributes to spindle checkpoint inactivation. *Mol Biol Cell* **19**, 4918-29.

Morris, N. R. (2000). Nuclear migration. From fungi to the mammalian brain. *J Cell Biol* **148**, 1097-101.

Morris, N. R., Xiang, X. and Beckwith, S. M. (1995). Nuclear migration advances in fungi. *Trends Cell Biol* **5**, 278-82.

Nogales, E., Wolf, S. G. and Downing, K. H. (1998). Structure of the alpha beta tubulin dimer by electron crystallography. *Nature* **391**, 199-203.

North, B. J., Marshall, B. L., Borra, M. T., Denu, J. M. and Verdin, E. (2003). The human Sir2 ortholog, SIRT2, is an NAD+-dependent tubulin deacetylase. *Mol Cell* **11**, 437-44.

Palazzo, A., Ackerman, B. and Gundersen, G. G. (2003). Cell biology: Tubulin acetylation and cell motility. *Nature* **421**, 230.

Parks, A. L., Cook, K. R., Belvin, M., Dompe, N. A., Fawcett, R., Huppert, K., Tan, L. R., Winter, C. G., Bogart, K. P., Deal, J. E. et al. (2004). Systematic generation of high-resolution deletion coverage of the Drosophila melanogaster genome. *Nat Genet* **36**, 288-92.

Payne, C., Rawe, V., Ramalho-Santos, J., Simerly, C. and Schatten, G. (2003). Preferentially localized dynein and perinuclear dynactin associate with nuclear pore complex proteins to mediate genomic union during mammalian fertilization. *J Cell Sci* **116**, 4727-38.

Perrod, S., Cockell, M. M., Laroche, T., Renauld, H., Ducrest, A. L., Bonnard, C. and Gasser, S. M. (2001). A cytosolic NAD-dependent deacetylase, Hst2p, can modulate nucleolar and telomeric silencing in yeast. *Embo J* **20**, 197-209.

Plamann, M., Minke, P. F., Tinsley, J. H. and Bruno, K. S. (1994). Cytoplasmic dynein and actin-related protein Arp1 are required for normal nuclear distribution in filamentous fungi. *J Cell Biol* **127**, 139-149.

Quarmby, L. M. and Lohret, T. A. (1999). Microtubule severing. *Cell Motil Cytoskeleton* **43**, 1-9.

Quintyne, N. J. and Schroer, T. A. (2002). Distinct cell cycle-dependent roles for dynactin and dynein at centrosomes. *J Cell Biol* **159**, 245-54.

Rebollo, E. and Gonzalez, C. (2000). Visualizing the spindle checkpoint in Drosophila spermatocytes. *EMBO Rep* **1**, 65-70.

Rebollo, E., Llamazares, S., Reina, J. and Gonzalez, C. (2004). Contribution of noncentrosomal microtubules to spindle assembly in Drosophila spermatocytes. *PLoS Biol* **2**, E8.

Reed, N. A., Cai, D., Blasius, T. L., Jih, G. T., Meyhofer, E., Gaertig, J. and Verhey, K. J. (2006). Microtubule acetylation promotes kinesin-1 binding and transport. *Curr Biol* **16**, 2166-72.

Reinsch, S. and Gonczy, P. (1998). Mechanisms of nuclear positioning. *J Cell Sci* **111 (Pt 16)**, 2283-95.

Reinsch, S. and Karsenti, E. (1994). Orientation of spindle axis and distribution of plasma membrane proteins during cell division in polarized MDCKII cells. *J Cell Biol* **126**, 1509-26.

Reinsch, S. and Karsenti, E. (1997). Movement of nuclei along microtubules in Xenopus egg extracts. *Curr Biol* **7**, 211-4.

Rivas, R. J. and Hatten, M. E. (1995). Motility and cytoskeletal organization of migrating cerebellar granule neurons. *J Neurosci* **15**, 981-9.

Robinson, J. T., Wojcik, E. J., Sanders, M. A., McGrail, M. and Hays, T. S. (1999). Cytoplasmic dynein is required for the nuclear attachment and migration of centrosomes during mitosis in Drosophila. *J Cell Biol* **146**, 597-608.

Rodrigues-Martins, A., Riparbelli, M., Callaini, G., Glover, D. M. and Bettencourt-Dias, M. (2008). From centriole biogenesis to cellular function: centrioles are essential for cell division at critical developmental stages. *Cell Cycle* **7**, 11-6.

Rodriguez, S., Jafer, O., Goker, H., Summersgill, B. M., Zafarana, G., Gillis, A. J., van Gurp, R. J., Oosterhuis, J. W., Lu, Y. J., Huddart, R. et al. (2003). Expression profile of genes from 12p in testicular germ cell tumors of adolescents and adults associated with i(12p) and amplification at 12p11.2-p12.1. *Oncogene* **22**, 1880-91.

Rorth, P. (1998). Gal4 in the Drosophila female germline. *Mech Dev* **78**, 113-8.

Roth, S., Neuman-Silberberg, F. S., Barcelo, G. and Schupbach, T. (1995). cornichon and the EGF receptor signaling process are necessary for both anterior-posterior and dorsal-ventral pattern formation in Drosophila. *Cell* **81**, 967-78.

Rubin, G. M. and Spradling, A. C. (1982). Genetic transformation of Drosophila with transposable element vectors. *Science* **218**, 348-53.

Rusan, N. M., Fagerstrom, C. J., Yvon, A. M. and Wadsworth, P. (2001). Cell cycle-dependent changes in microtubule dynamics in living cells expressing green fluorescent protein-alpha tubulin. *Mol Biol Cell* **12**, 971-80.

Rusan, N. M., Tulu, U. S., Fagerstrom, C. and Wadsworth, P. (2002). Reorganization of the microtubule array in prophase/prometaphase requires cytoplasmic dynein-dependent microtubule transport. *J Cell Biol* **158**, 997-1003.

Saji, S., Kawakami, M., Hayashi, S., Yoshida, N., Hirose, M., Horiguchi, S., Itoh, A., Funata, N., Schreiber, S. L., Yoshida, M. et al. (2005). Significance of HDAC6 regulation via estrogen signaling for cell motility and prognosis in estrogen receptor-positive breast cancer. *Oncogene* **24**, 4531-9.

Salina, D., Bodoor, K., Eckley, D. M., Schroer, T. A., Rattner, J. B. and Burke, B. (2002). Cytoplasmic dynein as a facilitator of nuclear envelope breakdown. *Cell* **108**, 97-107.

Sasaki, S., Shionoya, A., Ishida, M., Gambello, M. J., Yingling, J., Wynshaw-Boris, A. and Hirotsune, S. (2000). A LIS1/NUDEL/cytoplasmic dynein heavy chain complex in the developing and adult nervous system. *Neuron* **28**, 681-96.

Schroer, T. A. (2004). Dynactin. *Annu Rev Cell Dev Biol* **20**, 759-79.

Schroer, T. A. and Sheetz, M. P. (1991). Two activators of microtubule-based vesicle transport. *J Cell Biol* **115**, 1309-18.

Siller, K. H. and Doe, C. Q. (2008). Lis1/dynactin regulates metaphase spindle orientation in Drosophila neuroblasts. *Dev Biol* **319**, 1-9.

Siller, K. H., Serr, M., Steward, R., Hays, T. S. and Doe, C. Q. (2005). Live imaging of Drosophila brain neuroblasts reveals a role for Lis1/dynactin in spindle assembly and mitotic checkpoint control. *Mol Biol Cell* **16**, 5127-40.

Sivaram, M. V., Wadzinski, T. L., Redick, S. D., Manna, T. and Doxsey, S. J. (2009). Dynein light intermediate chain 1 is required for progress through the spindle assembly checkpoint. *Embo J* **28**, 902-14.

Smith, D. S., Niethammer, M., Ayala, R., Zhou, Y., Gambello, M. J., Wynshaw-Boris, A. and Tsai, L. H. (2000). Regulation of cytoplasmic dynein behaviour and microtubule organization by mammalian Lis1. *Nat Cell Biol* **2**, 767-75.

Stebbings, L., Grimes, B. R. and Bownes, M. (1998). A testis-specifically expressed gene is embedded within a cluster of maternally expressed genes at 89B in Drosophila melanogaster. *Dev Genes Evol* **208**, 523-30.

Susalka, S. J. and Pfister, K. K. (2000). Cytoplasmic dynein subunit heterogeneity: implications for axonal transport. *J Neurocytol* **29**, 819-29.

Svejstrup, J. Q. (2007). Elongator complex: how many roles does it play? *Curr Opin Cell Biol* **19**, 331-6.

Swan, A., Nguyen, T. and Suter, B. (1999). Drosophila Lissencephaly-1 functions with Bic-D and dynein in oocyte determination and nuclear positioning. *Nat Cell Biol* **1**, 444-9.

Swan, A. and Suter, B. (1996). Role of Bicaudal-D in patterning the Drosophila egg chamber in mid-oogenesis. *Development* **122**, 3577-86.

Tai, A. W., Chuang, J. Z. and Sung, C. H. (2001). Cytoplasmic dynein regulation by subunit heterogeneity and its role in apical transport. *J Cell Biol* **153**, 1499-509.

Tai, C. Y., Dujardin, D. L., Faulkner, N. E. and Vallee, R. B. (2002). Role of dynein, dynactin, and CLIP-170 interactions in LIS1 kinetochore function. *J Cell Biol* **156**, 959-68.

Tanaka, T., Serneo, F. F., Higgins, C., Gambello, M. J., Wynshaw-Boris, A. and Gleeson, J. G. (2004). Lis1 and doublecortin function with dynein to mediate coupling of the nucleus to the centrosome in neuronal migration. *J Cell Biol* **165**, 709-21.

Texada, M. J., Simonette, R. A., Johnson, C. B., Deery, W. J. and Beckingham, K. M. (2008). Yuri gagarin is required for actin, tubulin and basal body functions in Drosophila spermatogenesis. *J Cell Sci* **121**, 1926-36.

Thibault, S. T., Singer, M. A., Miyazaki, W. Y., Milash, B., Dompe, N. A., Singh, C. M., Buchholz, R., Demsky, M., Fawcett, R., Francis-Lang, H. L. et al. (2004). A complementary transposon tool kit for Drosophila melanogaster using P and piggyBac. *Nat Genet* **36**, 283-7.

Tran, A. D., Marmo, T. P., Salam, A. A., Che, S., Finkelstein, E., Kabarriti, R., Xenias, H. S., Mazitschek, R., Hubbert, C., Kawaguchi, Y. et al. (2007). HDAC6 deacetylation of tubulin modulates dynamics of cellular adhesions. *J Cell Sci* **120**, 1469-79.

Tsai, L. H. and Gleeson, J. G. (2005). Nucleokinesis in neuronal migration. *Neuron* **46**, 383-8.

Tulu, U. S., Rusan, N. M. and Wadsworth, P. (2003). Peripheral, non-centrosome-associated microtubules contribute to spindle formation in centrosome-containing cells. *Curr Biol* **13**, 1894-9.

Umeshima, H., Hirano, T. and Kengaku, M. (2007). Microtubule-based nuclear movement occurs independently of centrosome positioning in migrating neurons. *Proc Natl Acad Sci U S A* **104**, 16182-7.

Vallee, R. B. and Hook, P. (2006). Autoinhibitory and other autoregulatory elements within the dynein motor domain. *J Struct Biol* **156**, 175-81.

Vallee, R. B., Shpetner, H. S. and Paschal, B. M. (1989). The role of dynein in retrograde axonal transport. *Trends Neurosci* **12**, 66-70.

Vardy, L. and Orr-Weaver, T. L. (2007). The Drosophila PNG kinase complex regulates the translation of cyclin B. *Dev Cell* **12**, 157-66.

Vardy, L., Pesin, J. A. and Orr-Weaver, T. L. (2009). Regulation of Cyclin A protein in meiosis and early embryogenesis. *Proc Natl Acad Sci U S A* **106**, 1838-43.

Vaughan, K. T. and Vallee, R. B. (1995). Cytoplasmic dynein binds dynactin through a direct interaction between the intermediate chains and p150Glued. *J Cell Biol* **131**, 1507-16.

Vaughan, P. S., Leszyk, J. D. and Vaughan, K. T. (2001). Cytoplasmic dynein intermediate chain phosphorylation regulates binding to dynactin. *J Biol Chem* **276**, 26171-9.

Vaughan, P. S., Miura, P., Henderson, M., Byrne, B. and Vaughan, K. T. (2002). A role for regulated binding of p150(Glued) to microtubule plus ends in organelle transport. *J Cell Biol* **158**, 305-19.

Verdel, A., Curtet, S., Brocard, M. P., Rousseaux, S., Lemercier, C., Yoshida, M. and Khochbin, S. (2000). Active maintenance of mHDA2/mHDAC6 histone-deacetylase in the cytoplasm. *Curr Biol* **10**, 747-9.

Vogt, N., Koch, I., Schwarz, H., Schnorrer, F. and Nusslein-Volhard, C. (2006). The gammaTuRC components Grip75 and Grip128 have an essential microtubule-anchoring function in the Drosophila germline. *Development* **133**, 3963-72.

Wakefield, J. G., Bonaccorsi, S. and Gatti, M. (2001). The drosophila protein asp is involved in microtubule organization during spindle formation and cytokinesis. *J Cell Biol* **153**, 637-48.

Wakimoto, B. T., Lindsley, D. L. and Herrera, C. (2004). Toward a comprehensive genetic analysis of male fertility in Drosophila melanogaster. *Genetics* **167**, 207-16.

Wei, H. C., Rollins, J., Fabian, L., Hayes, M., Polevoy, G., Bazinet, C. and Brill, J. A. (2008). Depletion of plasma membrane PtdIns(4,5)P2 reveals essential roles for phosphoinositides in flagellar biogenesis. *J Cell Sci* **121**, 1076-84.

Westermann, S. and Weber, K. (2003). Post-translational modifications regulate microtubule function. *Nat Rev Mol Cell Biol* **4**, 938-47.

Willins, D. A., Liu, B., Xiang, X. and Morris, N. R. (1997). Mutations in the heavy chain of cytoplasmic dynein suppress the nudF nuclear migration mutation of Aspergillus nidulans. *Mol Gen Genet* **255**, 194-200.

Wittschieben, B. O., Otero, G., de Bizemont, T., Fellows, J., Erdjument-Bromage, H., Ohba, R., Li, Y., Allis, C. D., Tempst, P. and Svejstrup, J. Q. (1999). A novel histone acetyltransferase is an integral subunit of elongating RNA polymerase II holoenzyme. *Mol Cell* **4**, 123-8.

Wojcik, E., Basto, R., Serr, M., Scaerou, F., Karess, R. and Hays, T. (2001). Kinetochore dynein: its dynamics and role in the transport of the Rough deal checkpoint protein. *Nat Cell Biol* **3**, 1001-7.

Wong, R., Hadjiyanni, I., Wei, H. C., Polevoy, G., McBride, R., Sem, K. P. and Brill, J. A. (2005). PIP2 hydrolysis and calcium release are required for cytokinesis in Drosophila spermatocytes. *Curr Biol* **15**, 1401-6.

Xiang, X., Roghi, C. and Morris, N. R. (1995). Characterization and localization of the cytoplasmic dynein heavy chain in Aspergillus nidulans. *Proc Natl Acad Sci U S A* **92**, 9890-4.

Yamashita, Y. M., Jones, D. L. and Fuller, M. T. (2003). Orientation of asymmetric stem cell division by the APC tumor suppressor and centrosome. *Science* **301**, 1547-50.

Yamashita, Y. M., Mahowald, A. P., Perlin, J. R. and Fuller, M. T. (2007). Asymmetric inheritance of mother versus daughter centrosome in stem cell division. *Science* **315**, 518-21.